Electrospun nanofiber membranes as supports for enzyme immobilization and its application in wastewater treatment

Zhao, Dan

Publication date:
2023

Document Version
Publisher's PDF, also known as Version of record

Electrospun nanofiber membranes as supports for enzyme immobilization and its application in wastewater treatment

Dan Zhao

Ph.D. Thesis
March 2023

DTU Sustain
Department of Environmental and Resource Engineering
Technical University of Denmark

Electrospun nanofiber membranes as supports for enzyme immobilization and its application in wastewater treatment

Dan Zhao

Ph.D. Thesis, March 2023

Address: DTU Sustain
Department of Environmental and Resource Engineering
Technical University of Denmark
Bygningstorvet, Building 115
2800 Kgs. Lyngby
Denmark

Phone reception: +45 4525 1600

Homepage: http://www.env.dtu.dk
E-mail: reception@env.dtu.dk

Cover: STEP

Preface

This Ph.D. thesis, entitled "Electrospun nanofiber membranes as supports for enzyme immobilization and its application in wastewater treatment," comprises the research carried out at the Department of Environmental and Resource Engineering, Technical University of Denmark, from 1st December 2019 to 31st November 2022. This thesis was supported by the Novo Nordisk Foundation (NNF18OC0034918), and Danish Research Council (8022-00237B), and China Scholarship Council. The research was performed under the main supervision of Associate Professor Wenjing Zhang (DTU Sustain) and the co-supervision of Professor Claus Hélix-Nielsen (DTU Sustain) and Professor Maher Abou Hachem (DTU Bioengineering)

The thesis is organized in two parts: the first part puts into context the findings of the Ph.D. project in an introductive review; the second part consists of the papers listed below.

I **Zhao, D**, Leth, M. L., Abou Hachem, Hélix-Nielsen, C., and Zhang, W. Thin-film composite biocatalytic Nanofibrous membranes for Pharmaceutical Residues Degradation: Performance, stability, and Continuity. *Manuscript in preparation.*

II **Zhao, D**, Leth, M. L., Abou Hachem, Hélix-Nielsen, C., and Zhang, W. A novel eco-friendly degradable laccase-immobilized electrospun nanofibers targeting contaminant of emerging concerns. *Manuscript in preparation.*

III **Zhao, D**., Leth, M. L., Abou Hachem, M., Aziz, I., Jančič, N., Luxbacher, T., Hélix-Nielsen, C., and Zhang, W. (2023). Facile fabrication of flexible ceramic nanofibrous membranes for enzyme immobilization and transformation of emerging pollutants. *Chemical Engineering Journal*, *451*, 138902.

In addition, the following publications, not included in this thesis, were also concluded during this Ph.D. study:

IV Xu, M., **Zhao, D**., Zhu, X., Su, Y., Angelidaki, I. and Zhang, Y. (2021). Biogas upgrading and valorization to single-cell protein in a bioinorganic electrosynthesis system. *Chemical Engineering Journal*, *426*, 131837.

V Wang, G., Hambly, A.C., **Zhao, D.,** Wang, G., Tang, K. and Andersen, H.R. (2023). Peroxymonosulfate activation by suspended biogenic manganese oxides for polishing micropollutants in wastewater effluent. *Separation and Purification Technology*, *306*, 122501.

VI Qin J., Dou Y., **Zhao D**., Yang X., Andersen, H.R., Hélix-Nielsen, C., and Zhang, W. Encapsulation of Carbon-Nanodots into MOFs for Efficient Upcycling of Polyvinyl Chloride Plastics. *Manuscript in preparation*

Acknowledgments

Words cannot express my gratitude to the people who have contributed to this work. First, I would like to express my most profound appreciation to my main supervisor, Associate Professor Wenjing (Angela) Zhang, for her invaluable trust, encouragement, and enthusiasm. During the project, she has always supported my ideas and put forward valuable suggestions, making the project both exciting and meaningful. I am truly grateful and fortunate to have worked with Angela since 2019.

I sincerely appreciate my co-supervisor, Professor Maher Abou Hachem, who introduced me to the biology field. The professional guidance and expertise for the enzyme study are priceless. I still recognize the time we discussed the detailed experiment plans, and we both tried our best to keep up the thoughts.

Likewise, I would like to thank my co-supervisor, Professor Claus Hélix-Nielsen. Thank you for providing me with a broad view of the research. Claus has provided excellent feedback and suggestions for my study, for which I am truly grateful.

Special thanks go to Posdoc Maria Louise Leth, who has been my closest and most respected collaborator since the start of the project. She has helped set up enzymatic experiments, discussed results, and reviewed the manuscript.

I would like to extend my sincere thanks to all collaboration partners throughout this work: Professor Per Amstrup Pedersen and Assistant Professor Irena Petrinić for excellent cooperation in the NEPWAT project.

Additionally, this endeavor would not have been possible without the generous support from our group members past or present: Yibo Dou, Sung Yul Lim, Yuechao Yao, Tao Jiang, Feiyan Wu, Jibo Qin, Tian Tian, Xuhui Hu, Yiwen Chen, Qian Jia, Xing Chen, Ruijuan Qu, Iram Aziz, Gege Wu, Shaoxiong Zhai, Arshad Iqbal, and Begüm Tanis. I learned a lot from you guys and I hope to work with you in the future.

Besides, I would also like to thank Mikael Emil Olsson, Hector Garcia, Sinh Hy Nguyen, Lene Kirstejn Jensen, Hanne Bøggild, and Kristin Kostadinova for their technical assistance in the lab.

In addition, I would also like to appreciate the financial support from China Scholarship Council and Otto Mønsted Fond.

Most importantly, I would like to express my sincere appreciation to my family, who has always supported my decisions. Especially, I am deeply grateful to my husband, Mingyi Xu, for your unconditioned love and support.

Summary

Life on earth depends on water, which covers 71% of the planet's surface. Despite this, the availability of freshwater is endangered by factors such as climate change and excessive extraction, unable to keep up with the rising global demand. Moreover, the discharge of vast quantities of wastewater by industry, municipalities, and agriculture worsens the shortage of water resources and poses a threat to human health due to pollution. Water treatment, thus, is crucial for ensuring a clean water supply in the future.

Presently, wastewater treatment plants (WWTPs) face a challenge in monitoring and regulating contaminants of emerging concerns (CECs) due to their persistence and trace concentrations. The discharge of such compounds in the effluent can potentially have adverse effects on aquatic ecosystems and wildlife. To mitigate this issue, there is an increasing emphasis on employing advanced treatment technologies to reduce the discharge of CECs from WWTPs. However, due to their low concentrations, traditional treatment technologies like active sludge and moving bed biofilms have limited efficacy in removing CECs. In contrast, membrane technology has demonstrated high-quality removal of CECs, which may result in concentrated pollutants. One potential solution is to incorporate enzymes into membrane technology, taking advantage of the eco-friendly biotransformation of CECs and regulating water quality.

This thesis aims to investigate the potential of using three different types of membranes to immobilize enzymes, with a particular focus on adjusting the membranes' structure and functional groups. The initial phase of the research indicates the possibility and suitability of a polymer-based membrane system for enzyme immobilization. Specifically, the study used laccase, which was attached to nanofibers made of polyacrylonitrile (PAN), as well as a lab-created nanofibrous membrane with a selective layer. Results suggested that introducing β-cyclodextrin into the fibers and incorporating –OH and $–NH_2$ functional groups into the membrane surface could enhance the enzymatic activity of the membranes. The immobilized enzyme also demonstrated greater thermal stability and a wider range of pH tolerance compared to free enzymes.

The second part of the thesis focuses on the development of biodegradable materials and their potential for enzyme immobilization. Building on earlier research, a new process was utilized to produce biodegradable fibrous membranes, utilizing β-cyclodextrin as the primary material and citric acid as

a crosslinker. The study examined the ability to immobilize laccase in the molecular sieving structure of β-cyclodextrin, finding that the immobilized enzymes retained their catalytic activity. Implementing this biodegradable membrane system offers a solution to the plastic waste commonly associated with the disposal of polymeric membranes.

Despite the potential benefits of biodegradable membranes as carriers for enzymes, concerns persist regarding their reusability and durability due to inconsistent material properties and limited shelf life. To address these issues, the third segment of the study focuses on developing ceramic membranes as enzyme carriers that are mechanically stable, recyclable, and flexible. The findings demonstrated that the flexible ceramic membranes achieve a high immobilization yield of 57.9 ± 0.5% with a specific activity of 0.53 ± 0.09 U mg^{-1}. Furthermore, the membranes exhibited efficient removal of up to 95% of five emerging pollutants, providing the first proof of concept that laccase-immobilized ceramic nanofiltration membranes could effectively transform emerging pollutants while being easy to retrieve, making them a promising option for environmental bioremediation processes.

Dansk sammenfatning

Livet på jorden afhænger af vand, som dækker 71% af planetens overflade. På trods af dette er tilgængeligheden af ferskvand truet af faktorer såsom klimaændringer og overdreven udvinding, der ikke kan følge med den stigende globale efterspørgsel. Derudover forværrer udledning af store mængder spildevand fra industri, kommuner og landbrug mangel på vandressourcer og udgør en trussel mod menneskers sundhed på grund af forurening. Vandbehandling er derfor afgørende for at sikre en ren vandforsyning i fremtiden.

I øjeblikket står spildevandsrensningsanlæg (WWTP'er) over for en udfordring med at overvåge og regulere nyopdagede uønskede stoffer (CEC'er) på grund af deres vedholdenhed og sporstoffer. Udsivningen af sådanne forbindelser i spildevandet kan potentielt have negative virkninger på vandlevende økosystemer og dyreliv. For at mindske dette er der en stigende vægt på at anvende avancerede behandlingsteknologier for at reducere udledningen af CEC'er fra WWTP'er. Dog har traditionelle behandlingsteknologier som aktivt slam og bevægelige biofilmbede begrænset effektivitet i at fjerne CEC'er på grund af deres lave koncentrationer. I modsætning hertil har membranteknologi demonstreret højkvalitets fjernelse af CEC'er, men dette kan resultere i problemet med koncentrerede forureningsstoffer. En potentiel løsning er at inkorporere enzymer i membranteknologi, udnytte den miljøvenlige biotransformation af CEC'er og regulere vandkvaliteten.

Denne afhandling har til formål at undersøge potentialet ved at anvende tre forskellige typer af membraner til transport af enzymer, med særligt fokus på at justere membranernes struktur og funktionelle grupper. Den indledende fase af forskningen indikerer muligheden og egnetheden af et polymerbaseret membransystem til enzymimmobilisering. Specifikt bruger studiet laccase, som er fastgjort til nanofibre lavet af polyacrylonitril (PAN), samt en selvskabt nanofibøs membran med en selektiv lag. Resultaterne antyder, at introduktionen af β-cyclodextrin i fibrene og inkorporeringen af –OH og $–NH_2$ funktionelle grupper på membranoverfladen kan forbedre enzymatisk aktivitet i membranerne. Den immobiliserede enzym demonstrerer også større termisk stabilitet og et bredere pH-toleranceområde sammenlignet med frie enzymer.

Den anden del af afhandlingen fokuserer på udviklingen af biologisk nedbrydelige materialer og deres potentiale til enzymimmobilisering. Byggende på tidligere forskning anvendes en ny proces til at producere biologisk nedbrydelige fibermembraner ved hjælp af β-cyclodextrin som det primære materiale og

citronsyre som et tværforbinder. Studiet undersøger evnen til at immobilisere laccase i molekylsienestrukturen af β-cyclodextrin og finder, at de immobiliserede enzymer bevarer deres katalytiske aktivitet. Implementering af dette biologisk nedbrydelige membransystem tilbyder en løsning på plastaffald, der ofte er forbundet med bortskaffelse af polymermembraner.

Trods de potentielle fordele ved biologisk nedbrydelige membraner som bærere for enzymer, består bekymringer om deres genanvendelighed og holdbarhed på grund af inkonsekvente materialeegenskaber og begrænset holdbarhed. For at tackle disse problemer fokuserer den tredje del af undersøgelsen på at udvikle keramiske membraner som enzymerbærere, der er mekanisk stabile, genanvendelige og fleksible. Resultaterne viser, at de fleksible keramiske membraner opnår en høj immobiliseringsudbytte på 57,9 ± 0,5% med en specifik aktivitet på 0,53 ± 0,09 U mg^{-1}. Derudover viser membranerne effektiv fjernelse af op til 95% af fem nye forurenende stoffer og giver den første konceptbevis for, at laccase-immobiliserede keramiske nanofiltreringsmembraner kan effektivt transformere nye forurenende stoffer, samtidig med at de er nemme at hente, hvilket gør dem til en lovende mulighed for miljømæssig bioremedieringsprocesser.

Table of contents

Lists of Abbreviations

AOPs	Advanced oxidation processes
APTES	(3-Aminopropyl)triethoxysilane
BE	Backscattering electrons
BMRs	Biocatalytic membrane reactors
CAS	Conventional activated sludge
CD	β-cyclodextrin
CLSM	Confocal laser scanning microscopy
CECs	Contaminants of Emerging Concerns
DCF	Diclofenac
DS	Draw solution
EDCs	Endocrine-disrupting compounds
FO	Forward osmosis
FTIR	Fourier Transform Infrared Spectroscopy
FTIR-ATR	Fourier Transform Infrared Attenuated Total Reflectance
IP	Interfacial polymerisation
MOFs	Metal-organic frameworks
MF	Microfiltration
MFA	Mefenamic acid
MPs	Microplastics
NF	Nanofiltration
NFMs	Nanofiber membrane
PAN	Polyacrylonitrile
PDA	Polydopamine
PEI	Polyethyleneimine
PPCPs	Pharmaceutical and personal care products
POPs	Persistent organic pollutants
PVA	Poly(vinyl alcohol)
PVDF	Polyvinylidene fluoride
RO	Reverse osmosis
SE	Secondary electrons
SEM	Scanning electron microscopy
SW	Swelling ratio
TEOS	Tetraethyl orthosilicate
TFCs	Thin-film composite membranes
UF	Ultrafiltration
WS	Water scarcity
WU	Water uptake
WWTPs	Wastewater treatment plants

1 Introduction

1.1 Water, resources, and Emerging pollutants

While water covers 71% of the earth's surface, only approximately 3% is fresh water. Unfortunately, over two-thirds of this freshwater is frozen in glaciers and polar ice caps, leaving a minimal amount of freshwater, mainly as groundwater. In fact, only 1% of freshwater is present as surface water that is available for human activities [1]. Although freshwater is considered a renewable resource, it cannot meet the ever-increasing demand for water due to population growth and economic development. Some highly populated and water-stressed areas are already experiencing water scarcity (WS). Approximately one-fifth of the world's population lacks access to potable water [2]. Many regions are already undergoing pervasive water scarcity conditions. Additionally, by 2050, areas including Northern and Southern Africa, the Middle East, and Central and Eastern Asia are projected to experience severe water scarcity conditions [3,4].

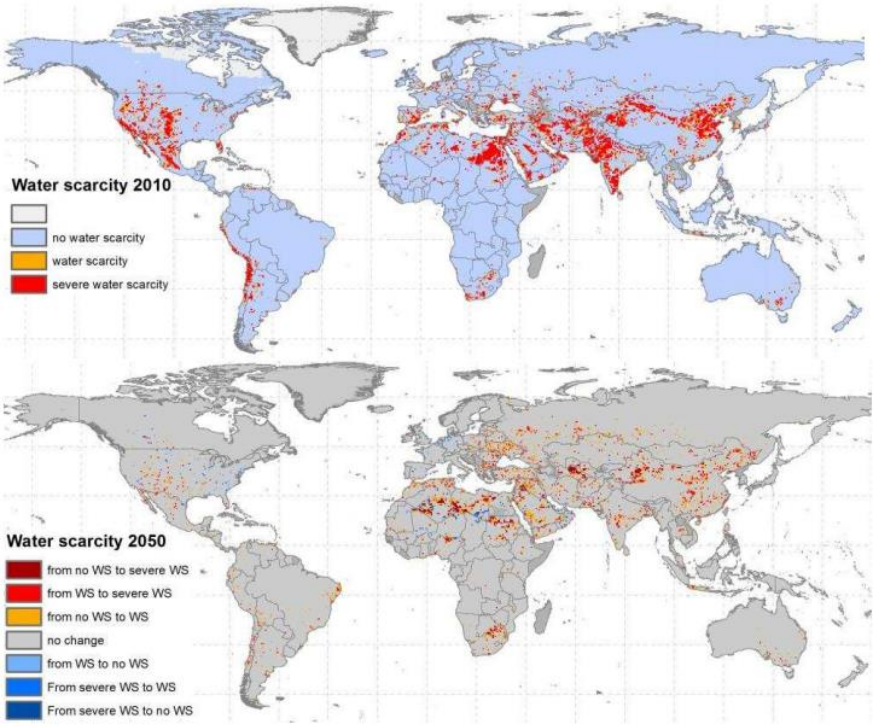

Figure 1.1 Water scarcity [4]

Despite the growing water demand, water pollution aroused by human activities has worsened the situation. Annually, 12,500 tons of renewable freshwater is utilized for domestic, agricultural, and industrial applications, thereby re-

sulting in contamination by a wide range of synthetic compounds [2]. An estimated 80% of industrial and municipal wastewaters containing pharmaceuticals, cosmetics, microplastics, and heavy metals are discharged into the environment without prior treatment, posing a threat to both human beings and the ecosystem [5]. As a result, continuous effort is required to treat these wastewaters. Over the past three decades, various physical, chemical, and biological technologies such as flotation [6], precipitation [7], oxidation, carbon adsorption [8], membrane filtration [9], electrochemistry, and biodegradation have been developed and implemented in wastewater treatment plants (WWTPs) [10].

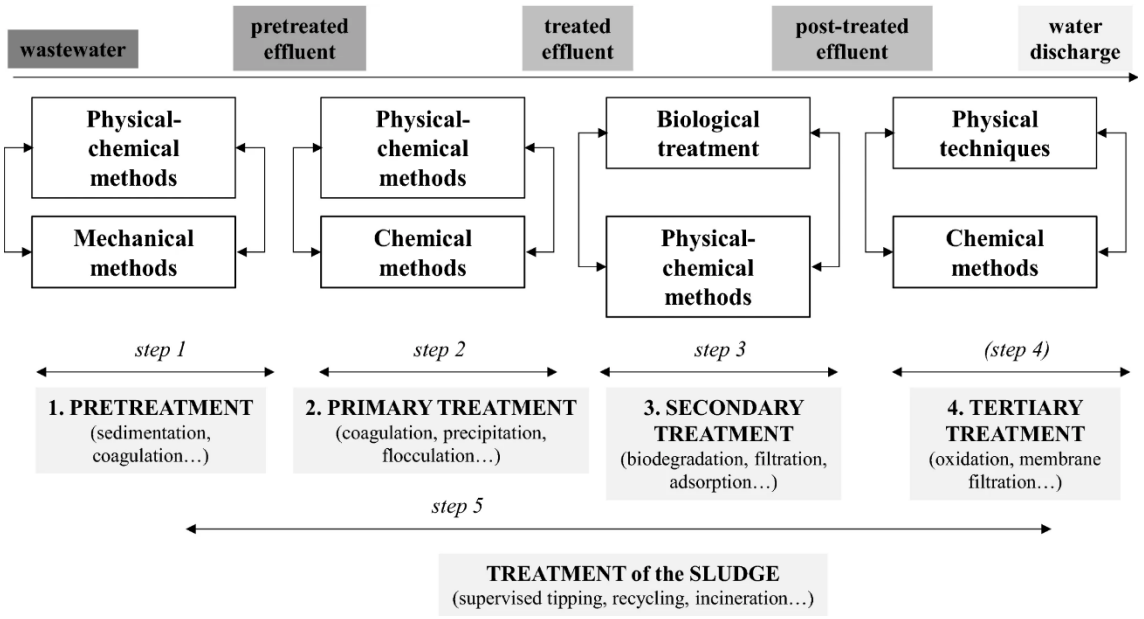

Figure 1.2 General scheme of wastewater treatment [10]. Reprinted with permission of *Springer*.

WWTPs are crucial for pollutant removal, while the very fact is that they can also be hot spots for releasing recalcitrant compounds into the environment [11]. These contaminants, known as Contaminants of Emerging Concerns (CECs), are highly persistent at low concentrations (ng L^{-1} ~ µg L^{-1} range). They have the potential to cause negative effects on both the environment and human health. There are more than 700 CECs, including their metabolites and transformation products, that are reported to be present in the aquatic environment in Europe [12]. Common categories of CECs include pharmaceutical and personal care products (PPCPs), microplastics (MPs), endocrine-disrupting compounds (EDCs), and persistent organic pollutants (POPs). CECs are currently not included in (inter)national routine monitoring programs, and their fate, behavior, and ecotoxicological effects are not well understood.

1.2 Wastewater Treatment

Conventional wastewater treatment consists of a combination of physical, chemical, and biological processes [13], following the listed sequence, as shown in **Figure 1.2**: (1) preliminary treatment; (2) primary treatment; (3) secondary treatment; (4) Tertiary treatment; and (5) treatment of sludge formed. However, most WWTPs are designed to remove nitrogen, phosphorus, and chemical oxygen demand from wastewater. Removal of the CECs through conventional treatment processes remains limited. As a result, they can be released from point pollution sources, in particular, WWTPs. Many CECs are frequently detected in treated wastewater (**Figure 1.3**), and their concentrations could potentially pose a threat to the environment [14].

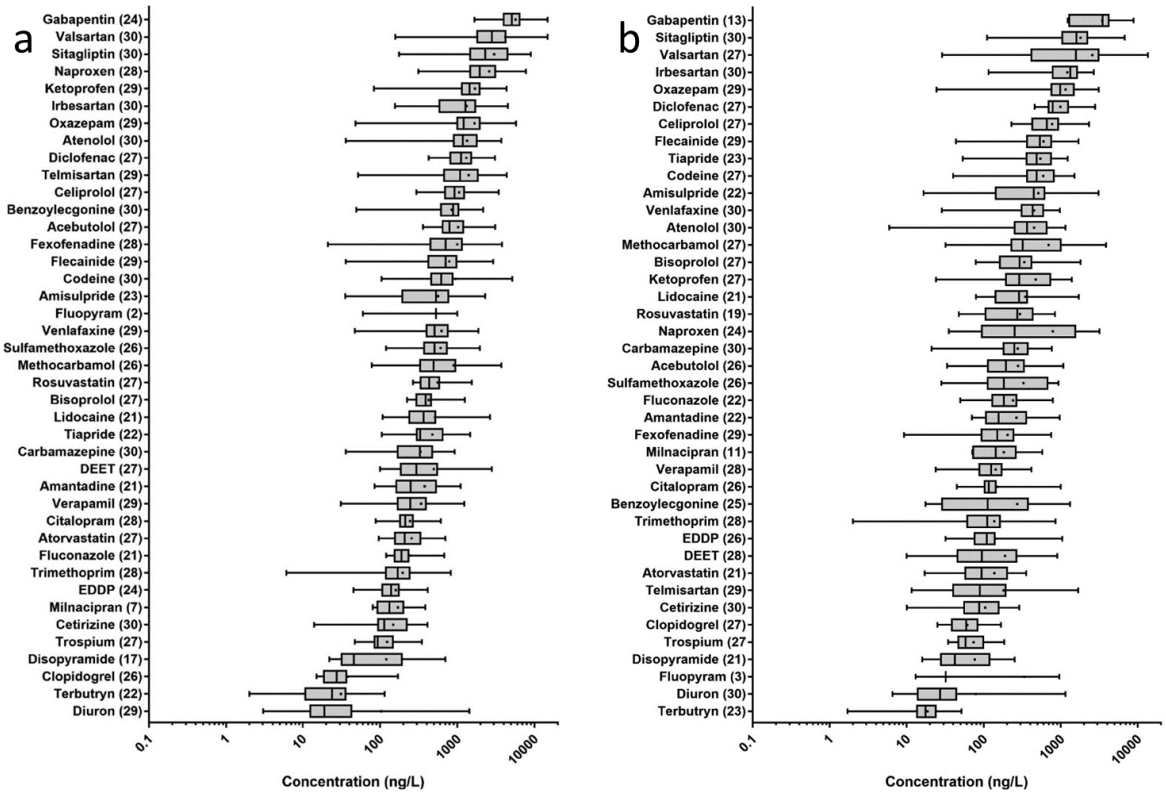

Figure 1.3 Concentrations of each identified CEC in a) influent; b) effluent for all WWTPs [14]. Adapted with permission from *Elsevier*.

Until now, reliable techniques to eliminate the CECs from wastewater are yet to be developed due to political, technological, and economic reasons. A few physicochemical and/or biological methods are evaluated and applied to the removal of pollutants from wastewater. This section presents an overview of the most relevant treatment technologies available.

1.2.1 Advanced oxidation processes (AOPs)

Advanced oxidation processes (AOPs) are a practical solution for treating recalcitrant pollutants as they utilize highly reactive hydroxyl radicals (·OH) to attack a broad range of organic pollutant molecules. This results in a series of oxidation reactions and eventually leads to the complete mineralization products of CO_2 and H_2O. Based on different possible processes for ·OH generation, commonly used AOPs include: 1) photocatalysis, 2) Fenton oxidations, 3) plasma oxidation, and 4) ozonation, as shown in **Figure 1.4**. However, a limitation of AOPs is the production of degradation intermediates that can be more toxic than the original compounds, posing a significant challenge to overcome.

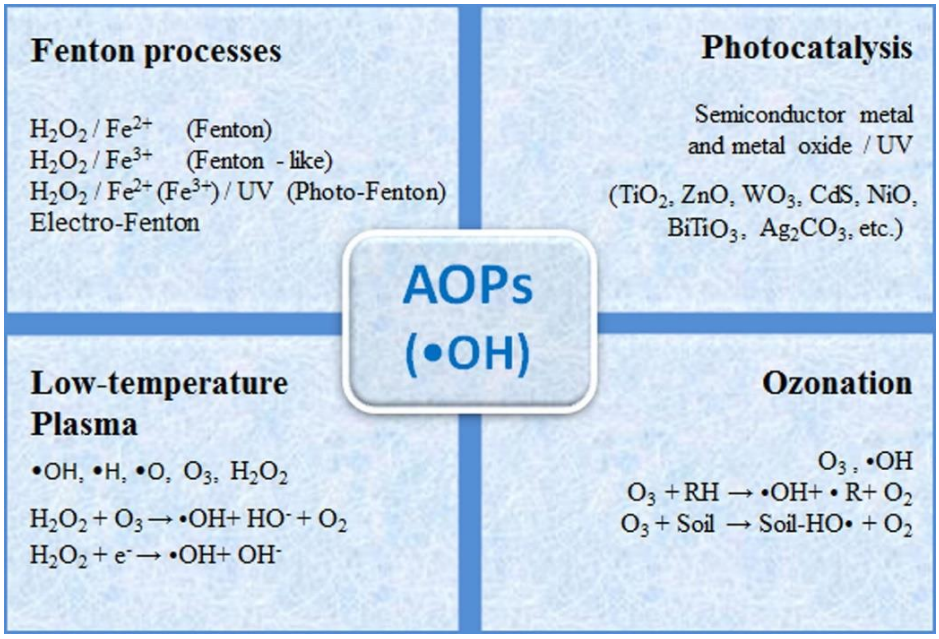

Figure 1.4 Hydroxyl radicals formed according to advanced oxidation technologies [15]. Reprinted with permission from *Elsevier*

1.2.2 Physical treatment process

Adsorption is a simple physical process for CECs elimination. The adsorption mechanisms of various adsorbents are associated with Van der Waal forces, electrostatic interaction, and hydrogen bonding [16]. The effectiveness of adsorption is determined by the type of adsorbent material and the characteristics of the contaminants. In addition, reaction conditions such as pH, temperatures, and contact time significantly influenced the process. One of the most used adsorbents is activated carbon [17]. Advanced materials with a high specific surface area, such as graphene [18,19], carbon nanotubes [20,21], and metal-organic frameworks (MOFs) [22,23], have also been investigated. However,

the high costs of adsorbent regeneration and disposal of waste adsorbent are the main constraints for this technique.

Membrane processes have been widely developed in wastewater treatment processes, including reverse osmosis (RO), microfiltration (MF), nanofiltration (NF), and ultrafiltration (UF), as depicted in **Figure 1.5**. Numerous studies [24–26] have reported efficient rejection of a wide range of CECs through pressure-driven membranes. The permeation mechanisms of CECs through these membranes involve size exclusion, hydrophobic adsorption, and electrostatic repulsion, which rely on various factors, such as the compound's physicochemical properties, solution chemistry, and membrane properties. Instead of using hydraulic pressure difference, forward osmosis (FO), which operates based on osmotic pressure differences between the draw solution (DS) and feed solution, is also a promising alternative for wastewater treatment [27,28]. Although membrane processes exhibit high CEC rejection rates, the concentrated pollutants require further chemical treatment, and the membranes applied, mostly polymeric membranes, raise the environmental issue of plastic waste after use.

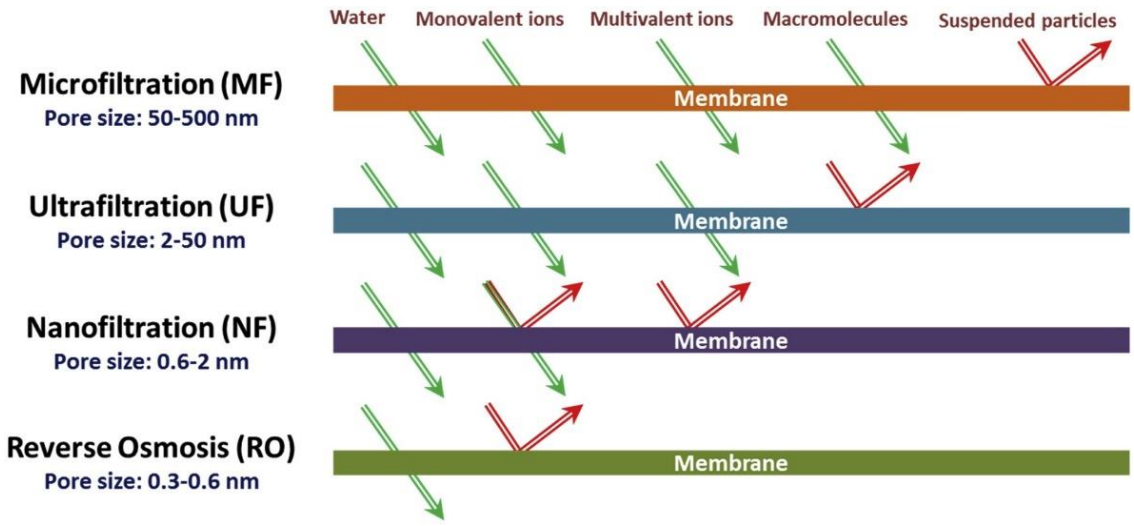

Figure 1.5 Schematic diagrams of microfiltration, ultrafiltration, nanofiltration, and reverse osmosis [29]. Reprinted with permission from *Elsevier*

1.2.3 Biological treatment processes

Conventional activated sludge (CAS) is a widely used biological treatment for reducing organic matter in WWTPs [30]. The process involves adsorption and biodegradation, resulting in a broad range of removal efficiencies from negative to 100% (**Figure 1.6**). Possible reasons for the apparent negative efficiencies could be: Firstly, glucuronides of compounds from the human metabolites

might be CECs sources yet discovered [31]. As such, these conjugates can convert to their parent compounds, leading to increased concentrations in treated effluents. Secondly, CECs enclosed in solids, such as fecal particles, could be gradually released during the biological treatment process.

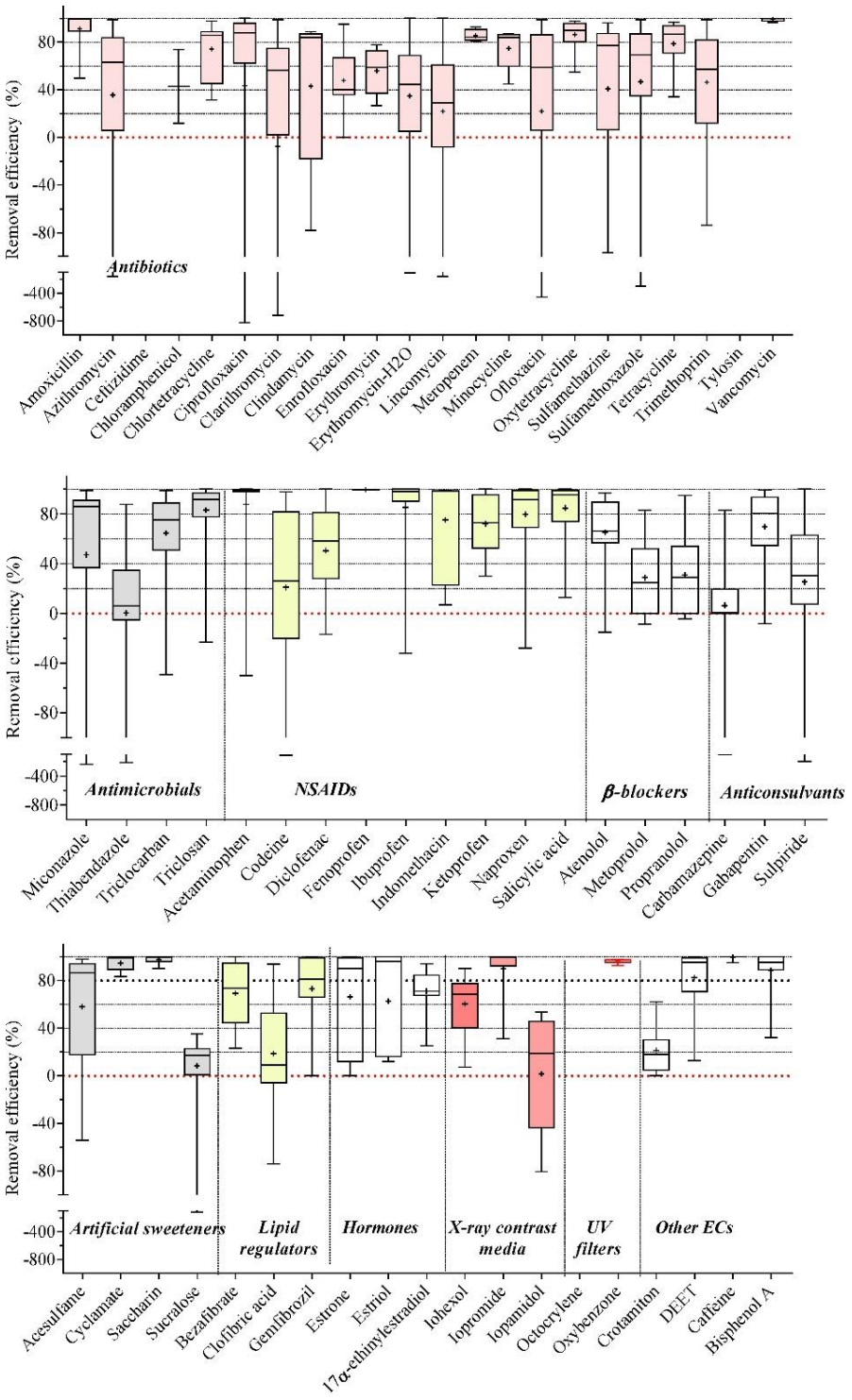

Figure 1.6 Schematic diagrams of microfiltration, ultrafiltration, nanofiltration, and reverse osmosis [32]. Reprinted with permission from *Elsevier*

Awareness is needed regarding the accumulation of adsorbed micropollutants and their by-products in sludge. Several studies have reported the frequent presence of CECs in sewage sludge and biosolids from WWTPs, with relatively high concentrations [33,34]. For instance, ciprofloxacin has been found in sewage sludge and biosolids from WWTPs at concentrations of up to 160 μg g^{-1} dry weight [33]. As a result, advanced methods for sludge management and disposal are necessary to prevent the re-exposure of these pollutants to the environment.

Enzymatic treatment is a highly effective and environmentally friendly method that has gained attention for transforming CECs [35,36]. Enzymes possess several desirable properties compared to chemical catalysts, such as high efficiency, selectivity, and mild operating conditions, which result in low energy consumption and cost reduction. Additionally, enzymes are biodegradable due to their natural origins, making them less environmentally harmful. A variety of enzymes, including hydrolases [37], lyases [38], and oxidoreductases [39], could be employed for the biotransformation of pollutants.

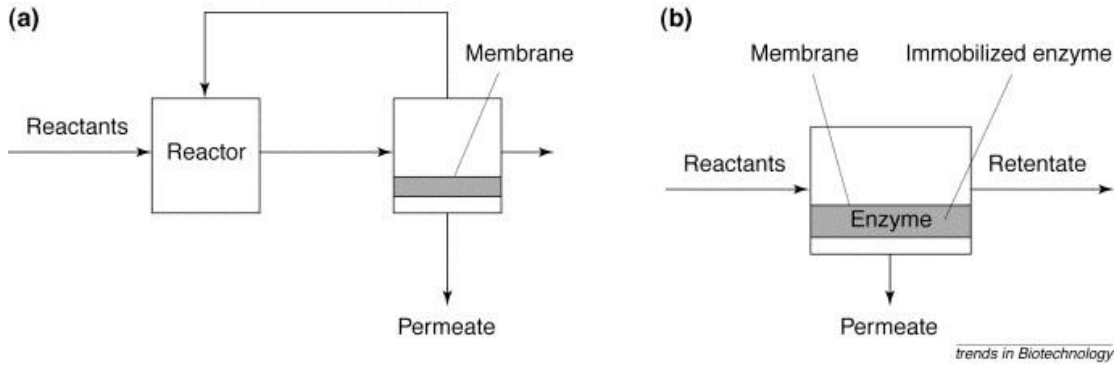

Figure 1.7 Two types of membrane reactors: (a) a reactor combined with a membrane operation unit, (b) a reactor with the membrane acts as a catalytic and separation unit.[40]. Reprinted with permission from *Elsevier*

However, most enzyme research is conducted using enzymes in a free form, on small laboratory scales, in artificial water, and with an extremely high concentration of reactants. It is still challenging to apply these findings to actual wastewater treatment situations. Additionally, other factors, such as the non-reusability of the enzymes and the susceptibility to environmental conditions, must also be considered when exploring potential applications. In order to overcome the limitations, biocatalytic membrane reactors (BMR), where biochemical transformations catalyzed by enzymes are combined with permeation or mass transfer through the membranes, have been developed [40]. Biocatalysts can be suspended in solution or immobilized within the membrane matrix.

The first system (**Figure 1.7a**) consists of a traditional reactor equipped with a membrane separation unit, while enzymes in the reactor are hard to reuse and collect. On the other hand, biocatalytic membranes where biocatalysts are embedded or immobilized in **Figure 1.7b** combine the benefits of bioremediation, and membrane technology markedly facilitates the reuse of immobilized enzymes.

1.3 Oxidoreductases

Oxidoreductases, including dehydrogenases, oxidases, oxygenases, and peroxidases, can catalyze electron transfer from one molecule to another [41]. Dehydrogenases, known as reductases, generally catalyze reversible reactions and, therefore, can be used for both oxidative and reductive biocatalysis. On the other hand, oxygenases, oxidases, and peroxidases facilitate irreversible oxidation reactions due to their high standard enthalpy change of reaction. Research on utilizing oxidoreductases in chemical and pharmaceutical industries has gained widespread attention owing to their inherent selectivity and intriguing chemistry, including introducing oxygen from O_2 into C–H bonds, functionalizing C=C and C–N bonds, and oxidating alcohols, aldehydes, and aromatic compounds.

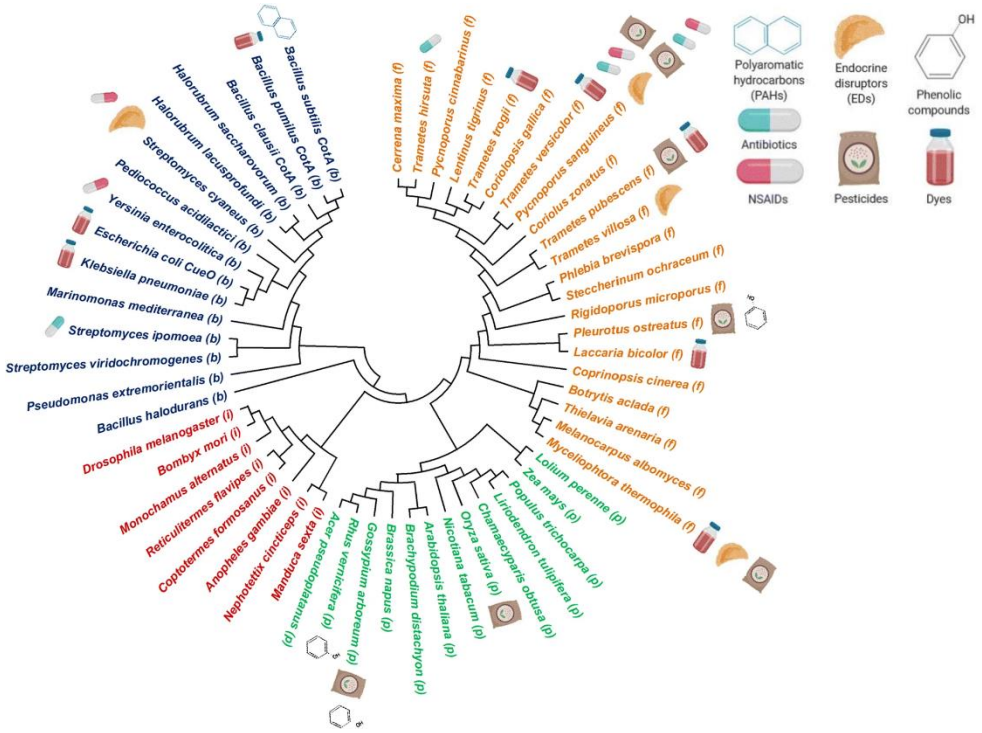

Figure 1.8 Phylogenetic tree constructed with different sources of laccases and their applications in bioremediation [42]. Reprinted under the Creative Commons CC BY license.

1.3.1 Laccase

Laccases (benzenediol: oxygen oxidoreductase, EC 1.10.3.2), known as multicopper oxidases, were first discovered in the lacquer of the Japanese tree *Rhus vernicifera* by Yoshida in 1883 [43]. Since then, it has been reported that laccases are widely distributed in nature (**Figure 1.8**) [42], such as higher plants, fungi, bacteria, and insects. They are model industrial enzymes with a broad range of substrate specificity towards synthetic dyes, chlorinated phenolics, and polycyclic aromatic hydrocarbons [44]. Therefore, it is possible to anticipate that enzymes produced by various organisms may have numerous applications in the field of water treatment.

Laccases, belonging to the blue multicopper oxidase family, possess copper centers within their catalytic core. These enzymes have an active center with four copper atoms, which can be categorized into three groups based on their distinct spectroscopic properties (**Figure 1.9**). Type 1 (T1) site copper atom exhibits a strong absorption at 600 nm due to charge transfer from cysteine sulfur to the copper atom. This charge transfer contributes to the blue color of the laccase. Type 2 (T2) normal copper is invisible in the UV-Vis absorption spectrum. Type 3 coppers consist of a pair of Cu atoms in a binuclear conformation and have a weak absorbance at 330 nm. The laccase-mediated oxidation process comprises three primary steps: Firstly, the T1 copper center acts as the primary electron acceptor site, accepting electrons from the reducing substrate. Secondly, electrons are subsequently transferred from T1 copper to the trinuclear T2/T3 copper cluster. Thirdly, electrons reduce molecular oxygen to water at the trinuclear T2/T3 cluster.

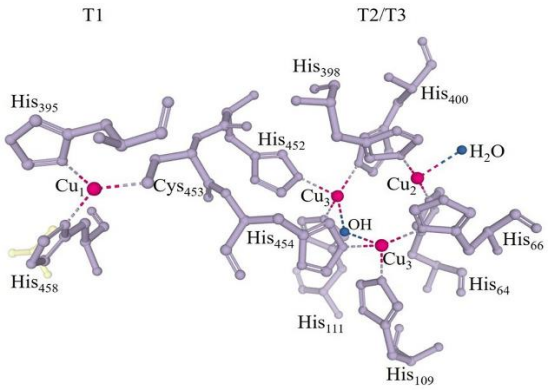

Figure 1.9 Representation of the copper catalytic site of *Trametes versicolor* laccases (RCBS—Protein Data Bank code 1GYC). His and Cys refers to histidines and cysteíne. Pink spheres refers to te copper atoms [45]. Reprinted under the Creative Commons CC BY license.

In general, laccases oxidize substrates into free radicals. These free radicals and unstable chemical products initiate domino reactions, leading to complex chemical transformations [46]. The reaction with laccases can give rise to the production of quinoid derivatives or homomolecular dimers [47] through intermolecular nucleophilic attack by the radicals (**Figure 1.10**).

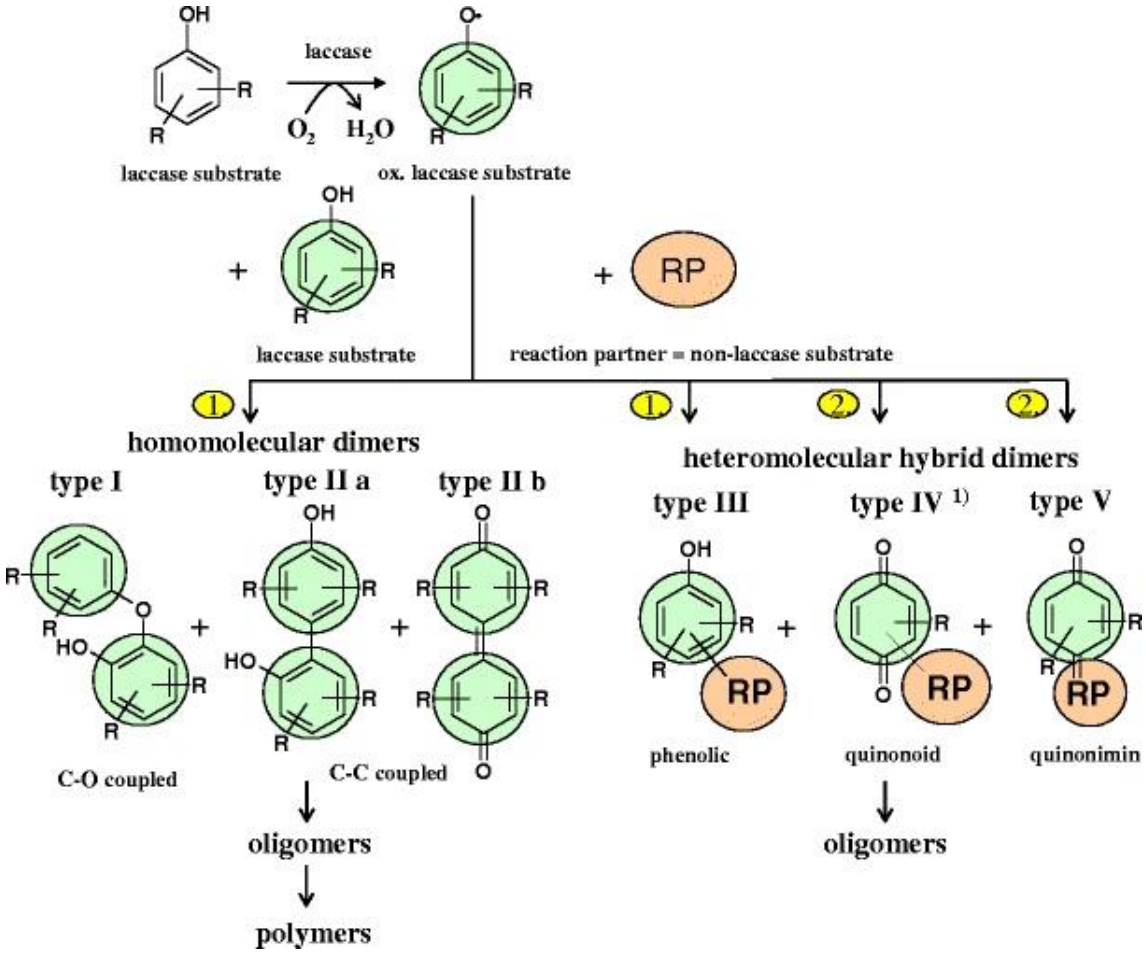

Figure 1.10 Formation of homomolecular and heteromolecular dimers [47]. Reprinted with permission from *Springer Nature*

Over 15 commercial laccase products are utilized in the food [48], paper [49], and textile industries [45,50]. One of the most successful applications is the bleaching of indigo-stained denim [51]. Unfortunately, the complex composition of organic matter and salt, and the pH values of contaminant media largely limit commercial laccase applications for water treatment. Additionally, the large-scale production of laccases poses a constraint on their application in water treatment.

1.3.2 Laccase immobilization

As previously stated, although free enzymes exhibit high catalytic efficiency, their non-reusability and susceptibility to deactivation in industrial conditions pose challenges to their utilization in water treatment. Targeting the aforementioned problems, enzyme immobilization, a process of attaching enzymes to support or matrix, has attracted growing attention owing to several advantages, including the ability to retrieve the catalyst, increased durability under harsh conditions, and continued utilization in enzymatic processes [52]. Enzyme immobilization techniques involve adsorption, covalent binding, entrapment and encapsulation, and cross-linked aggregate, as listed in **Table 1.1**.

Table 1.1 Comparison of different enzyme immobilization methods

Binding method	Adsorption	Encapsulation	Entrapment	Covalent Binding	Cross-linking
Complexity	Simple	Difficult	Difficult	Difficult	Difficult
Binding force	Variable	Weak	Weak	Strong	Strong
Enzyme leakage	Yes	Yes	Yes	No	No
Large diffusion barrier	No	Yes	Yes	No	No
Cost	Low	Moderate	Moderate	High	Low

Adsorption is a common and simple technique for enzyme immobilization, where enzymes are attached to the outer surface of supporting materials. The attractive interactions between enzymes and support normally involve hydrogen bonding, van der Waals forces, hydrophobic interactions, ionic bonding, and metallic chelation interactions. Little damage is applied to enzymes during this adsorption process. However, its shortcomings are obvious, including enzyme leakage [53], the clogged catalytic site of enzymes, non-specific adsorption of products, residual contaminants, and other substances [54].

Covalent binding is achieved through covalent bonds between functional groups of residual amino acid from enzyme surfaces and substrate materials or bi-functional reagents that attach enzymes at one side and substrate on the other side. It has been reported that many amino acid functional groups could be considered reactive enough to participate in covalent bonds formation, such as amino groups of lysine or arginine, the carboxyl group of aspartic acid or glutamic acid, sulfhydryl group of cysteine, phenolic of tyrosine, the hydroxyl group of serine or threonine, and guanidine of arginine [55]. Generally, strong interactions between enzymes and substrates enhance stability and reusability

due to increased enzyme rigidity. At the same time, chemical reactions confirm that the catalytic sites of enzymes remain unaffected, which ensures immobilized enzymes with higher activities [56]. Therefore, it, by far, has been the most effective technique for enzyme immobilization.

Different from the adsorption and covalent binding method, entrapment and encapsulation provide another pathway for enzyme immobilization [57]. In the case of immobilization by encapsulation or entrapment, the biomolecule is physically inserted into the pores of the supporting material while maintaining its original structure. The advantages of entrapment and encapsulation are fast, cheap, and mild conditions required for the reaction process. The support matrix, in addition, protects the enzyme from microbial contamination. However, the disadvantage of these techniques is the mass transfer limitation [58].

Cross-linked enzyme aggregates [59], as a type of immobilization, involve concatenating enzymes to each other to form three-dimensional complex enzyme aggregates instead of forming an enzyme monolayer on top of supporting materials, which increases the promising extent of enzyme loading. The most commonly used cross linkers are glutaraldehyde-ethylene diamine polymers, glutaraldehyde, dextran aldehyde, and toluene diisocyanate [53,54]. High enzyme loading compensates for the loss of enzyme activity caused by cross-linking reactions and finally represents a high overall enzymatic reaction activity. Several studies [60,61] could be found to covalently attach cross-linked enzyme aggregates to PS/PSMA nanofibers via glutaraldehyde treatment. Both enzyme stability and initial reaction activity showed highly improved with negligible damage to enzymes.

1.3.3 Choice of membrane material and structure

Previous research has explored various types of support for enzyme immobilization, including nanofibers [62], nano/microspheres [63], beads [64], gels [65], and capsules [66]. Considering the functions of the membrane (carrier material for enzyme immobilization and separation layer in the reactor), the choice of membrane materials is supposed to fulfill the following characteristics:

1) High surface area providing sufficient active sites for enzyme immobilization

2) Functional groups with strong interactions with the enzymes

3) Suitable mechanical strength fit for the actual wastewater treatment

4) Easy to scale up

Up to date, diverse types of nano-materials have been found to fit those requirements, such as mesoporous silica [67], nanoparticles [68], nanotubes [69], and nanofibers [70–72]. These nanomaterials with extremely high specific surface area display a highly efficient immobilization rate distinguishing from those of other materials. Yet some shortages are still not to be neglected. For instance, mesoporous silica [73] usually encloses enzymes on the inner surface leading to low enzyme activities. Nanoparticles and nanotubes suffer from recycling and certain concerns of health and environmental issues [68]. Nanofibers with high porosity and interconnectivity are easier to fabricate and modify, standing out of those mentioned materials. Regarding this, electrospun nanofibers, as enzyme carriers coupled with membrane reactors, have attracted much attention in recent years. The process of electrospinning is widely acknowledged as the most effective and facile method [74] for producing nanofibers with controlled fiber diameters and morphology from synthetic and natural polymers [23,75], polymer alloys [76], and polymers containing nanoparticles [77], active agents, metals [23], and ceramics [73,74]. Selected samples for electrospun nanofiber as enzyme carriers in wastewater treatment have shown in **Table 1.2**.

Table 1.2. Selected samples for electrospun nanofiber as enzyme carriers in wastewater treatment

Enzyme species	**Fiber types**	**Immobilization**	**Pollutants**	**Removal rate (%)**	**Ref**
Laccase	Biochar-PAN	Covalent binding	Chlortetracycline, Diclofenac	63.3%, 72.7%	[78]
Laccase	PAN/PVDF/Cu	Covalent binding	2,4,6-trichlorophenol	95.4%	[79]
Laccase	PDLLA	Encapsulation	Phenanthrene, Naphthalene	86.6%, 80.2%	[80]
Laccase	Vinyl-modified PAA-SiO_2	Covalent binding	Triclosan	65%	[81]
Laccase	PLCL	Encapsulation and adsorption	Naproxen and Diclofenac	Over 90%	[82]
Laccase	PA_6/CHIT nanofibers	Covalent binding	Bisphenol A, 17α-ethinylestradiol	92% and 96%	[83]
Laccase	PMMA/Fe_3O_4	Covalent binding	Tetracycline	100% and 94%	[71]
Laccase	TiO_2/PES	Covalent binding	-	-	[84]
Horseradish peroxidase	Fe_3O_4/PAN	Adsorption and covalent binding	Phenol	85%	[85]
Horseradish peroxidase	PLGA/F108	Encapsulation	Pentachlorophenol	83%	[86]
Hydrolase	PCL	Entrapment	Neurotoxin	81%	[87]

1.4 Objectives and thesis structure

This work intends to investigate different materials for enzyme immobilization with a particular focus on adjusting the membranes' structure and functional groups and the potential use of laccase-immobilized membranes in CECs depletion. The specific aims are listed below:

Aim 1 obtains a fundamental understanding of laccase, laccase immobilization, and biocatalytic membranes.

Aim 2 investigates different materials from polymer to ceramics adapted to enzyme immobilization

Aim 3 utilizes obtained biocatalytic membranes in dead-end and cross-flow filtration membrane setups and studies the potentiality for CECs elimination.

1.5 Outline of the Thesis

The thesis is based on the three studies presented in Paper I-III. The thesis is written with the presentation of the background research of each study, necessary experimental information, and discussions outlined in each chapter so that a reader can easily follow.

Chapter 1 presents the current situation in water and an overview of possible treatment techniques applied in WWTPs for CECs removal as well as general information about laccases, an industrial enzyme. Specifically, it describes the structure of laccases, different immobilization techniques, and the materials that can be used as enzyme carriers.

Chapter 2 elucidates the experimental work and characteristic techniques employed in Paper I-III to facilitate the comprehension of the results presented in the subsequent chapters.

Chapter 3 discusses laccase immobilization on designed polymeric fibrous membranes (**Paper I**). Compared with free laccase activity, the apparent activity, chemical stability, and thermal resistance are discussed. Additionally, the chapter makes an attempt to utilize the laccase-immobilized membrane and a thin-film composite membrane as a system in cross-flow filtration mode for CECs depletion.

Chapter 4 designs a novel biodegradable nanofiber mat using the findings from Chapter 3, as outlined in **Paper II**. The objective of this design is to address the problem of plastic waste. The resulting biodegradable membranes are analyzed using SEM, FTIR spectrum, and enzyme assays. Furthermore, the potential applications of these biodegradable membranes are evaluated and discussed.

Chapter 5 presents a novel approach to fabricating flexible ceramic membranes and applies the obtained for enzyme immobilization, as described in **Paper III**. Additionally, the chapter utilizes the laccase-immobilized membrane and a commercial microfiltration membrane as a system in dead-end filtration mode for CECs depletion.

Chapter 6 summarizes the obtained knowledge and future perspectives for biocatalytic membrane applications.

2 Methodology

Main experimental work and characteristic techniques are elucidated to facilitate the comprehension of the thesis, including membrane fabrication and characterization, enzyme assays, and CECs depletion performances.

2.1 Membrane fabrication

2.1.1 Electrospun nanofibrous membranes

Electrospinning is a versatile technique for generating uniform nanofibrous membranes with controlled fiber diameters and morphology from synthetic and natural polymers. As depicted in **Figure 2.1a**, this process involves a metallic needle spinneret, a syringe pump, a high-voltage power supply, and a ground collector. Initially, a solution of polymer, sol-gel, or composite is placed in the syringe, forming a droplet at the needle tip. Upon applying high voltage, the droplet stretches into a Taylor-cone structure and then transforms into an electrified jet. The jet is further elongated, whipped, and solidified into nanofibers, which accumulate on the collector to form a nonwoven fibrous mat. Since each needle generates only one polymer jet, needle-based electrospinning is limited by low productivity. Needle-less electrospinning, instead, using different spinnerets, produces fibers directly from an open liquid surface. **Figure 2.1b** depicts a needless electrospinning setup with a wire-shaped motionless spinneret.

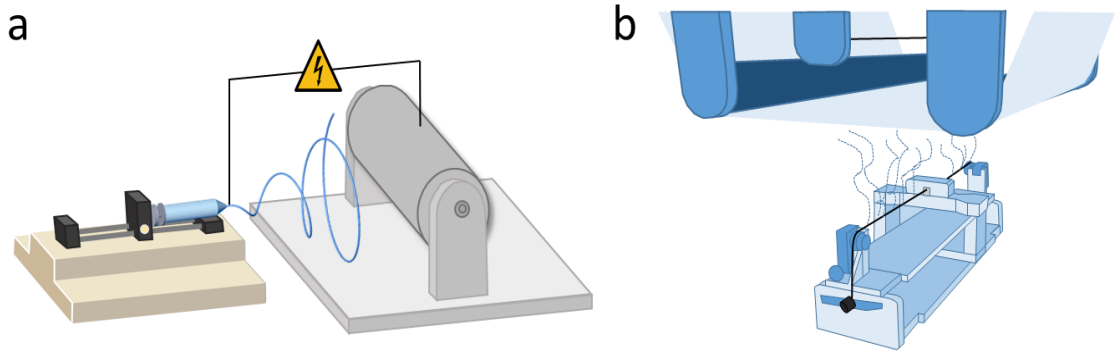

Figure 2.1 a) Needle-based, b) Needless electrospinning setups

2.1.2 Nanofiber-supported thin-film composite membranes (TFCs)

Interfacial polymerization (IP) has been utilized for the fabrication of functional materials [88]. This process typically involves the reaction of two active monomers, namely diamine and acyl chloride, at the interface of water and oil (**Figure 2.2**). The rapid polymerization leads to the formation of a thin polymer

film. The monomers within the two solutions subsequently become partitioned, and the polymerization slows down due to monomer diffusion through the film. As the film thickness grows, the reaction ultimately halts due to the increasing diffusion barrier.

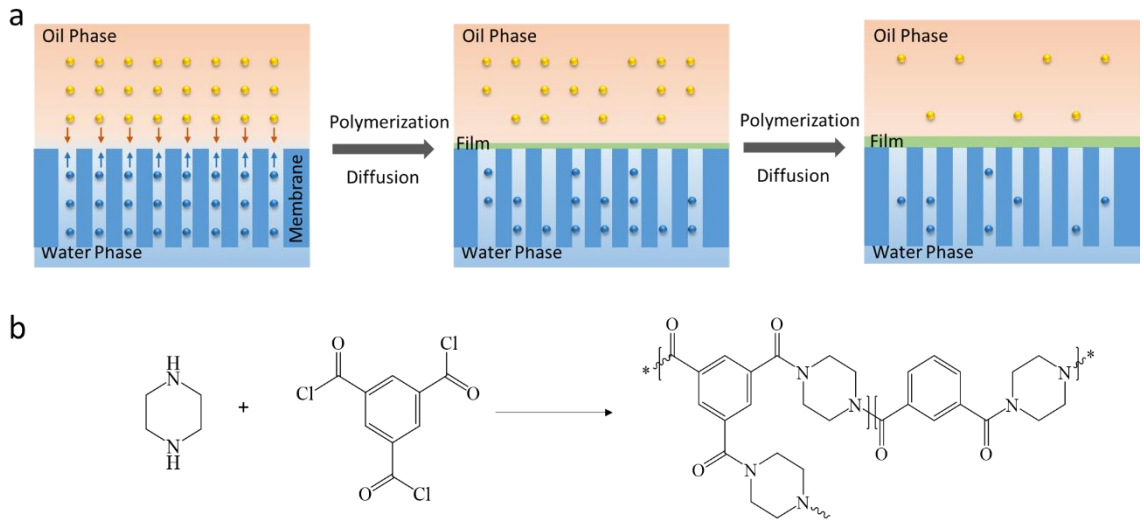

Figure 2.2 Interfacial polymerization. a) Schematic representation of the interfacial polymerization process with membrane. b) The reaction schemes of interfacial polymerization involved in the thesis

2.2 Membrane characterization

2.2.1 Microscopy

Identifying the morphology, structure, and material components is an essential factor in the material study. Here, scanning electron microscopy (SEM) and confocal laser scanning microscopy (CLSM) are demonstrated, as depicted in **Figure 2.3**. SEM is an advanced microscopy technology using a beam of electrons to generate high-resolution images of the material surface. As the primary electrons interact with atoms of the sample, various signals are produced, including secondary electrons (SE), backscattering electrons (BSE), X-rays, and visible light. Among these, secondary and backscattered electrons are commonly employed, with secondary electrons revealing morphology and topography and backscattered electrons highlighting composition contrasts in multiphase samples.

CLSM is an optical imaging technique that enhances the optical resolution and contrast of micrographs during image formation. This is achieved by illuminating the specimen with a laser beam and using a confocal pinhole to eliminate

out-of-focus light, resulting in a sharp and highly-contrasted image. CLSM is particularly useful in visualizing and analyzing the structure and function of biological specimens.

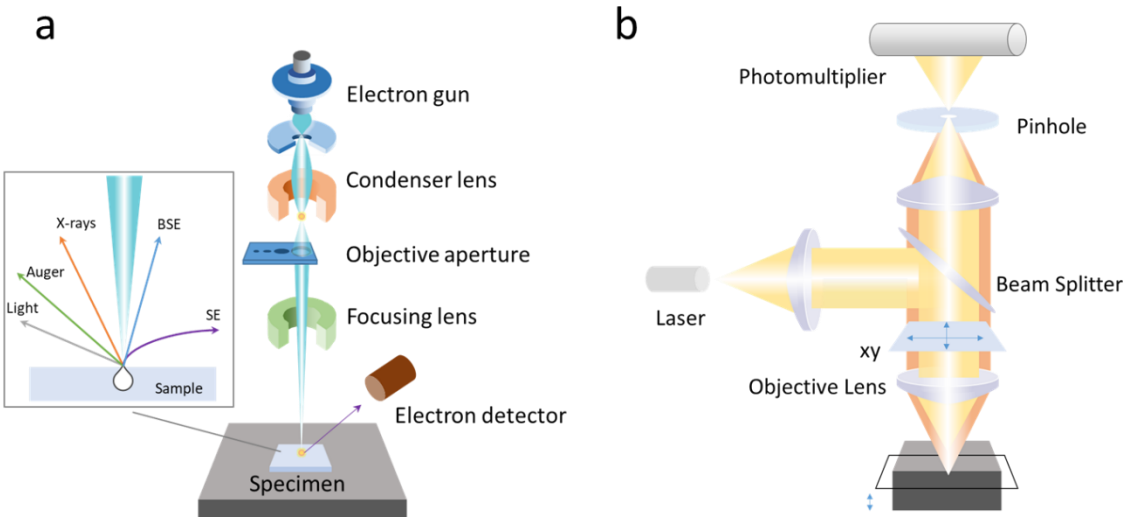

Figure 2.3 Schematic of a) SEM microscope components. b) CLSM microscope components

2.2.2 Fourier Transform Infrared Spectroscopy (FTIR)

FTIR is a powerful analytical technique that enables the identification and characterization of the chemical composition of various specimens by measuring the absorption of infrared light. In FTIR, a beam of infrared radiation is directed through the specimens, making it particularly useful for analyzing transparent samples. In Fourier Transform Infrared Attenuated Total Reflectance (FTIR-ATR), the infrared radiation is directed onto a crystal in contact with the sample to be analyzed. The radiation partially penetrates the sample, interacting with its surface, causing a decrease in the intensity of reflected radiation. FTIR-ATR is often favored over FTIR for analyzing solid or semi-solid samples, providing a representative sample spectrum without sample preparation.

2.2.3 Zeta-potential

Zeta potential is an indicator of surface charge in membrane study and describes the difference in electrical potential between the membrane surface and the surrounding fluid. The streaming potential method is used to determine the zeta potential of the membranes.

2.3 Enzyme Assays

2.3.1 Laccase loadings

The amount of immobilized laccase is calculated by the amount of protein remaining in the immobilization supernatant compared to the total protein. The protein concentrations in solutions were determined by the Bradford method on a microplate reader. The total amount (m) of the immobilized enzyme (μg) was calculated as follows:

$$m = (C_0 - C_r)V - \sum C_w V_w \quad (1)$$

Where,

C_0 : the enzyme concentrations in the initial stock, [μg mL^{-1}]

C_w : the enzyme concentrations in washing buffer, [μg mL^{-1}]

C_r : the enzyme concentrations in the residual solution, , [μg mL^{-1}]

V, V_w : volumes of the enzyme solution and washing buffer, [mL]

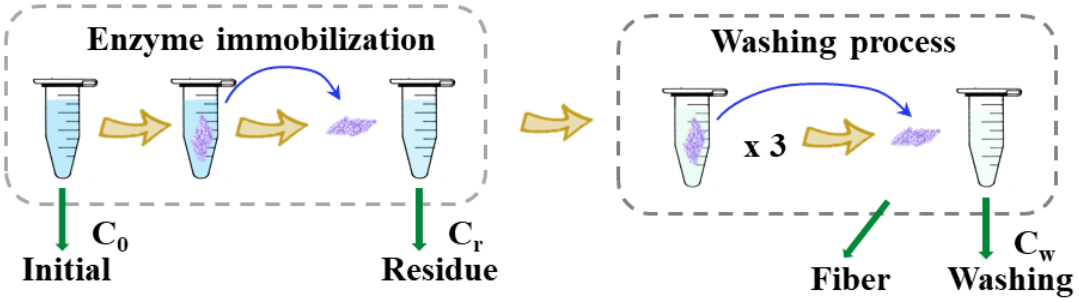

Figure 2.4 Schematic enzyme immobilization process

2.3.2 Laccase activity

To determine the apparent enzyme activity (A) of either an enzyme solution (A_{free}) or a fiber (A_{fiber}), the initial slope of the absorbance versus time curve (Abs420 min^{-1}) was used to calculate it. The enzyme activity was measured in units (U), where one unit of enzyme activity (U) was defined as the amount of enzyme necessary to convert 1 μmol of ABTS per minute under the given assay conditions (μmol min^{-1}).

$$A = \frac{\alpha \times V_{\text{Total}}}{\varepsilon \times d} \quad (2)$$

Where,

V_{Total}: the volume of total assay, [μL]

α : the absorbance per minute at 420 nm, [min^{-1}],

d : the light path of the assay, [cm]

ε : the molar absorption coefficient of ABTS at 420 nm, 36,000 $M^{-1}\cdot cm^{-1}$.

The specific activity of free enzyme (SA_{free}), specific activities of the immobilized enzyme (SA_{imm}) and fiber (SA_{fiber}) were defined as the enzyme activity of enzyme solution per weight of free enzyme (U mg^{-1} enzyme), enzyme activity of fiber per weight of immobilized enzyme (U mg^{-1} enzyme) and support membrane(U g^{-1} fiber) separately.

$$SA_{\text{free}} = \frac{A_{\text{free}}}{M_{\text{free}}} \quad (3)$$

$$SA_{imm} = \frac{A_{\text{fiber}}}{M_{\text{imm}}} \quad (4)$$

$$SA_{\text{fiber}} = \frac{A_{\text{fiber}}}{M_{\text{fiber}}} \quad (5)$$

Where,

M_{free} : the amount of free enzyme in the assay, [mg]

M_{imm} : the amount of immobilized enzyme on tested fiber, [mg]

M_{fiber} : the mass of tested fibers, [g]

2.3.3 Optimum pH and thermal inactivation curve

To assess the impact of pH on laccase activity, the free and immobilized enzymes were examined at pH 3.5-6.5 in 20 mM NaOAc, and their absorbance at 420 nm was measured at 25°C. Additionally, a thermal-irreversible inactivation test was carried out to assess the stability of both the free and immobilized enzymes at 50°C.

2.3.4 Kinetic parameters

The apparent Michaelis-Menten kinetic parameters of both free and immobilized enzymes are obtained by determining the specific activity of the enzymes using various concentrations of ABTS ranging from 0.1 to 5 mM:

$$\upsilon = V_{\max}\frac{[S]}{K_{\text{m}}+[S]} \quad (6)$$

$$\frac{1}{V} = \frac{K_{\mathrm{m}}}{V_{\max}[S]} + \frac{1}{V_{\max}} \quad (7)$$

Where,

υ : the initial reaction rate

$[S]$: substrate concentration, [mM]

$V_{\max}$: the apparent maximum rate of the bio-catalyst

K_{m} : the apparent Michaelis–Menten constant, [mM]

2.4 Membrane filtration setups

The thesis involves two kinds of filtration modes: dead-end filtration and cross-flow filtration.

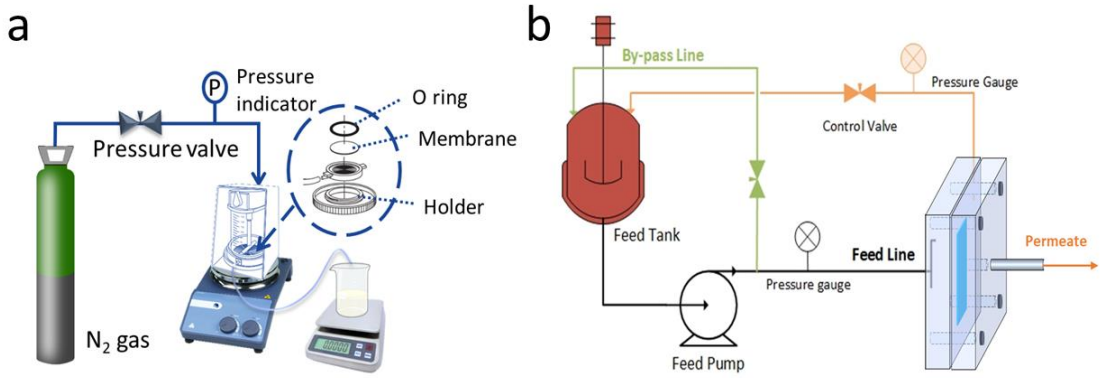

Figure 2.5 Schematic of a) dead-end filtration setup, b)cross-flow filtration setup

The concentrations of EPs were analyzed by High-Performance Liquid Chromatography–Mass Spectrometry (HPLC-MS). The depletion efficiency (D) was calculated as

$$D = \frac{C_{\mathrm{EP_0}} - C_{\mathrm{EP}}}{C_{\mathrm{EP_0}}} \times 100\% \quad (8)$$

Where,

C_{EP0} : EP concentrations in initial solutions, [μg L^{-1}]

C_{EP} : EP concentrations in the permeate, [μg L^{-1}]

3 Polymeric Membranes for Laccase Immobilization and CECs Depletion

Chapter 3 will implement a laccase-assisted polymeric membrane system for laccase immobilization. This chapter is related to **Paper I**.

3.1 Introduction and Motivation

Bio-catalytic degradation of recalcitrant micropollutants with enzymes such as laccase offers an environmentally appealing option to traditional filtration and adsorption methods. Numerous studies [23,89,90] have been dedicated to immobilizing laccases onto various membrane supports. Polymeric membranes are favored for membrane-based water treatment applications due to their ease of processing and inexpensive manufacturing cost, making them the most commonly utilized materials. Lante et al. [91] successfully adsorbed laccases onto polyethersulphone membranes by recirculating enzyme solution through. Hou et al. [77] covalently immobilized laccases onto the TiO_2 sol-gel coated polyvinylidene fluoride (PVDF) membrane, where nearly 80% of the original laccase activity was preserved. Costa et al. efficiently immobilized laccases over polysulfone membranes blended with functionalized carbon nanotubes [92]. However, the enzyme performance of each membrane above was limited to a batch study.

Herein, we developed a novel enzyme immobilization strategy to build a biocatalytic membrane reactor with efficient degradation performance. For this purpose, Polyacrylonitrile (PAN), with good stability and mechanical properties, was chosen as the primary material for electrospinning [78]. Besides, β-cyclodextrin (CD) was employed as an additive material due to its remarkable adsorption property on protein and pollutants resulting from its cone-shaped structure and unique hydrophilicity [93]. Several steps of functionalization and modification were applied to introduce functional groups into the polymer fibers. This is the first study to employ scalable biocatalytic membranes and a self-constructed TFC membrane in a cross-flow filtration arrangement for the purpose of transforming emerging contaminants.

3.2 Experimental Design

As shown in **Figures 3.1a-b**, the electrospun PAN NFMs and PAN/β-CD NFMs are obtained by electrospinning. The obtained PAN/β-CD membranes were further functionalized by following steps: 1) Amidoxime synthesis was achieved by immersing 0.32 g PAN/β-CD NFMs in 100 mL 0.15 M hydroxylamine aqueous solution at 65 °C for two hours. The pH value of the solution was adjusted to 7 by the addition of Na_2CO_3. The obtained NFMs were washed with distilled water three times and vacuum-dried overnight at 40 °C. 2) To perform the silanization treatment, the treated membranes were immersed in a 100 ml ethanol solution containing 10% (w/w) of (3-Aminopropyl)triethoxysilane (APTES) and heated to 70 °C for two hours. The resulting NFMs were then washed thrice with distilled water and dried overnight at 40 °C. Afterward, the functionalized NFMs were placed in a laccase solution with a concentration of 5 mg mL^{-1} (by weight) in 50 mM NaOAc buffer, pH 4.5, and incubated at 25 °C for one hour, followed by a transfer to a 4 °C fridge for 24 hours. **Figure 3.1c** illustrates the process of preparation of a thin-film composite (TFC) membrane by interfacial polymerization of polyamide onto the electrospun PAN NFMs. Finally, the biocatalytic membranes and the thin-film composite membranes were tested in a cross-flow filtration membrane cell. The PAN, PAN/β-CD, amidoxime treated PAN/β-CD, and silanized PAN/β-CD NFMs are labeled as M1, M2, M3, and M4 NFMs, respectively.

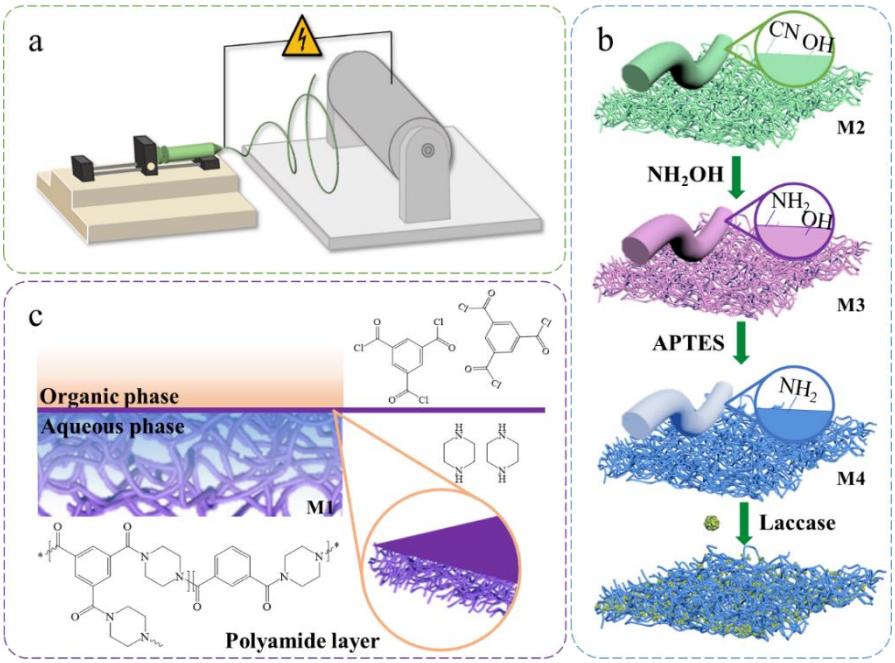

Figure 3.1 Schematic illustration of needle-based electrospinning a), enzyme immobilization b), and thin-film composite membrane fabrication.

3.3 Membrane Characterisation

Figures 3.2A-C depict the morphology of M2, M3, and M4 NFMs. Compared with M2 NFMs, shown in **Figure 3.2A**, surface-treated M3 and M4 NFMs maintained a smooth and uniform structure with a fiber diameter distribution at 450 ± 130 nm, 465 ± 120 nm, and 452 ± 159 nm. The addition of β-CD, amidoxime treatment, and silanization did not change the surface morphology of the NFMs. **Figures 3.2D-F** show the surface and cross-section of the TFC membrane. The thin nanofiber nonwoven matt with high porosity and low tortuosity reduced the severity of internal concentration polarization. A continuous polyamide film was expected to adhere on top of the nanofiber matt, consistent with the results from **Figure 3.2D**. The nanofibers were partially embedded in the top layer, indicating a tight polyamide adhesion to the nanofibers. In addition, wrinkles were noticed on the surface, which the shrinkage of the polyamide layer might cause during the thermal treatment. From the cross-section image (**Figures 3.2E-F**), the polyamide layer and TFC membrane thicknesses were 155 ± 5 nm and 25 ± 1 μm, respectively.

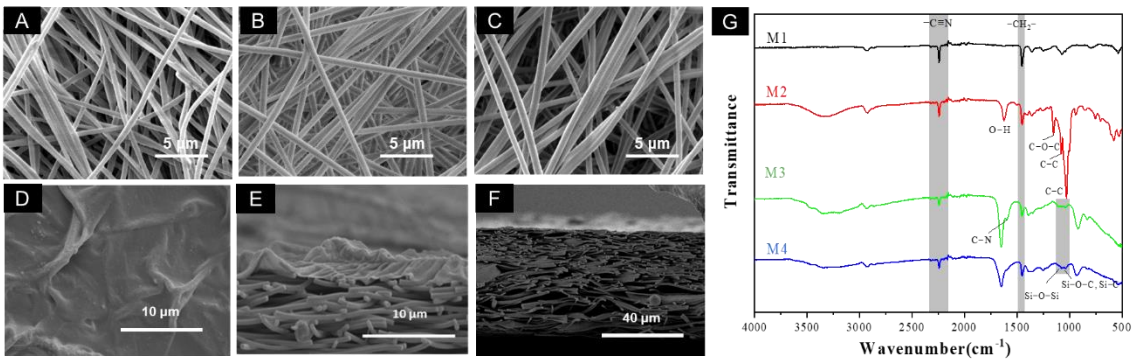

Figure 3.1 A-C) SEM image of M2, M3, and M4 NFMs. D) Surface SEM image of TFC NFMs. E-F) Cross-section SEM images of TFC NFMs with different magnifications. G) FTIR-ATR spectrum of M1, M2, M3, and M4 NFMs.

Figure 3.2G reveals differences between the electrospun fibers before and after surface functionalization. The prominent peaks of PAN at 2243, 2925, and 1452 cm^{-1} can be ascribed to the stretching vibrations of cyano groups (−C≡N) and the stretching and bending vibrations of methylene groups (−CH_2−), respectively [94]. Characteristic peaks for β-CD were observed at 1628 cm^{-1}, 1152 cm^{-1}, 1078 cm^{-1}, and 1031 cm^{-1}, assigning to bending vibration of hydroxyl groups (O−H), stretching vibrations of glycosidic linkage (C−O−C), stretching vibrations of C−C bond, and stretching vibrations of C−H bonds from cyclodextrin ring [93,95]. A new peak formed on M3 NFMs at 1597 cm^{-1}, corresponding to C−N stretching bonds, and weakened cyano groups at 2243

cm^{-1}, indicated that some cyano groups were converted into $–C(NH_2)=NOH$ groups. Following the silanization process, absorption peaks at approximately 1050 cm^{-1} corresponded to Si–O–C and Si–O–Si. It is likely that these peaks were caused by the extensive chain of the Si–O–Si network from the APTES molecules.

3.4 Enzyme Characterization

Figure 3.3A shows the specific activity of biocatalytic membranes. It was observed that M3 NFMs exhibited the highest values in terms of unit weight and area of the membrane. The amount of protein immobilized onto the fiber was difficult to quantify in M2-M4 NFMs, where the β-CD interfaces the Bradford and BCA reagent. Therefore, enzyme performance in this study was mainly focused on the apparent specific activities of fibers.

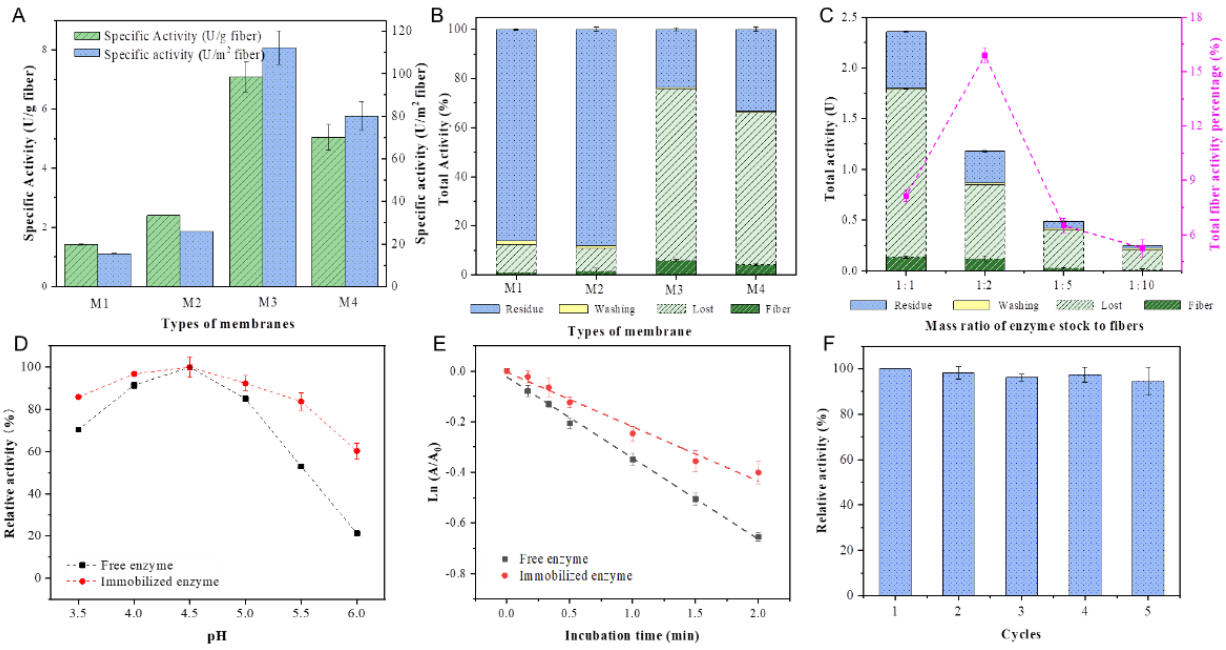

Figure 3.3 A) Specific activity of different fibers in terms of weight and area. B-C) Total enzyme activity in the residue solution, washing buffer, immobilized fibers, and the calculated lost activity with different NFMs and different mass ratios of enzyme stock. D) The pH-dependent relative activity of both free laccase and laccase-immobilized M3 NFMs and free laccase. E) Thermal inactivation kinetics of laccase-immobilized M3 NFMs and free laccase. F) Relative activity of laccase-immobilized NFMs with recycling usage.

M3 and M4 NFMs showed a high enzyme activity of fiber loss, correlated to the high protein load. However, M3 NFMs exhibited the highest enzyme activity of fiber (112 ± 5 U m^{-2}), corresponding to 8% of total activity, as shown in **Figure 3.3B**. The decrease in activity could be due to the overcrowding of immobilized enzymes on the fibers, supported by the results in **Figure 3.3C**. When the enzyme load was reduced by 50%, fiber retained 86% of the activity, while activity losses decreased from 70% to 62%. A significant loss of fiber activity was observed when the enzyme load was further reduced.

In **Figures 3.3D-E**, the impact of pH and thermal treatment on both free and immobilized laccase on M3 NFMs is presented. Immobilized laccase demonstrated more than 60% of its optimum activity within a wider pH range as compared to the free enzyme. The optimum pH values of both free and immobilized laccase were found to be the same at 4.5. The residual activity of immobilized laccase was observed to be 67%, while it was only 53% for the free laccase after heating for 120 minutes at 50°C. These results indicated that immobilization enhanced the thermal stability of laccase compared to its free form. Additionally, the repeated use of immobilized laccase is presented in **Figure 3.3F**, demonstrating up to 95% retention of initial activity after five cycles of reuse.

3.5 Enzymatic membrane system performance

The enzymatic membrane system was applied with a laccase-immobilized M3 membrane and a lab-made TFC membrane. The CECs depletion performance involved both separation and biocatalytic reaction. Both the concentrations of selected CECs were measured in both retentate and permeate. **Figure 3.4A** depicts the increased concentrations of both diclofenac (DCF) and mefenamic acid (MFA) during the filtration process with the TFC membrane. Different from the performance of a TFC membrane, the additional layer of a biocatalytic membrane led to a decrease in the concentrations of CECs in the feed (retentate) side, which indicated a valid enzymatic reaction in the system (**Figure 3.4B**). Notably, the depletion of both DCF and MFA in the permeate side was > 85%, largely improved by adding a biocatalytic membrane to the membrane system (**Figure 3.4C**).

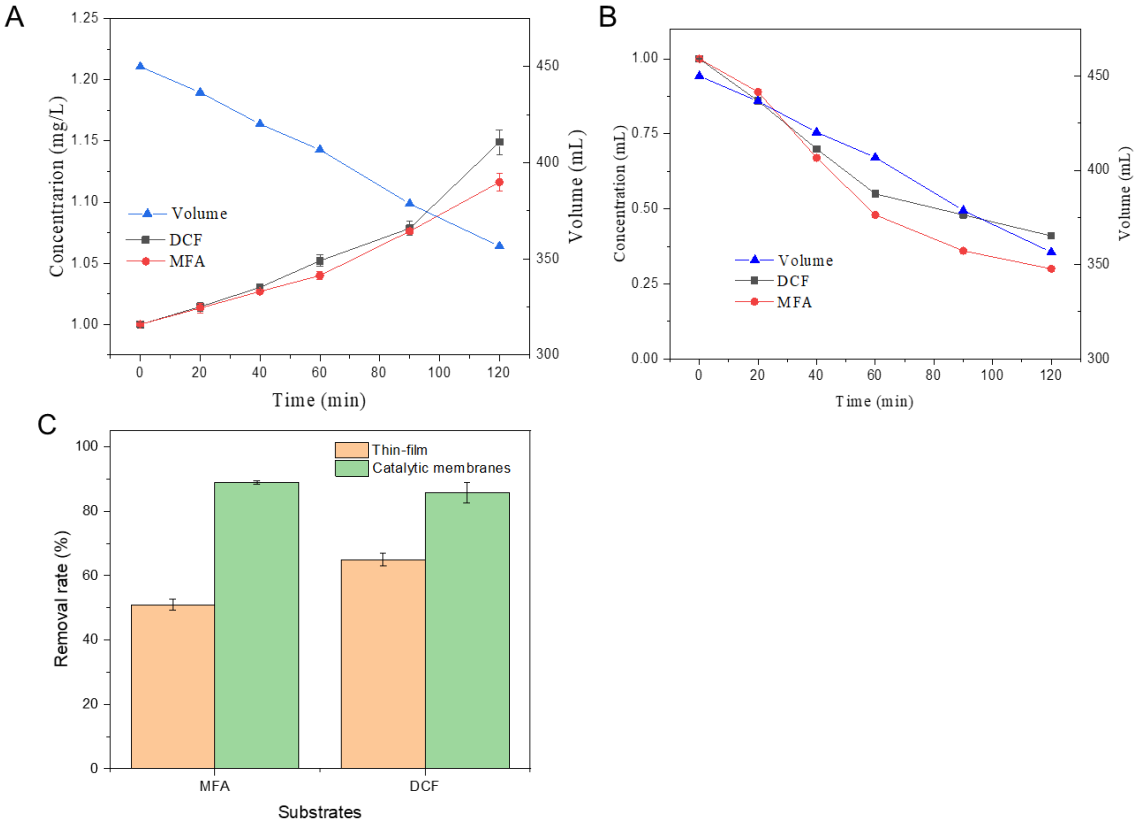

Figure 3.4 CECs concentrations in the retentate A) with a TFC membrane, B) with a TFC and catalytic membrane. C) CECs depletion in the permeate.

3.6 Conclusions

Laccase immobilization onto functionalized PAN/β-CD NFMs was successfully achieved, and the potential of using biocatalytic NFMs for CECs depletion was investigated. The findings suggested that incorporating β-cyclodextrin into the fibers and introducing –OH and –NH_2 functional groups onto the membrane surface could enhance the enzymatic activity of the membranes. Furthermore, the enzyme immobilization process was found to promote the biocatalyst performance, broadening the range of pH and improving the thermal tolerance of immobilized enzymes, which indicates a great potential for industrial application. Additionally, compared to free enzymes, the ability to recycle biocatalysts offers an economic advantage due to the high cost of bio-catalyst production. Our work demonstrates the feasibility of applying laccase-immobilized membranes to filtration systems for the removal of CECs, as evidenced by the high depletion efficiency observed for two selected CECs.

4 Biodegradable Membranes for Laccase Immobilization and CECs Depletion

This chapter will implement a new material, flexible ceramic membranes, for laccase immobilization. This chapter is related to **Paper II**.

4.1 Introduction and Motivation

Inspired by earlier research, the observation that introducing β-cyclodextrin (CD) into the fibers enhanced the specific activity of enzyme-immobilized NFMs has drawn our attention. β-CD is a naturally occurring compound found in starch, characterized by a distinctive toroidal cavity with a hydrophobic interior and a hydrophilic exterior. This peculiar structure functions as a supramolecular complexation agent for a wide range of molecules, including poorly soluble drug molecules [96] and large polymer chains that form pseudorotaxanes [97]. As such, β-CD polymers have gained significant attention in research due to their high surface-to-volume ratio and high functional β-CD content, which are highly advantageous in environmental applications.

Herein, we designed insoluble biodegradable NFMs for enzyme immobilization to build a biocatalytic membrane reactor with efficient degradation performance. The biodegradable NFMs, utilizing HP-β-cyclodextrin as the primary material, citric acid as a crosslinker, and polyvinyl alcohol (PVA) as a spinning polymer, were fabricated by electrospinning followed by thermal cross-linking. The highly insoluble NFMs have a potential for laccase immobilization. This is the first study to employ scalable insoluble biodegradable cross-linked HP-β-cyclodextrin NFMs as laccase carriers for emerging contaminant transformation applications.

4.2 Experimental Design

As shown in **Figure 4.1**, the electrospun HP-β-CD NFMs were obtained by electrospinning. The spinning solutions contained different ratios of PVA, HP-β-CD, and CA. The obtained HP-β-CD membranes were thermally cross-linked at high temperatures for four hours. The cross-linked HP-β-CD membranes with different conditions are listed in **Table 4.1**. Then the membranes were soaked into a 5 mg mL^{-1} (by weight) laccase solution in 50 mM NaOAc buffer, pH 4.5, incubated for one hour at 25 °C, and then transferred to 4 °C for 2, 6, 12, and 24 h. CECs depletion experiments were individually performed by treating the membranes (36 cm^2) with a 250 mL CECs mixture with each concentration of 200 μg L^{-1} as a function of time.

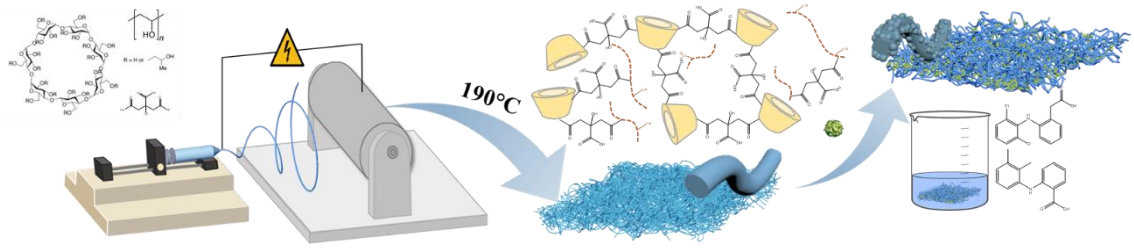

Figure 4.1 Schematic illustration of laccase-immobilized insoluble β-CD NFMs and their catalytic performance in a batch study.

The solubility experiment was conducted, where the fiber mats were soaked in 1 mM NaCl aqueous solution for 24 h. Afterward, the mats were taken out of the water and vacuum dried until a constant weight was achieved. The insoluble fraction (%) water uptake (WU) and in-plane swelling ratio (SR) was determined as follows:

$$\text{Insoluble fraction}(\%) = \frac{W_i}{W_0} \times 100\% \quad (8)$$

$$\text{WU} = \frac{W_a - W_d}{W_d} \quad (9)$$

$$\text{SR} = \frac{L_a - L_d}{L_d} \quad (10)$$

Where,

W_0, W_i : the fiber weight of initial and after drying, [mg]

W_a, W_d : the weight of wet and dry fibers, [mg]

L_a and L_d : the length of the wet and dry membranes, [cm]

4.3 Membrane Characterization

Figures 4.3A-B depict the morphology of HP-β-CD and cross-linked NFMs. The ribbon structure of the HP-β-CD nanofibers was noticed, and the surface of the NFMs was smooth without any apparent porous textures, suggesting steady water evaporation during the electrospinning. No significant difference in fiber diameter was observed before and after thermal crosslinking. The average diameters of HP-β-CD and cross-linked NFMs are 883 ± 58 nm and 850 ± 103 nm. The success of the cross-linking process was validated through stability tests in water (**Figure 4.2C**). Upon contact with water, HP-β-CD rapidly dissolved, while the cross-linked fibers remained insoluble, demonstrating their enhanced stability. Additionally, pH was found that influence the membrane morphology.

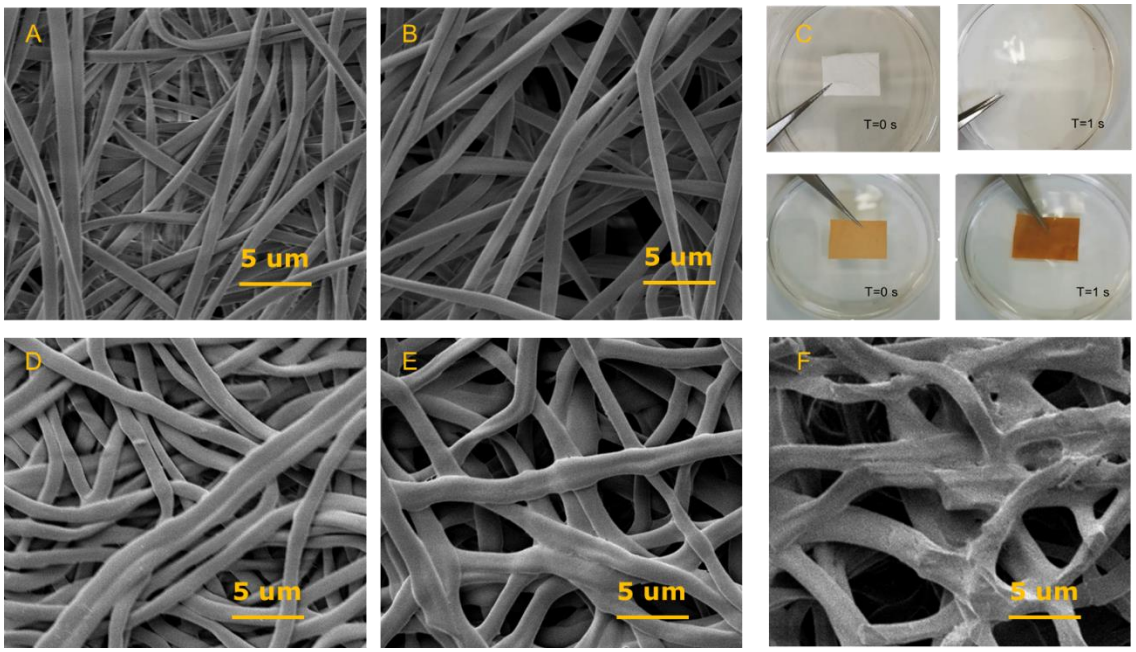

Figure 4.2 Characterization of HP-β-CD and cross-linked NFMs. A-B) SEM images of β-CD NFMs before and after thermal treatment. C) Water treatment of HP-β-CD and cross-linked NFMs. D-F) SEM images of cross-linked HP-β-CD NFMs after 24 h treatment in aqueous solutions with different pH at 4.5, 7, and 9.

Figures 4.2D-F depict that the cross-linked NFMs maintained their structure in an acidic or moderate pH. In contrast, the NFMs poorly maintained their shapes in an alkaline condition, where breakage, defects, and frizziness were observed. In addition, a noticeable increase in the fiber diameter was observed with the raising of pH values, whereas the fibers aggregated owing to their hydrophilic nature. The fiber diameter distribution treated in pH 4.5, 7, and 9,

compared with the pristine NFMs (850 ± 103 nm), was 1065 ± 75 nm, 1570 ± 406 nm, and 1593 ± 251 nm. The percentage increase of average fiber diameter with different pH at 4.5, 7, and 9 were determined as 0.26, 0.85, and 0.87, correspondingly. It should be noticed that the swelling ratio of cross-linked NFMs was as high as 0.26 ± 0.02. Therefore, it is difficult to fit these NFMs into a membrane mold.

4.4 Enzyme Characterization

High enzyme activity of fiber (A_{fiber}) loss, correlated to reaction time, is observed on cross-linked NFMs. Nonetheless, the apparent activity of cross-linked fibers only reached 3% of the total activity input, as shown in **Figure 4.3A**. A possible reason for the high activity loss may be the unreacted citric acid released from the fibers, resulting in a pH shift in the residue solution. Immobilized laccase on the cross-linked NFMs exhibited a potential for repeated use. The fibers maintained over 80% of initial activity after three-time testing. However, during the fierce washing process, fractions of fibers were washed off and left in the washing solution, leading to a sharp drop in fiber activity (**Figure 4.3B**).

Figures 4.3D-E illustrate the impact of pH and thermal treatment on free and immobilized laccase on cross-linked NFMs. The optimum pH values of the free and immobilized laccase were found to be 4.5 and 5.0, respectively. This shift in optimum pH towards a higher value, in agreement with the literature [98], may be attributed to the presence of acidic cross-linkers in the NFMs, resulting in the surface of the support being more acidic than the buffer solution. The enzyme immobilization resisted enzyme denaturation, with the immobilized laccase retaining more than 30% of its optimal activity at a wider range of pH values. Improved thermal stability was also observed where the residual activity of immobilized laccase was 72.5 ± 3.1% as compared to 50.7 ± 0.4% for free laccase after heating for 120 min at 50 °C.

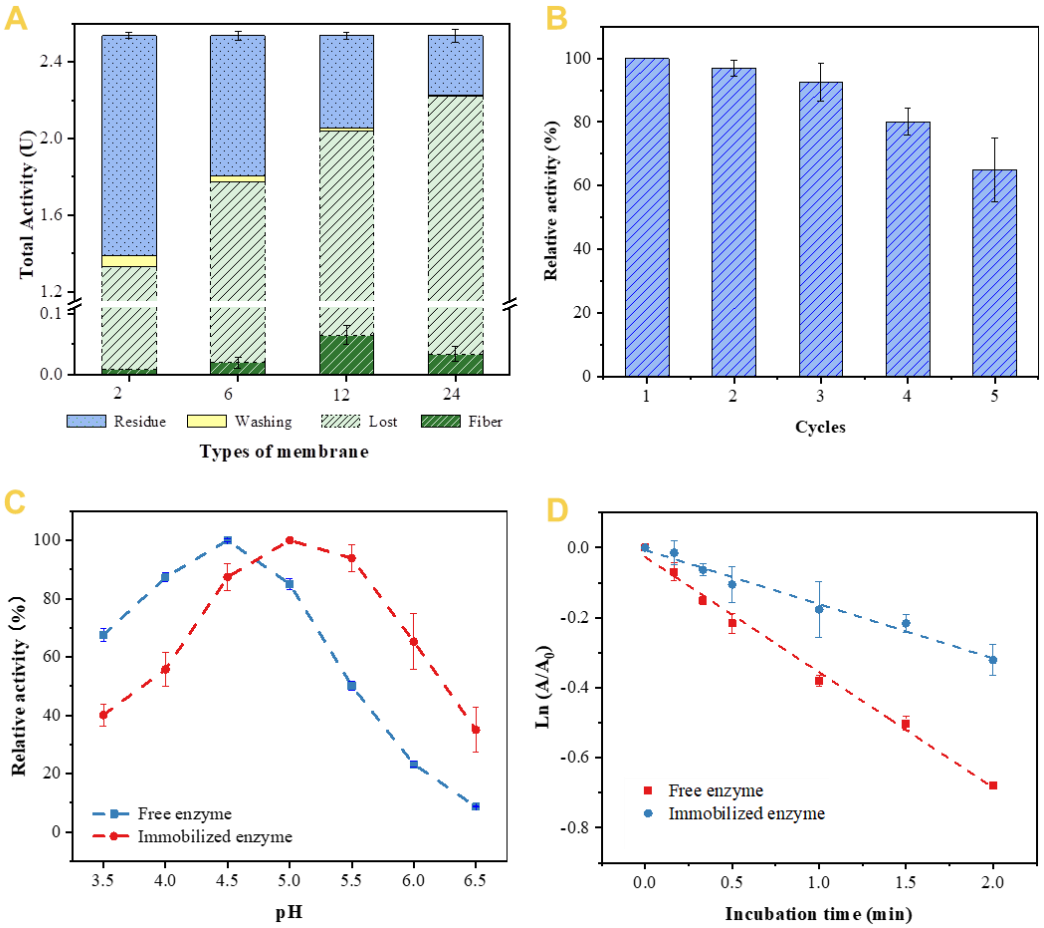

Figure 4.3 A) Total enzyme activity in the residue solution, washing buffer, immobilized fibers, and the calculated lost activity with different immobilization times. B) Relative activity of laccase-immobilized NFMs with recycling usage. C) The pH-dependent relative activity of Lac-C2-190 NFMs and free laccase. D) Thermal inactivation kinetics of Lac-C2-190 NFMs and free laccase.

4.5 Enzymatic membrane system performance

The cross-linked HP-β-CD NFMs have shown a certain degree of depletion outcomes on both CECs due to the adsorption properties. Within three hours, about 20% and 56% of DCF and MFA were removed, whereas the biocatalytic membranes largely enhanced the depletion performance to 60% and 89%, correspondingly (**Figures 4.4A-B**). Additionally, up to 90% of the initial depletion efficiency was retained three times of reuse on both CECs (**Figures 4.4C-D**).

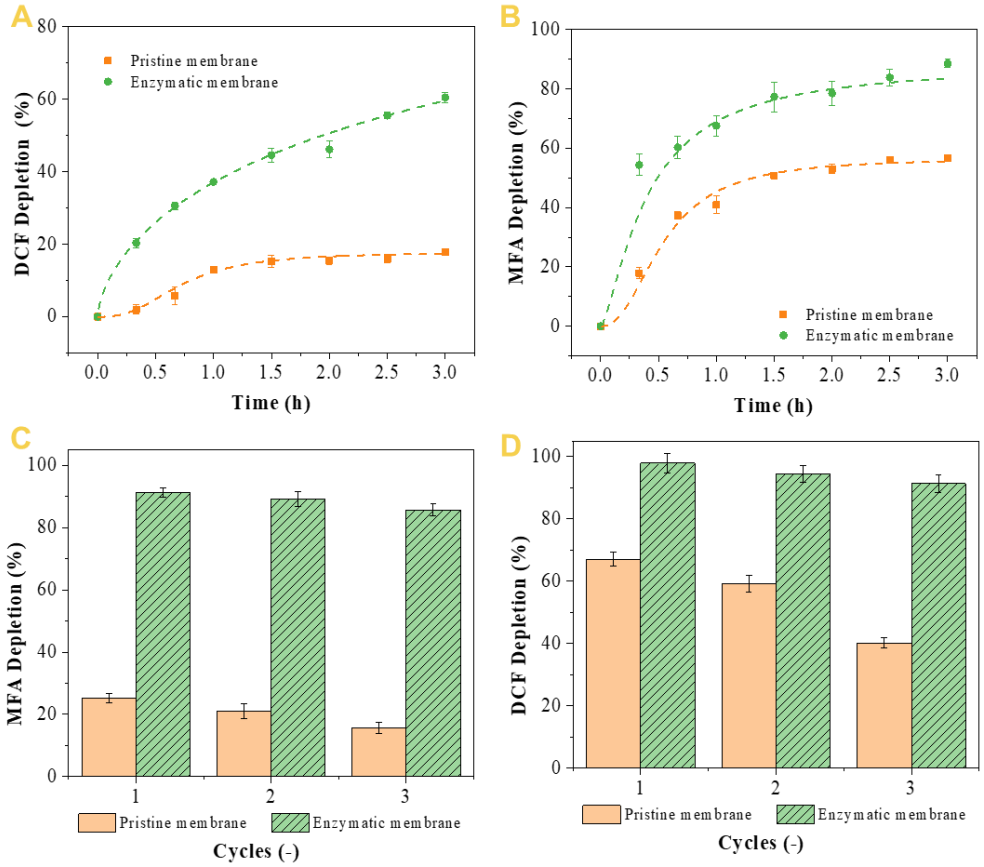

Figure 4.4 Membrane depletion efficiency of A) DCF, B) MFA; Depletion efficiency of the reused membrane of C) DCF, D) MFA.

4.6 Conclusions

We successfully produced biodegradable cross-linked β-cyclodextrin NFMs. These membranes possessed high insolubility and could resist different solvents such as water, ethanol, DMAc, and n-hexane, indicating their potential applications in various fields. We also investigated the catalytic activities of immobilized laccase using these NFMs as enzyme carriers. The results showed that the immobilized laccase had better stability compared to the free enzyme, particularly with higher resistance towards neutral pH, making it suitable for industrial applications. However, we need to consider their key features before applying these NFMs, particularly their high water uptake and swelling ratio, which suggests that batch reactors with full contact with substrate compounds may be more appropriate than fixed membrane modules. These biodegradable NFMs offer a solution to the environmental issue of disposing of contaminated polymeric modules as plastic waste. Overall, our study demonstrates a promising potential for using biodegradable NFMs for CECs treatment.

5 Ceramic Membranes for Laccase Immobilization and CECs Depletion

This chapter will implement a new material, flexible ceramic membranes, for laccase immobilization. This chapter is related to **Paper III**.

5.1 Introduction and Motivation

As discussed in **Chapters 3** and **4**, polymeric membranes are widely used owing to their easy processability and low manufacturing cost. However, it is important to consider environmental and economic factors when disposing of these membranes or recycling them. As a result, there has been a push to reduce the use of non-biodegradable polymers and explore alternative materials like biodegradable polymers and inorganic materials. Nevertheless, inorganic membranes often have drawbacks such as being expensive, difficult to prepare, brittle, and rigid, which limit their practical use [99]. A novel flexible self-standing ceramic nanofiber membrane was fabricated by electrospinning for the first time in 2002 [100], and subsequent studies have revealed the relationship between length-to-diameter ($L\ D^{-1}$) ratios and the flexibility of the nanofibers [101]. The superior flexibility of ceramic membranes has promoted applications in various fields of thermal insulation [102], sensors [103], and battery separators [104], but rarely in water treatment.

In this study, we presented a simple and effective method for flexible ceramic membrane fabrication and applied the materials as enzyme carriers in water treatment. Our approach involved a one-step co-deposition process using polydopamine (PDA) and polyethyleneimine (PEI). To the best of our knowledge, this is the first report on the development of highly flexible and efficient biocatalytic ceramic membranes that can be readily scaled up for the removal of emerging contaminants

5.2 Experimental Design

As shown in **Figure 5.1**, the electrospun flexible ceramic membranes are obtained by the sol-gel method by following steps: 1) Preparation of a spinning solution containing poly(vinyl alcohol) (PVA) and tetraethyl orthosilicate (TEOS); 2) Electrospinning the solution into ceramic precursor fibers; 3) Calcination at high temperature in order to eliminate the organic components. Three different approaches were used to functionalize SiO_2 NFMs. These included silanization treatment, dopamine coating, and co-deposition of PDA and PEI. After the treatment, the resulting NFMs were designated as SiO_2-SA, SiO_2-PD, and SiO_2-PE, respectively. The functionalized membranes were then washed with water and dried overnight at 40 °C. Following this, the membranes were immersed in a laccase solution in 50 mM NaOAc buffer (pH 4.5) for one hour at 25 °C and transferred to 4 °C for 24 h. Finally, the resulting biocatalytic membranes were tested in a dead-end filtration membrane cell.

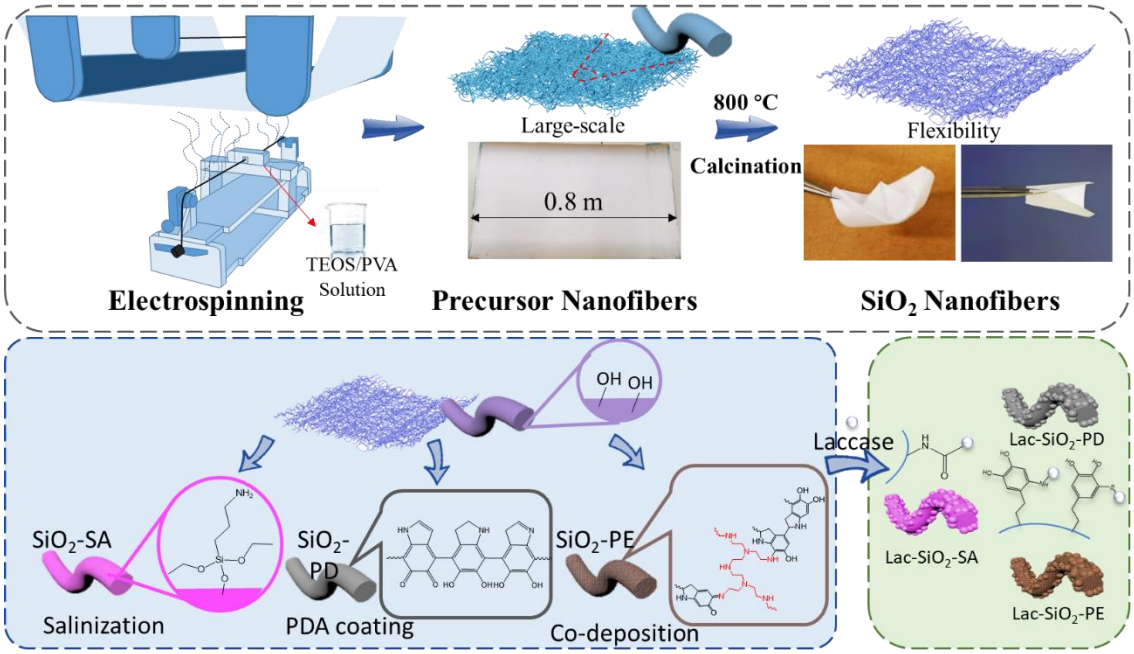

Figure 5.1 Schematic illustration of laccase-immobilized SiO_2 NFMs preparation.

5.3 Membrane Characterization

Figures 5.2a-d depict the morphology of calcined SiO_2, SiO_2-SA, SiO_2-PD, and SiO_2-PE NFs. SiO_2 calcined fibers were smooth and uniform in a narrower fiber diameter distribution at 168 ± 40 nm (**Figure 5.2e**). The surface morphology of SiO_2-SA exhibited the existence of thin films in between fibers. In comparison to silanization, both the dopamine coating and co-deposition methods introduced particles onto the surfaces of the fibers, thus elevating the roughness of the nanofibers. Furthermore, the inclusion of PEI also affected the development of PDA aggregates. According to previous reports, PEI can form covalent bonds with the phenyl group of dopamine, which in turn hinders the PDA from self-aggregating. This impacts the composition and morphology of the NFMs [105].

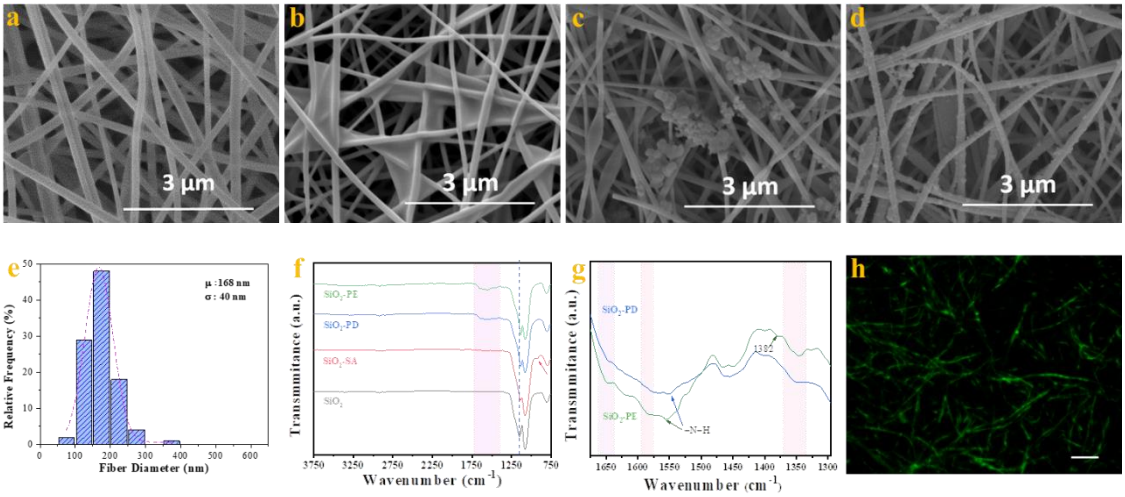

Figure 5.3. a-d) SEM image of SiO_2, SiO_2-SA, SiO_2-PD, and SiO_2-PE NFMs. e) Fiber diameter distribution of calcined SiO_2 nanofibers. f-g) Cross-section SEM image of precursor nanofiber membrane and calcined SiO_2 nanofiber membrane. h) LCSM image of Lac-SiO_2-PE. The green fluorescence signal is from fluorescence-labeled enzymes. The scale of the unlabeled bar is 10 µm.

Figures 5.2f-g reveal differences between the electrospun fibers before and after surface functionalization. Compared to the pristine SiO_2 membrane, SiO_2-SA showed a new band at 922 cm^{-1}, indicating the presence of Si−O and amino groups due to APTES conjugation. The characteristic shoulder peak of PDA at 1351 cm^{-1} in both SiO_2-PD and SiO_2-PE spectra was assigned to indole ring CNC stretching. Successful grafting of PEI onto the membrane was confirmed by a characteristic peak at 1382 cm^{-1} attributed to CH_2 bending. To visualize

the distribution of immobilized laccase on SiO_2-PE NFMs, laccase was fluorescence-labeled before immobilization, and confocal laser scanning microscopy was employed. **Figure 5.2h** displays an ultrafine fiber that emits green fluorescence when exposed to excitation light. It is clear from the observation that the process of immobilization led to a uniform distribution of laccase molecules on the surfaces of the fiber.

5.4 Enzyme characterizations

Figure 5.3a shows fiber-dependent changes in protein amount distribution. The pristine SiO_2, SiO_2-SA, SiO_2-PD, and SiO_2-PE NFMs could achieve 24.9%, 7%, 30%, and 57.9% of the total protein immobilized onto the fibers, respectively. A similar finding was observed in **Figure 5.4b** that the SiO_2-PE NFMs showed the highest specific activity of fibers (6.4 ± 1.1 U g^{-1} membrane), indicating that more enzymes were immobilized on the same weight of membrane pieces. While there were slight differences in the functionalized NFMs, the specific activity of the immobilized enzymes was the most notable distinction. The highest value was obtained by SiO_2-PE NFMs, which was 0.53 ± 0.09 U mg^{-1}enzyme.

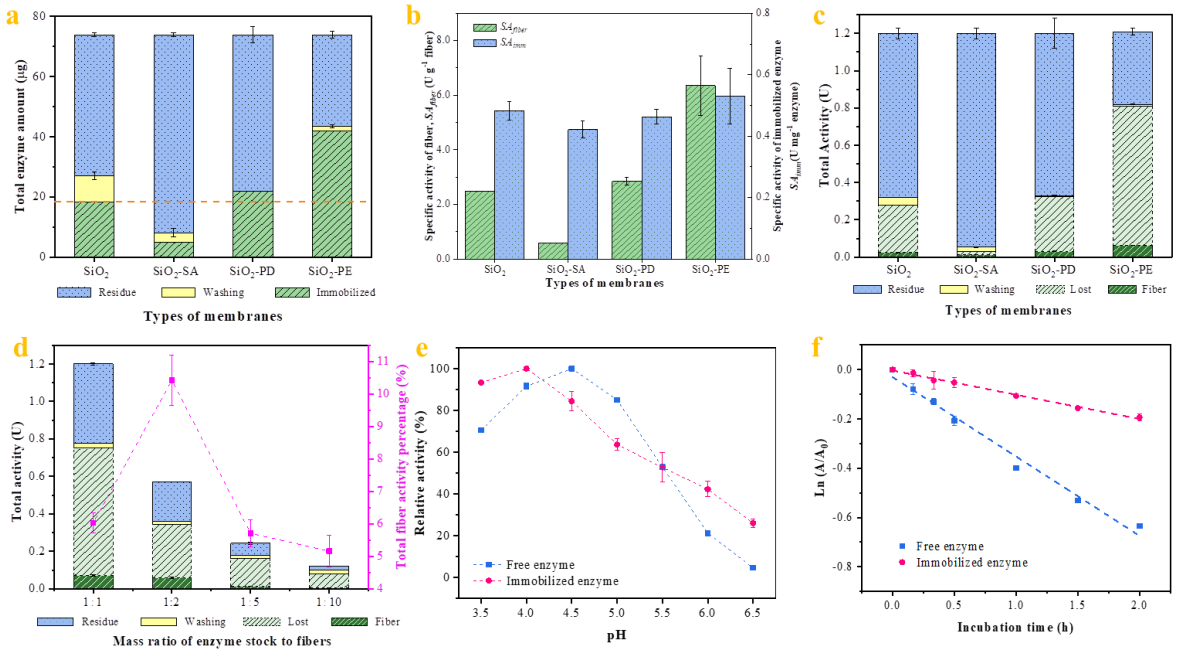

Figure 5.3 a) Enzyme amount distribution in residue solution, washing buffers and immobilized fiber during the immobilization b) Specific activity of fiber (SA_{fiber}) and specific activity of immobilized laccase (SA_{imm}) on different fibrous membranes. c-d) Total residue activity in the residue solution, washing

buffer, immobilized fibers, and the calculated lost activity with different NFMs and mass ratios of enzyme stock. e) The pH-dependent relative activity of Lac-SiO_2-PE NFMs and free laccase. f) Thermal inactivation kinetics of Lac-SiO_2-PE NFMs and free laccase.

SiO_2-PE NFMs showed a correlation between high protein load and high enzyme activity loss of fiber (A_{fiber}). Despite this, the membrane type still exhibited the highest enzyme activity of fiber (6.4 ± 1.1 U g^{-1} membrane), which was only 6% of the total activity, as illustrated in **Figure 5.3c**. The decrease in activity could potentially be attributed to the crowding of immobilized enzymes on the fibers, as indicated by the findings in **Figure 5.3d**. When the enzyme load was reduced by 50%, the fiber could maintain 80% of its activity, resulting in a decrease in activity losses from 56% to 47%. Thus it is crucial to optimize the enzyme load on the fiber in order to achieve maximum yield of immobilized active enzyme per unit mass of membrane.

Figures 5.3e-f describe the effect of pH and thermal treatment on free and immobilized laccase on SiO_2-PE NFMs. The immobilized laccase exhibited optimal activity retention of over 40% within a wider pH range compared to the free enzyme. The optimal pH value of the free and immobilized laccase was 4.5 and 4.0, respectively. This apparent pH shift, in accordance with the literature [106], might be due to the high charge density of SiO_2-PE NFMs changing the microenvironment around the enzyme. Furthermore, the thermal stability of the immobilized laccase was observed to be improved, as evidenced by the retention of 82.4 ± 1.2% of residual activity after heating for 120 min at 50 °C, in comparison to only 53.0 ± 0.01% for the free laccase.

5.5 Enzymatic membrane system performance

As illustrated in **Figure 5.4a**, the control membrane demonstrated adsorption properties for selected CECs, in particular clarithromycin and bicalutamide, as evidenced by the ability of both mentioned CECs to achieve over 70% depletion. The biocatalytic membrane was found to further enhance the depletion of CECs, and promising depletion outcomes (≥95%) for selected EPs were achieved. Notably, Lac-SiO_2-PE NFMs showed stable performance for the selected EPs, with transformation efficiency maintained above 90% even after being reused three times (**Figure 5.4b**).

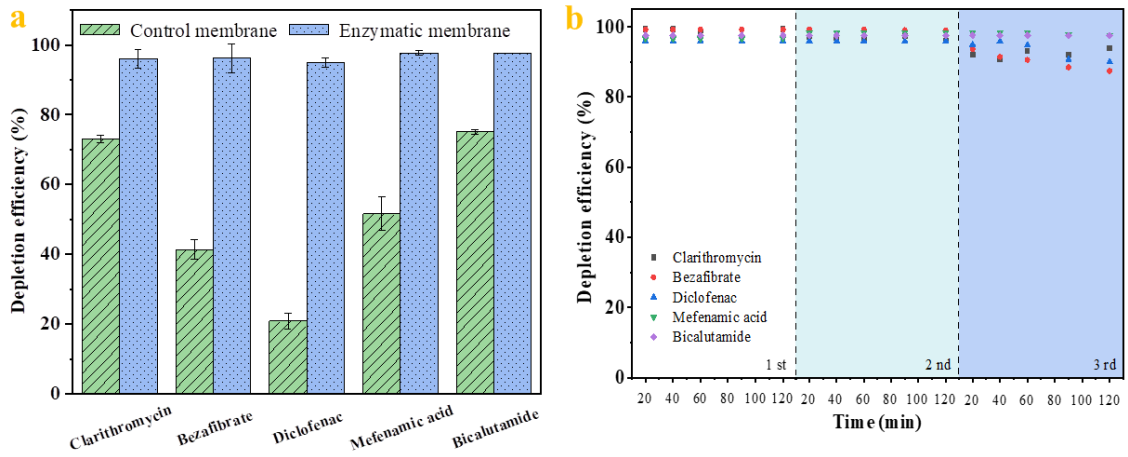

Figure 4.4 Membrane performance on EPs removal. a) Depletion efficiency by control membranes and lac-SiO_2 NFMs. b) Cycling performance of lac-SiO_2 NFMs.

5.6 Conclusions

Our work presented a simple method to fabricate scalable and flexible ceramic membranes, overcoming the bottlenecks of conventional ceramic membranes, including brittleness and complex production procedures. Further, laccases were successfully immobilized onto functionalized SiO_2 NFMs. It was found that the biocatalyst's performance in terms of loading and stability was significantly impacted by both the immobilization procedure and the properties of the immobilized support. Our findings revealed that the Lac-SiO_2-PE NFMs enabled high protein loading (57.9 ± 0.5%), improved stability compared to the free enzyme, and allowed for biocatalyst recycling. The study also highlighted the promising potential of Lac-SiO_2-PE NFMs in addressing the environmental issue of discarding contaminated polymeric modulus through the reuse of biocatalytic membranes. Overall, we demonstrate the potential of flexible ceramics in membrane filtration for environmental remediation purposes.

6 Conclusion and Future Perspective

The thesis was motivated by the increasing demand for advanced treatment technologies to reduce the discharge of CECs from WWTPs. Based on Papers I-III, the focus was on creating new materials, ranging from polymers to ceramics, to serve as carriers for enzymes, investigating their catalytic performance, and demonstrating the potential of using laccase-immobilized membranes in water treatment. The main findings are summarized below:

1. PAN/β-CD NFMs were fabricated and designed for laccase immobilization. The addition of β-CD into the M3 NFMs led to the highest specific activity of 7.1 ± 0.5 U g^{-1}_{fiber} and improved stability compared to the free enzyme. We successfully demonstrated the feasibility of applying laccase-immobilized membranes in a cross-flow filtration system, which led to high depletion efficiency for two common CECs. Our research is the first to investigate the laccase-immobilized membrane, together with a thin-film composite membrane, in this area.

2. Building on the previous work, we studied and characterized cross-linked insoluble β-CD NFMs. Cross-linked β-CD NFMs, used in laccase immobilization, have several advantages, including high tolerance in acidic conditions and are an environmentally-friendly biodegradable material. However, the main challenges were their high swelling degree and water uptake. To meet the feasibility of real-scale treatment, specific efforts were directed towards this, prioritizing them over ongoing laboratory-scale studies.

3. We fabricated functionalized SiO_2 NFMs and used them for enzyme immobilization for the first time. The results showed that the immobilization procedure and the properties of the immobilized support significantly affected the biocatalyst performance in terms of loading and stability. Our research successfully attained a high protein load (57.9 ± 0.5%) and enhanced stability, while also demonstrating the recyclability of the membrane carrier. In summary, our findings underscored the promising potential of enzyme-immobilized ceramics in the removal of EPs during wastewater treatment. The straightforward method employed to fabricate scalable and flexible ceramic membranes in our study overcomes the challenges posed by traditional ceramic membranes, including brittleness and a complicated production process.

Nanostructured materials incorporated with immobilized enzymes have shown significant potential for enzymatic wastewater treatment technology. However, there is still a long way to go before practical applications can be achieved. Large-scale production of enzymes is critical for making biocatalysts more commercially viable and cost-effective. However, this process involves various complexities, such as production, separation, and purification. The lack of commercial availability of enzymes presents significant technical and economic challenges to large-scale enzymatic treatment processes. While recombinant DNA technology could be a potential solution to reduce costs, it has not yet been widely implemented at the industrial level.

One of the challenges in using enzymes for wastewater treatment is the unknown products of enzymatic reactions in a complex environment. Many studies focused on removing a specific pollutant from a synthetic solution. Although the toxicity of pollutants like diclofenac and naproxen was shown to be reduced after laccase treatment, in some cases, the products of enzymatic reactions could be more toxic than the original compounds, which defeats the purpose of water treatment. For example, adding syringaldehyde to laccase treatment of a broad range of antibiotics resulted in a time-dependent increase in toxicity [107]. Another challenge is the disposal of membrane carriers. Although immobilization extends enzyme stability and reusability, the lifetime of modules is limited by the decay of the immobilized enzyme. Therefore, the practical application of immobilized enzymes in large-scale industrial processes can be facilitated by the ability to reuse the polymeric support once the enzyme becomes inactive. Reversible covalent immobilization of enzymes can be investigated in the future [108].

In addition to these challenges, many current studies deal with high concentrations of contaminants, whereas most environmental compartments typically have much lower concentrations in the range of ng to $\mu g \cdot L^{-1}$. This creates difficulties in transferring experimental results to practical applications, particularly in WWTPs. To overcome this challenge, two strategies are proposed: 1) Onsite WWTPs can be implemented at point sources, such as hospitals and pharmaceutical industries, where contaminant concentrations are high; 2) Enzymatic treatment of contaminants can be used as a treatment process for concentrated wastewater streams. However, pre-treatment steps, such as FO, UF, and RO, are required to concentrate contaminants.

Hence, an environmentally friendly and cost-effective enzymatic treatment for WWTPs requires much more in-depth research.

7 References

[1] R.B. Jackson, S.R. Carpenter, C.N. Dahm, D.M. McKnight, R.J. Naiman, S.L. Postel, S.W. Running, Water in a Changing World, Ecol. Appl. 11 (2001) 1027–1045. doi:https://doi.org/10.1890/1051-0761(2001)011[1027:WIACW]2.0.CO;2.

[2] R. Schwarzenbach, B. Escher, K. Fenner, T. Hofstetter, C. Johnson, U. von Gunten, B. Wehrli, The Challenge of Micropollutants, Sci. Technol. 313 (2006) 1072–1077. doi:10.1126/science.1127291.

[3] WWDR, 2018 UN World Water Development Report, Nature-based Solutions for Water, (2018).

[4] P. Burek, Y. Satoh, G. Fischer, M.T. Kahil, A. Scherzer, S. Tramberend, L.F. Nava, Y. Wada, S. Eisner, M. Flörke, Water futures and solution-fast track initiative, (2016).

[5] R. Connor, A. Renata, C. Ortigara, E. Koncagül, S. Uhlenbrook, B.M. Lamizana-Diallo, S.M. Zadeh, M. Qadir, M. Kjellén, J. Sjödin, The united nations world water development report 2017. wastewater: the untapped resource, United Nations World Water Dev. Rep. (2017).

[6] C. Wang, H. Wang, J. Fu, Y. Liu, Flotation separation of waste plastics for recycling—A review, Waste Manag. 41 (2015) 28–38.

[7] C.K. Mbamba, X. Flores-Alsina, D.J. Batstone, S. Tait, Validation of a plant-wide phosphorus modelling approach with minerals precipitation in a full-scale WWTP, Water Res. 100 (2016) 169–183.

[8] R. Guillossou, J. Le Roux, R. Mailler, E. Vulliet, C. Morlay, F. Nauleau, J. Gasperi, V. Rocher, Organic micropollutants in a large wastewater treatment plant: what are the benefits of an advanced treatment by activated carbon adsorption in comparison to conventional treatment?, Chemosphere. 218 (2019) 1050–1060.

[9] S. Kwon, E. Moon, T.-S. Kim, S. Hong, H.-D. Park, Pyrosequencing demonstrated complex microbial communities in a membrane filtration system for a drinking water treatment plant, Microbes Environ. 26 (2011) 149–155.

[10] G. Crini, E. Lichtfouse, Advantages and disadvantages of techniques used for wastewater treatment, Environ. Chem. Lett. 17 (2019) 145–155.

[11] L. Wiest, A. Gosset, A. Fildier, C. Libert, M. Hervé, E. Sibeud, B. Giroud, E. Vulliet, T. Bastide, P. Polomé, Y. Perrodin, Occurrence and removal of emerging pollutants in urban sewage treatment plants using LC-QToF-MS suspect screening and quantification, Sci. Total Environ. 774 (2021) 145779. doi:10.1016/J.SCITOTENV.2021.145779.

[12] Y. Tang, M. Yin, W. Yang, H. Li, Y. Zhong, L. Mo, Y. Liang, X. Ma, X. Sun, Emerging pollutants in water environment: Occurrence, monitoring, fate, and risk assessment, Water Environ. Res. 91 (2019) 984–991.

[13] G. Crini, E. Lichtfouse, Wastewater treatment: an overview, Green Adsorbents Pollut. Remov. Fundam. Des. (2018) 1–21.

[14] L. Wiest, A. Gosset, A. Fildier, C. Libert, M. Hervé, E. Sibeud, B. Giroud, E. Vulliet, T. Bastide, P. Polomé, Y. Perrodin, Occurrence and removal of emerging pollutants in urban sewage treatment plants using LC-QToF-MS suspect screening and quantification, Sci. Total Environ. 774 (2021) 145779.

doi:https://doi.org/10.1016/j.scitotenv.2021.145779.

[15] M. Cheng, G. Zeng, D. Huang, C. Lai, P. Xu, C. Zhang, Y. Liu, Hydroxyl radicals based advanced oxidation processes (AOPs) for remediation of soils contaminated with organic compounds: A review, Chem. Eng. J. 284 (2016) 582–598. doi:https://doi.org/10.1016/j.cej.2015.09.001.

[16] K.B. Tan, M. Vakili, B.A. Horri, P.E. Poh, A.Z. Abdullah, B. Salamatinia, Adsorption of dyes by nanomaterials: recent developments and adsorption mechanisms, Sep. Purif. Technol. 150 (2015) 229–242.

[17] X. Yang, R.C. Flowers, H.S. Weinberg, P.C. Singer, Occurrence and removal of pharmaceuticals and personal care products (PPCPs) in an advanced wastewater reclamation plant, Water Res. 45 (2011) 5218–5228. doi:10.1016/j.watres.2011.07.026.

[18] X. Wang, B. Liu, Q. Lu, Q. Qu, Graphene-based materials: fabrication and application for adsorption in analytical chemistry, J. Chromatogr. A. 1362 (2014) 1–15.

[19] S. Sarkar, S. Ahuja, Applications and limitations of graphene oxide for remediating contaminants of emerging concern in wastewater, in: Sep. Sci. Technol., Elsevier, 2022: pp. 209–222.

[20] C.F. de Azevedo, F.M. Machado, N.F. de Souza, L.L. Silveira, E.C. Lima, R. Andreazza, C.P. Bergamnn, Comprehensive adsorption and spectroscopic studies on the interaction of carbon nanotubes with diclofenac anti-inflammatory, Chem. Eng. J. 454 (2023) 140102.

[21] H. Cui, L. Zhang, D. Söder, X. Tang, M.D. Davari, U. Schwaneberg, Rapid and Oriented Immobilization of Laccases on Electrodes via a Methionine-Rich Peptide, ACS Catal. (2021) 2445–2453. doi:10.1021/acscatal.0c05490.

[22] J. Guo, L. Yang, Z. Gao, C. Zhao, Y. Mei, Y.Y. Song, Insight of MOF Environment-Dependent Enzyme Activity via MOFs-in-Nanochannels Configuration, ACS Catal. 10 (2020) 5949–5958. doi:10.1021/acscatal.0c00591.

[23] Z. Ren, J. Luo, Y. Wan, Highly permeable biocatalytic membrane prepared by 3D modification: Metal-organic frameworks ameliorate its stability for micropollutants removal, Chem. Eng. J. (2018). doi:10.1016/j.cej.2018.04.203.

[24] S. Kim, K.H. Chu, Y.A.J. Al-Hamadani, C.M. Park, M. Jang, D.-H. Kim, M. Yu, J. Heo, Y. Yoon, Removal of contaminants of emerging concern by membranes in water and wastewater: A review, Chem. Eng. J. 335 (2018) 896–914.

[25] J. Heo, S. Kim, N. Her, C.M. Park, M. Yu, Y. Yoon, Removal of contaminants of emerging concern by FO, RO, and UF membranes in water and wastewater, Contam. Emerg. Concern Water Wastewater. (2020) 139–176.

[26] M. Taheran, S.K. Brar, M. Verma, R.Y. Surampalli, T.C. Zhang, J.R. Valero, Membrane processes for removal of pharmaceutically active compounds (PhACs) from water and wastewaters, Sci. Total Environ. 547 (2016) 60–77. doi:10.1016/j.scitotenv.2015.12.139.

[27] M. Salamanca, R. Lopez-Serna, L. Palacio, A. Hernández, P. Prádanos, M. Pena, Study of the rejection of contaminants of emerging concern by a biomimetic aquaporin hollow fiber forward osmosis membrane, J. Water Process Eng. 40 (2021) 101914.

[28] D. Jang, S. Jeong, A. Jang, S. Kang, Relating solute properties of contaminants of emerging concern and their rejection by forward osmosis membrane, Sci. Total Environ. 639 (2018) 673–678.

[29] Z. He, Z. Lyu, Q. Gu, L. Zhang, J. Wang, Ceramic-based membranes for water and wastewater treatment, Colloids Surfaces A Physicochem. Eng. Asp. 578 (2019) 123513. doi:https://doi.org/10.1016/j.colsurfa.2019.05.074.

[30] O. Modin, F. Persson, B.-M. Wilén, M. Hermansson, Nonoxidative removal of organics in the activated sludge process, Crit. Rev. Environ. Sci. Technol. 46 (2016) 635–672.

[31] B. Zonja, S. Pérez, D. Barceló, Human Metabolite Lamotrigine-N2-glucuronide Is the Principal Source of Lamotrigine-Derived Compounds in Wastewater Treatment Plants and Surface Water, Environ. Sci. Technol. 50 (2016) 154–164. doi:10.1021/acs.est.5b03691.

[32] N.H. Tran, M. Reinhard, K.Y.-H. Gin, Occurrence and fate of emerging contaminants in municipal wastewater treatment plants from different geographical regions-a review, Water Res. 133 (2018) 182–207. doi:https://doi.org/10.1016/j.watres.2017.12.029.

[33] K. McClellan, R.U. Halden, Pharmaceuticals and personal care products in archived US biosolids from the 2001 EPA national sewage sludge survey, Water Res. 44 (2010) 658–668.

[34] P. Guerra, M. Kim, A. Shah, M. Alaee, S.A. Smyth, Occurrence and fate of antibiotic, analgesic/anti-inflammatory, and antifungal compounds in five wastewater treatment processes, Sci. Total Environ. 473–474 (2014) 235–243. doi:https://doi.org/10.1016/j.scitotenv.2013.12.008.

[35] S. Ba, L. Haroune, L. Soumano, J.-P. Bellenger, J.P. Jones, H. Cabana, A hybrid bioreactor based on insolubilized tyrosinase and laccase catalysis and microfiltration membrane remove pharmaceuticals from wastewater, Chemosphere. 201 (2018) 749–755.

[36] M. Bilal, H.M.N. Iqbal, Persistence and impact of steroidal estrogens on the environment and their laccase-assisted removal, Sci. Total Environ. 690 (2019) 447–459.

[37] A. Sharma, T. Sharma, T. Sharma, S. Sharma, S.S. Kanwar, Role of microbial hydrolases in bioremediation, Microbes Enzym. Soil Heal. Bioremediation. (2019) 149–164.

[38] P. Wu, S. Yang, Z. Zhan, G. Zhang, Origins and features of pectate lyases and their applications in industry, Appl. Microbiol. Biotechnol. 104 (2020) 7247–7260.

[39] A.T. Martínez, F.J. Ruiz-Dueñas, S. Camarero, A. Serrano, D. Linde, H. Lund, J. Vind, M. Tovborg, O.M. Herold-Majumdar, M. Hofrichter, C. Liers, R. Ullrich, K. Scheibner, G. Sannia, A. Piscitelli, C. Pezzella, M.E. Sener, S. Kılıç, W.J.H. van Berkel, V. Guallar, M.F. Lucas, R. Zuhse, R. Ludwig, F. Hollmann, E. Fernández-Fueyo, E. Record, C.B. Faulds, M. Tortajada, I. Winckelmann, J.A. Rasmussen, M. Gelo-Pujic, A. Gutiérrez, J.C. del Río, J. Rencoret, M. Alcalde, Oxidoreductases on their way to industrial biotransformations, Biotechnol. Adv. 35 (2017) 815–831. doi:10.1016/j.biotechadv.2017.06.003.

[40] L. Giorno, E. Drioli, Biocatalytic membrane reactors: applications and perspectives,

Trends Biotechnol. 18 (2000) 339–349. doi:https://doi.org/10.1016/S0167-7799(00)01472-4.

[41] L.M. Blank, B.E. Ebert, K. Buehler, B. Bühler, Redox Biocatalysis and Metabolism: Molecular Mechanisms and Metabolic Network Analysis, Antioxid. Redox Signal. 13 (2010) 349–394. doi:10.1089/ars.2009.2931.

[42] L. Arregui, M. Ayala, X. Gómez-Gil, G. Gutiérrez-Soto, C.E. Hernández-Luna, M. Herrera de los Santos, L. Levin, A. Rojo-Domínguez, D. Romero-Martínez, M.C.N. Saparrat, M.A. Trujillo-Roldán, N.A. Valdez-Cruz, Laccases: structure, function, and potential application in water bioremediation, Microb. Cell Fact. 18 (2019) 200. doi:10.1186/s12934-019-1248-0.

[43] P. Giardina, G. Sannia, Laccases: old enzymes with a promising future, Cell. Mol. Life Sci. 72 (2015) 855–856.

[44] G. Janusz, A. Pawlik, U. Świderska-Burek, J. Polak, J. Sulej, A. Jarosz-Wilkołazka, A. Paszczyński, Laccase properties, physiological functions, and evolution, Int. J. Mol. Sci. 21 (2020) 966.

[45] T. Brugnari, D.M. Braga, C.S.A. dos Santos, B.H.C. Torres, T.A. Modkovski, C.W.I. Haminiuk, G.M. Maciel, Laccases as green and versatile biocatalysts: from lab to enzyme market—an overview, Bioresour. Bioprocess. 8 (2021) 131. doi:10.1186/s40643-021-00484-1.

[46] L.P. Christopher, B. Yao, Y. Ji, Lignin biodegradation with laccase-mediator systems, Front. Energy Res. 2 (2014). doi:10.3389/fenrg.2014.00012.

[47] A. Mikolasch, F. Schauer, Fungal laccases as tools for the synthesis of new hybrid molecules and biomaterials, Appl. Microbiol. Biotechnol. 82 (2009) 605–624.

[48] J.F. Osma, J.L. Toca-Herrera, S. Rodríguez-Couto, Uses of laccases in the food industry, Enzyme Res. 2010 (2010).

[49] A.P. Virk, P. Sharma, N. Capalash, Use of laccase in pulp and paper industry, Biotechnol. Prog. 28 (2012) 21–32.

[50] S. Nisha, A. Karthick, N. Gobi, A review on methods, application and properties of immobilized enzyme, Chem. Sci. Rev. Lett. 1 (2012) 148–155.

[51] R. Campos, A. Kandelbauer, K.H. Robra, A. Cavaco-Paulo, G.M. Gübitz, Indigo degradation with purified laccases from Trametes hirsuta and Sclerotium rolfsii, J. Biotechnol. 89 (2001) 131–139.

[52] B.B. Tikhonov, E.M. Sulman, P.Y. Stadol'nikova, A.M. Sulman, E.P. Golikova, A.I. Sidorov, V.G. Matveeva, Immobilized Enzymes from the Class of Oxidoreductases in Technological Processes: A Review, Catal. Ind. 11 (2019) 251–263. doi:10.1134/S2070050419030115.

[53] S. Ul-Islam, Shahid-ul-Islam, Advanced Materials for Wastewater Treatment, John Wiley & Sons, Hoboken, NJ, USA, 2017. doi:10.1002/9781119407805.

[54] J.M. Guisan, G.F. Bickerstaff, Immobilization of enzymes and cells, Springer, 2006.

[55] P.A. Srere, K. Uyeda, Functional groups on enzymes suitable for binding to matrices, Methods Enzymol. 44 (1976) 11–19. doi:10.1016/S0076-6879(76)44004-1.

[56] M. Asgher, M. Shahid, S. Kamal, H.M.N. Iqbal, Recent trends and valorization of immobilization strategies and ligninolytic enzymes by industrial biotechnology, J.

Mol. Catal. B Enzym. 101 (2014) 56–66. doi:10.1016/j.molcatb.2013.12.016.

[57] A.C. Patel, S. Li, J.M. Yuan, Y. Wei, In situ encapsulation of horseradish peroxidase in electrospun porous silica fibers for potential biosensor applications, Nano Lett. 6 (2006) 1042–1046. doi:10.1021/nl0604560.

[58] S.M. Lee, S. Nair, H.K. Ahn, B.S. Kim, S.H. Jun, H.J. An, E. Hsiao, S.H. Kim, Y.M. Koo, J. Kim, Property control of enzyme coatings on polymer nanofibers by varying the conjugation site concentration, Enzyme Microb. Technol. 47 (2010) 216–221. doi:10.1016/j.enzmictec.2010.07.011.

[59] O. Barbosa, C. Ortiz, Á. Berenguer-Murcia, R. Torres, R.C. Rodrigues, R. Fernandez-Lafuente, Glutaraldehyde in bio-catalysts design: A useful crosslinker and a versatile tool in enzyme immobilization, RSC Adv. 4 (2014) 1583–1600. doi:10.1039/c3ra45991h.

[60] B.C. Kim, S. Nair, J. Kim, J.H. Kwak, J.W. Grate, S.H. Kim, M.B. Gu, Preparation of biocatalytic nanofibres with high activity and stability via enzyme aggregate coating on polymer nanofibres, Nanotechnology. 16 (2005). doi:10.1088/0957-4484/16/7/011.

[61] S.-H. Jun, M.S. Chang, B.C. Kim, H.J. An, D. Lopez-Ferrer, R. Zhao, R.D. Smith, S.-W. Lee, J. Kim, Trypsin Coatings on Electrospun and Alcohol-Dispersed Polymer Nanofibers for a Trypsin Digestion Column, Anal. Chem. 82 (2010) 7828–7834. doi:10.1021/ac101633e.

[62] C. Işik, G. Arabaci, Y.I. Doğaç, İ. Deveci, M. Teke, Synthesis and characterization of electrospun PVA/Zn2+ metal composite nanofibers for lipase immobilization with effective thermal, pH stabilities and reusability, Mater. Sci. Eng. C. 99 (2019) 1226–1235.

[63] Q.-G. Xiao, X. Tao, H.-K. Zou, J.-F. Chen, Comparative study of solid silica nanoparticles and hollow silica nanoparticles for the immobilization of lysozyme, Chem. Eng. J. 137 (2008) 38–44.

[64] R.-S. Juang, F.-C. Wu, R.-L. Tseng, Use of chemically modified chitosan beads for sorption and enzyme immobilization, Adv. Environ. Res. 6 (2002) 171–177.

[65] B. Thangaraj, P.R. Solomon, Immobilization of lipases–a review. Part I: enzyme immobilization, ChemBioEng Rev. 6 (2019) 157–166.

[66] X. Ma, H. Sui, Q. Yu, J. Cui, J. Hao, Silica capsules templated from metal–organic frameworks for enzyme immobilization and catalysis, Langmuir. 37 (2021) 3166–3172.

[67] C.-H. Lee, T.-S. Lin, C.-Y. Mou, Mesoporous materials for encapsulating enzymes, Nano Today. 4 (2009) 165–179. doi:10.1016/J.NANTOD.2009.02.001.

[68] P. Wang, Nanoscale biocatalyst systems, Curr. Opin. Biotechnol. 17 (2006) 574–579. doi:10.1016/J.COPBIO.2006.10.009.

[69] C. Chao, J. Liu, J. Wang, Y. Zhang, B. Zhang, Y. Zhang, X. Xiang, R. Chen, Surface modification of halloysite nanotubes with dopamine for enzyme immobilization, ACS Appl. Mater. Interfaces. 5 (2013) 10559–10564. doi:10.1021/am4022973.

[70] Z.G. Wang, J.Q. Wang, Z.K. Xu, Immobilization of lipase from Candida rugosa on electrospun polysulfone nanofibrous membranes by adsorption, J. Mol. Catal. B Enzym. 42 (2006) 45–51. doi:10.1016/j.molcatb.2006.06.004.

[71] J. Zdarta, K. Jankowska, K. Bachosz, E. Kijeńska-Gawrońska, A. Zgoła-Grześkowiak, E. Kaczorek, T. Jesionowski, A promising laccase immobilization using electrospun materials for biocatalytic degradation of tetracycline: Effect of process conditions and catalytic pathways, Catal. Today. (2019). doi:10.1016/J.CATTOD.2019.08.042.

[72] Q. Fu, X. Wang, Y. Si, L. Liu, J. Yu, B. Ding, Scalable Fabrication of Electrospun Nanofibrous Membranes Functionalized with Citric Acid for High-Performance Protein Adsorption, ACS Appl. Mater. Interfaces. 8 (2016) 11819–11829. doi:10.1021/acsami.6b03107.

[73] H. Shan, Y. Si, J. Yu, B. Ding, Facile access to highly flexible and mesoporous structured silica fibrous membranes for tetracyclines removal, Chem. Eng. J. 417 (2021) 129211. doi:10.1016/J.CEJ.2021.129211.

[74] S.X. Wang, C.C. Yap, J. He, C. Chen, S.Y. Wong, X. Li, Electrospinning: A facile technique for fabricating functional nanofibers for environmental applications, Nanotechnol. Rev. 5 (2016) 51–73. doi:10.1515/ntrev-2015-0065.

[75] R. Xu, Q. Zhou, F. Li, B. Zhang, Laccase immobilization on chitosan/poly(vinyl alcohol) composite nanofibrous membranes for 2,4-dichlorophenol removal, Chem. Eng. J. (2013). doi:10.1016/j.cej.2013.02.074.

[76] W.-C. Lee, K.-B. Kim, N.G. Gurudatt, K.K. Hussain, C.S. Choi, D.-S. Park, Y.-B. Shim, Comparison of enzymatic and non-enzymatic glucose sensors based on hierarchical Au-Ni alloy with conductive polymer, Biosens. Bioelectron. 130 (2019) 48–54.

[77] J. Hou, G. Dong, Y. Ye, V. Chen, Enzymatic degradation of bisphenol-A with immobilized laccase on TiO2 sol-gel coated PVDF membrane, J. Memb. Sci. (2014). doi:10.1016/j.memsci.2014.06.027.

[78] M. Taheran, M. Naghdi, S.K. Brar, E.J. Knystautas, M. Verma, R.Y. Surampalli, Covalent Immobilization of Laccase onto Nanofibrous Membrane for Degradation of Pharmaceutical Residues in Water, ACS Sustain. Chem. Eng. 5 (2017) 10430–10438. doi:10.1021/acssuschemeng.7b02465.

[79] R. Xu, J. Cui, R. Tang, F. Li, B. Zhang, Removal of 2,4,6-trichlorophenol by laccase immobilized on nano-copper incorporated electrospun fibrous membrane-high efficiency, stability and reusability, Chem. Eng. J. 326 (2017) 647–655. doi:10.1016/j.cej.2017.05.083.

[80] Y. Dai, J. Niu, L. Yin, J. Xu, J. Xu, Laccase-carrying electrospun fibrous membrane for the removal of polycyclic aromatic hydrocarbons from contaminated water, Sep. Purif. Technol. 104 (2013) 1–8. doi:10.1016/J.SEPPUR.2012.11.013.

[81] R. Xu, Y. Si, X. Wu, F. Li, B. Zhang, Triclosan removal by laccase immobilized on mesoporous nanofibers: Strong adsorption and efficient degradation, Chem. Eng. J. 255 (2014) 63–70. doi:10.1016/j.cej.2014.06.060.

[82] J. Zdarta, K. Jankowska, M. Wyszowska, E. Kijeńska-Gawrońska, A. Zgoła-Grześkowiak, M. Pinelo, A.S. Meyer, D. Moszyński, T. Jesionowski, Robust biodegradation of naproxen and diclofenac by laccase immobilized using electrospun nanofibers with enhanced stability and reusability, Mater. Sci. Eng. C. 103 (2019) 109789. doi:10.1016/J.MSEC.2019.109789.

[83] M. Maryšková, I. Ardao, C.A. García-González, L. Martinová, J. Rotková, A. Ševců,

Polyamide 6/chitosan nanofibers as support for the immobilization of Trametes versicolor laccase for the elimination of endocrine disrupting chemicals, Enzyme Microb. Technol. 89 (2016) 31–38. doi:10.1016/J.ENZMICTEC.2016.03.001.

[84] J. Hou, G. Dong, Y. Ye, V. Chen, Laccase immobilization on titania nanoparticles and titania-functionalized membranes, J. Memb. Sci. 452 (2014) 229–240.

[85] J. Li, X. Chen, D. Xu, K. Pan, Immobilization of horseradish peroxidase on electrospun magnetic nanofibers for phenol removal, Ecotoxicol. Environ. Saf. 170 (2019) 716–721. doi:10.1016/j.ecoenv.2018.12.043.

[86] J. Niu, J. Xu, Y. Dai, J. Xu, H. Guo, K. Sun, R. Liu, Immobilization of horseradish peroxidase by electrospun fibrous membranes for adsorption and degradation of pentachlorophenol in water, J. Hazard. Mater. 246–247 (2013) 119–125. doi:10.1016/J.JHAZMAT.2012.12.023.

[87] C. Delre, C. Huang, T. Li, P. Dennis, E. Drockenmuller, T. Xu, Reusable Enzymatic Fiber Mats for Neurotoxin Remediation in Water, ACS Appl. Mater. Interfaces. 10 (2018) 44216–44220. doi:10.1021/acsami.8b18484.

[88] F. Zhang, J. Fan, S. Wang, Interfacial polymerization: from chemistry to functional materials, Angew. Chemie Int. Ed. 59 (2020) 21840–21856.

[89] J. Zdarta, A.S. Meyer, T. Jesionowski, M. Pinelo, Developments in support materials for immobilization of oxidoreductases: A comprehensive review, Adv. Colloid Interface Sci. 258 (2018) 1–20. doi:10.1016/j.cis.2018.07.004.

[90] T. Taghizadeh, A. Talebian-Kiakalaieh, H. Jahandar, M. Amin, S. Tarighi, M.A. Faramarzi, Biodegradation of bisphenol A by the immobilized laccase on some synthesized and modified forms of zeolite Y, J. Hazard. Mater. 386 (2020) 121950. doi:10.1016/J.JHAZMAT.2019.121950.

[91] A. Lante, A. Crapisi, A. Krastanov, P. Spettoli, Biodegradation of phenols by laccase immobilised in a membrane reactor, Process Biochem. 36 (2000) 51–58. doi:10.1016/S0032-9592(00)00180-1.

[92] J.B. Costa, M.J. Lima, M.J. Sampaio, M.C. Neves, J.L. Faria, S. Morales-Torres, A.P.M. Tavares, C.G. Silva, Enhanced biocatalytic sustainability of laccase by immobilization on functionalized carbon nanotubes/polysulfone membranes, Chem. Eng. J. 355 (2019) 974–985. doi:10.1016/J.CEJ.2018.08.178.

[93] A.M. Khalil, A.I. Schäfer, Cross-linked β-cyclodextrin nanofiber composite membrane for steroid hormone micropollutant removal from water, J. Memb. Sci. 618 (2021) 118228. doi:10.1016/j.memsci.2020.118228.

[94] Y. Kuang, H. He, S. Chen, J. Wu, F. Liu, Adsorption behavior of CO2 on amine-functionalized polyacrylonitrile fiber, Adsorption. 25 (2019) 693–701.

[95] D. Sharma, B.K. Satapathy, Fabrication of optimally controlled electrosprayed polymer-free nano-particles of curcumin/β-cyclodextrin inclusion complex, Colloids Surfaces A Physicochem. Eng. Asp. 618 (2021) 126504.

[96] Y. Gao, G. Li, Z. Zhou, L. Guo, X. Liu, Supramolecular assembly of poly(β-cyclodextrin) block copolymer and benzimidazole-poly(ε-caprolactone) based on host-guest recognition for drug delivery, Colloids Surfaces B Biointerfaces. 160 (2017) 364–371. doi:10.1016/J.COLSURFB.2017.09.047.

[97] F.-F. Shen, Y. Chen, X. Dai, H.-Y. Zhang, B. Zhang, Y. Liu, Y. Liu, Purely organic

light-harvesting phosphorescence energy transfer by β-cyclodextrin pseudorotaxane for mitochondria targeted imaging, Chem. Sci. 12 (2021) 1851–1857.

[98] G. Li, A.G. Nandgaonkar, K. Lu, W.E. Krause, L.A. Lucia, Q. Wei, Laccase immobilized on PAN/O-MMT composite nanofibers support for substrate bioremediation: A: de novo adsorption and biocatalytic synergy, RSC Adv. 6 (2016) 41420–41427. doi:10.1039/c6ra00220j.

[99] Y.-L.E. Fung, H. Wang, Investigation of reinforcement of porous alumina by nickel aluminate spinel for its use as ceramic membrane, J. Memb. Sci. 444 (2013) 252–258.

[100] H. Dai, J. Gong, H. Kim, D. Lee, A novel method for preparing ultra-fine alumina-borate oxide fibres via an electrospinning technique, Nanotechnology. 13 (2002) 674.

[101] D. Han, S. Filocamo, R. Kirby, A.J. Steckl, Deactivating chemical agents using enzyme-coated nanofibers formed by electrospinning, ACS Appl. Mater. Interfaces. 3 (2011) 4633–4639. doi:10.1021/am201064b.

[102] X. Mao, L. Zhao, K. Zhang, Y.-Y. Wang, B. Ding, Highly flexible ceramic nanofibrous membranes for superior thermal insulation and fire retardancy, Nano Res. (2022) 1–7.

[103] Y. Wang, H. Wu, D. Lin, R. Zhang, H. Li, W. Zhang, W. Liu, S. Huang, L. Yao, J. Cheng, One-dimensional electrospun ceramic nanomaterials and their sensing applications, J. Am. Ceram. Soc. 105 (2022) 765–785.

[104] L. Dou, B. Yang, S. Lan, Y. Liu, Y.-H. Lin, C.-W. Nan, Nanonet-/fiber-structured flexible ceramic membrane enabling dielectric energy storage, J. Adv. Ceram. 12 (2023) 145–154.

[105] H.-C. Yang, K.-J. Liao, H. Huang, Q.-Y. Wu, L.-S. Wan, Z.-K. Xu, Mussel-inspired modification of a polymer membrane for ultra-high water permeability and oil-in-water emulsion separation †, (2014). doi:10.1039/c4ta00143e.

[106] M. Bilal, J. Cui, H.M.N. Iqbal, Tailoring enzyme microenvironment: State-of-the-art strategy to fulfill the quest for efficient bio-catalysis, Int. J. Biol. Macromol. 130 (2019) 186–196. doi:10.1016/J.IJBIOMAC.2019.02.141.

[107] D. Becker, S. Varela Della Giustina, S. Rodriguez-Mozaz, R. Schoevaart, D. Barceló, M. de Cazes, M.-P. Belleville, J. Sanchez-Marcano, J. de Gunzburg, O. Couillerot, J. Völker, J. Oehlmann, M. Wagner, Removal of antibiotics in wastewater by enzymatic treatment with fungal laccase – Degradation of compounds does not always eliminate toxicity, Bioresour. Technol. 219 (2016) 500–509. doi:https://doi.org/10.1016/j.biortech.2016.08.004.

[108] K. Ovsejevi, C. Manta, F. Batista-Viera, Reversible Covalent Immobilization of Enzymes via Disulfide Bonds BT - Immobilization of Enzymes and Cells: Third Edition, in: J.M. Guisan (Ed.), Humana Press, Totowa, NJ, 2013: pp. 89–116. doi:10.1007/978-1-62703-550-7_7.

8 Papers

I **Zhao, D**., Leth, M. L., Abou Hachem, M., Aziz, I., Jančič, N., Luxbacher, T., Hélix-Nielsen, C., and Zhang, W. (2023). Facile fabrication of flexible ceramic nanofibrous membranes for enzyme immobilization and transformation of emerging pollutants. *Chemical Engineering Journal*, *451*, 138902.

II **Zhao, D**, Leth, M. L., Abou Hachem, Hélix-Nielsen, C., and Zhang, W. Thin-film composite biocatalytic Nanofiberous membranes for Pharmaceutical Residues Degradation: Performance, stability and Continuity. *Manuscript in preparation.*

III **Zhao, D**, Leth, M. L., Abou Hachem, Hélix-Nielsen, C., and Zhang, W. A novel eco-friendly degradable laccase-immobilized electrospun nanofibers targeting contaminant of emerging concerns. *Manuscript in preparation.*

IV Xu, M., **Zhao, D**., Zhu, X., Su, Y., Angelidaki, I. and Zhang, Y. (2021). Biogas upgrading and valorization to single-cell protein in a bioinorganic electrosynthesis system. *Chemical Engineering Journal*, *426*, 131837.

V Wang, G., Hambly, A.C., **Zhao, D.,** Wang, G., Tang, K. and Andersen, H.R. (2023). Peroxymonosulfate activation by suspended biogenic manganese oxides for polishing micropollutants in wastewater effluent. *Separation and Purification Technology*, *306*, 122501.

VI Qin J., Dou Y., **Zhao D**., Yang X., Andersen, H.R., Hélix-Nielsen, C., and Zhang, W. Encapsulation of Carbon-Nanodots into MOFs for Efficient Upcycling of Polyvinyl Chloride Plastics. *Manuscript in preparation*

Supplementary Material for:

Thin-film Composite Biocatalytic Nanofibrous Membranes for Pharmaceutical Residues degradation: Performance, stability, and Continuity

Dan Zhao[a], Maher Abou Hachem[b], Claus Hélix-Nielsen[a], Wenjing (Angela) Zhang[a,*]

a. Department of Environmental and Resource Engineering, Technical University of Denmark, DTU, 2800 Kgs. Lyngby, Denmark

b. Department of Biotechnology and Biomedicine, Technical University of Denmark, DTU, 2800 Kgs. Lyngby, Denmark

[*] **Corresponding author:**

Dr. Wenjing (Angela) Zhang

Tel: (+45) 20352356; E-mail address: wen@dtu.dk

Dr. Claus Hélix-Nielsen

Tel: (+45) 45252228; E-mail address: clhe@dtu.dk

Text S1. Materials

Table S1. Twenty common emerging pollutants

	Emerging pollutants	CAS Number	Molecular weight (g/mol)	Formula	Supplier
1	Diclofenac sodium salt	15307-79-6	318.13	$C_{14}H_{11}Cl_2NNaO_2$	Sigma-Aldrich
2	Mefenamic acid	61-68-7	241.29	$C_{15}H_{15}NO_2$	Sigma-Aldrich

Text S2. Operation of cross-flow filtration

The flow diagram of the dead-end filtration system with the ceramic membrane is shown in **Figure S1.**

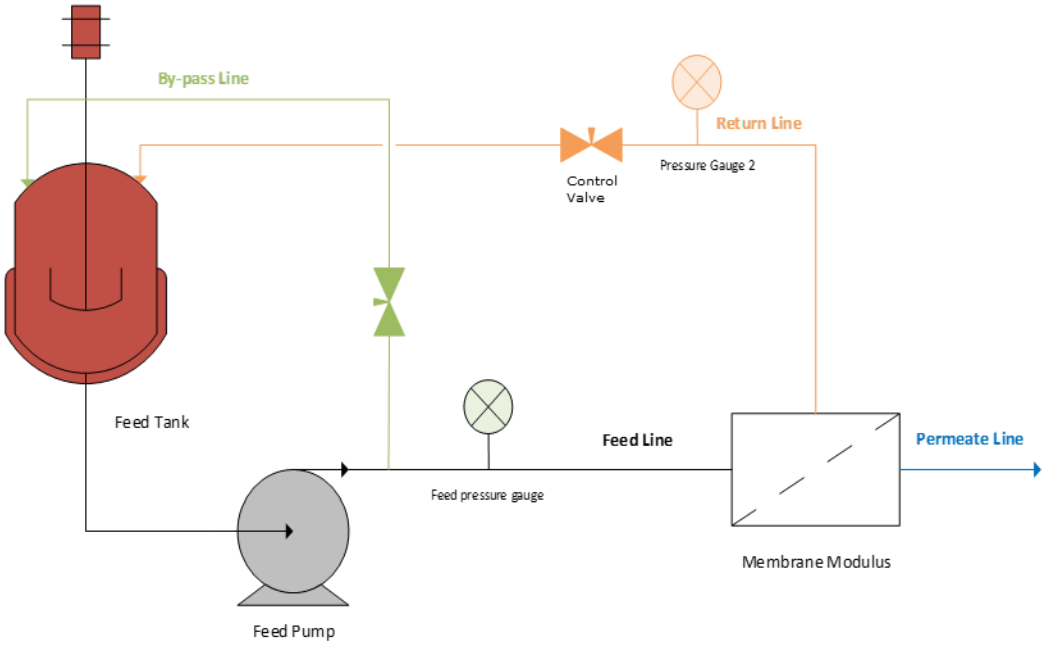

Figure S1. Cross-flow filtration diagram

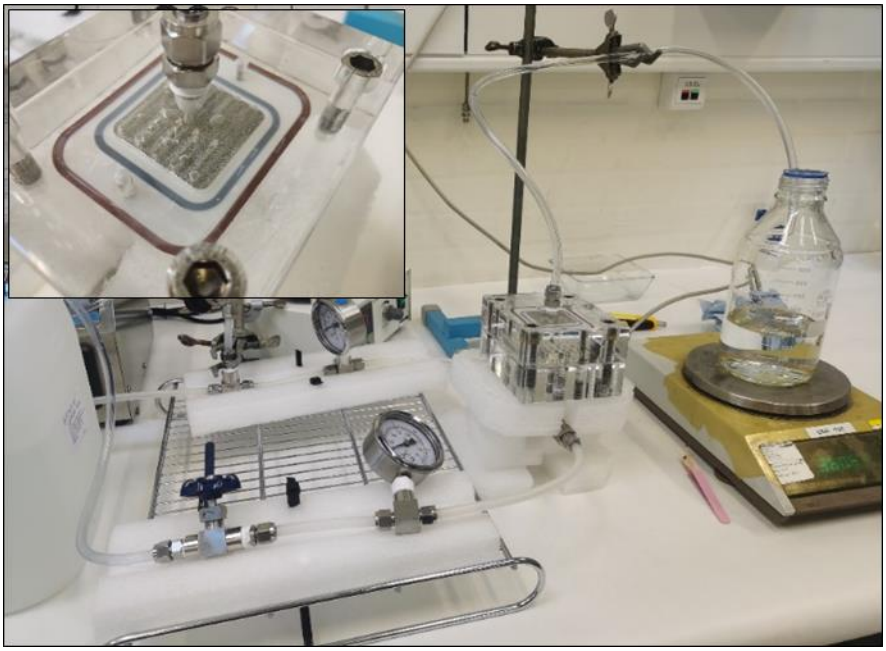

Figure S2. Cross-flow filtration setups

Text S3. Thermal inactivation kinetics

The thermal inactivation data for free and immobilized laccase was plotted for zero (residual activity versus time), first (natural logarithm of the residual activity versus time) and second-order (reciprocal activity versus time). The rate constant k_{inact} [h^{-1}] for first-order thermal inactivation was determined from the slope of the inactivation time:

$$ln\left(\frac{A_t}{A_0}\right) = -k_{inact}t \quad (1)$$

$$t_{0.5} = \frac{ln(2)}{k_{inact}} \quad (2)$$

Where At is the residual activity that remains after heating the enzyme for time t, and A_0 is the initial enzyme activity before heating. The half-time of thermal inactivation ($t_{0.5}$) was determined by equation S2.

Text S4. SEM image of the back of the polyamide layer.

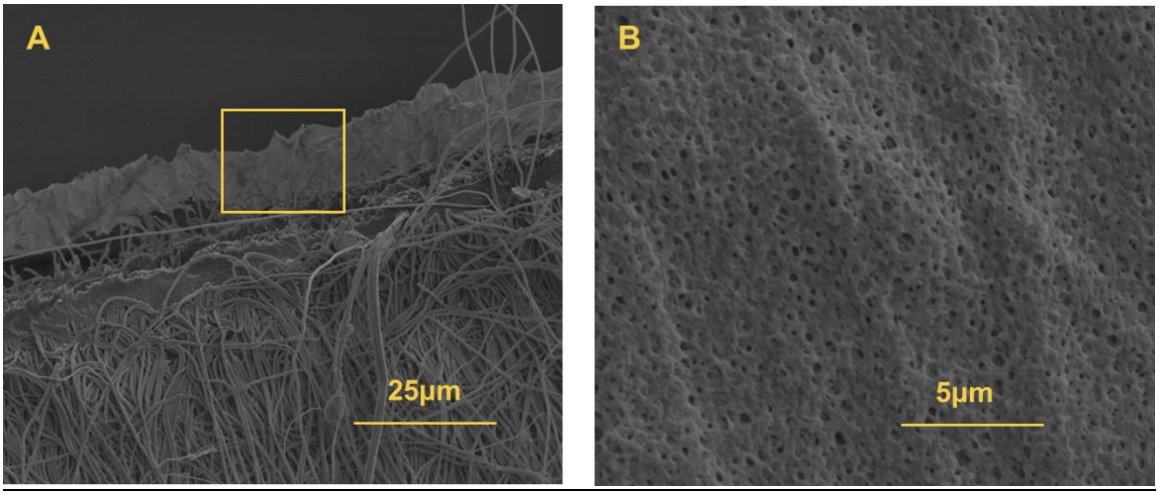

Figure S3. A) SEM image of the back of the polyamide layer. B) SEM image of the yellow square area

Thin-film Composite Biocatalytic Nanofibrous Membranes for Pharmaceutical Residues degradation: Performance, stability, and Continuity

Dan Zhao[a], Maher Abou Hachem[b], Claus Hélix-Nielsen[a], Wenjing (Angela) Zhang[a,*]

a. Department of Environmental and Resource Engineering, Technical University of Denmark, DTU, 2800 Kgs. Lyngby, Denmark

b. Department of Biotechnology and Biomedicine, Technical University of Denmark, DTU, 2800 Kgs. Lyngby, Denmark

***Corresponding author:**

Dr. Wenjing (Angela) Zhang

Tel: (+45) 20352356; E-mail address: wen@env.dtu.dk

Dr. Claus Hélix-Nielsen

Tel: (+45) 45252228; E-mail address: clhe@env.dtu.dk

Abstract

Biocatalytic nanofibrous membranes have recently become a popular choice for bioreactors due to their high specificity, prolonged reusability, increased stability, and low-cost separating unit. They have been utilized in various fields, such as biosensing and wastewater treatment. In this study, a novel technique was investigated that involved covalently immobilizing laccases on functionalized electrospun nanofibers containing β-cyclodextrin. The non-polar cavity of β-cyclodextrin can encapsulate various hydrophobic guest molecules. The incorporation of β-cyclodextrin into the fibers and the introduction of –OH and $–NH_2$ functional groups onto the membrane surface can enhance the enzymatic activity of the membranes. Moreover, the immobilization process has been shown to improve the performance of the biocatalyst. In particular, the immobilized enzymes exhibit a broader range of pH, enhanced thermal tolerance, and high reusability with 90% of the initial after five cycles, making them highly suitable for industrial applications. In this work, the biocatalytic membranes were applied with a lab-made thin-film composite membrane. The addition of a biocatalytic membrane largely enhanced the performance of pharmaceutical depletion, where over 85% of pharmaceuticals in the permeate were achieved. Overall, our study highlights the tremendous potential of biocatalytic membrane systems in removing pharmaceuticals during wastewater treatment.

Keywords: Laccase, Electrospun fibrous membrane, Immobilization, Biodegradation

37 **Graphical Abstract**

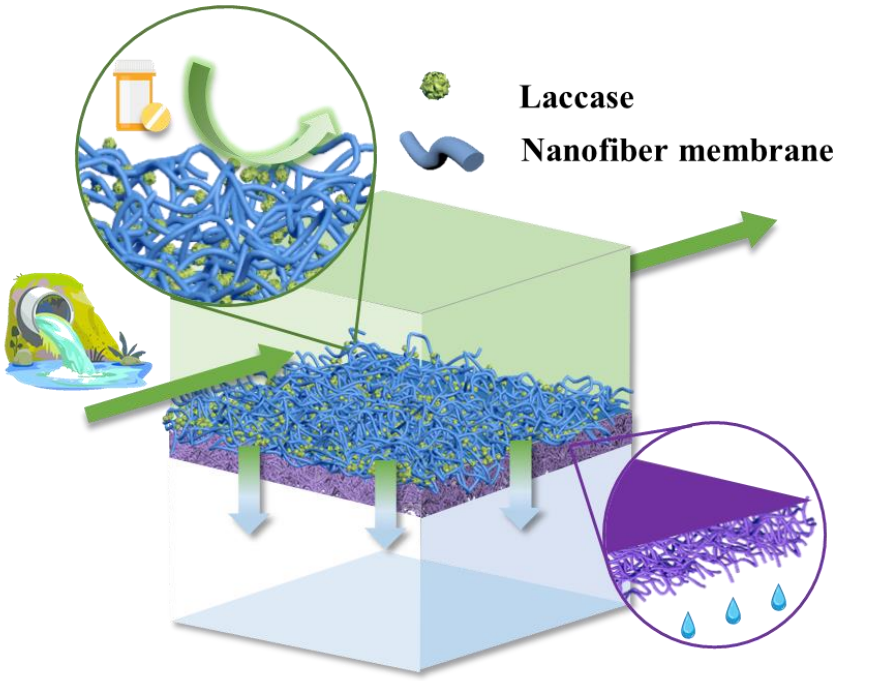

38

39

1. Introduction

In recent decades, the release of pharmaceutical active compounds (PhACs) has drawn emerging concerns because of consistent detection and potential ecotoxicological consequences regarding public health and aquatic ecosystems.[1] Mefenamic acid (MFA), a non-steroidal anti-inflammatory drug (NSAID), has been widely prescribed to decrease pain and blood loss from menstrual periods. Unfortunately, the conventional wastewater treatment plants (WWTPs) based on activated sludge[2] and moving bed biofilms[3] present an unmet need for removing resistant micropollutants. As a result, MFA has been frequently detected in wastewater effluents[4], and the effluents have been identified as one of the primary sources of pharmaceuticals in the environment.[5] To date, efforts have been proposed and investigated, including activated carbon adsorption[6,7], advanced oxidation processes (AOPs)[8–10], and membrane separation[11,12]. Nevertheless, several challenges, such as absorbent regeneration, toxic by-product formation, and disposal of the retentate, need to be addressed before applying these methods at a large scale.

Recently, enzymes have attracted attention for pharmaceutical detoxification mainly due to their high selectivity, mild reaction conditions, and minimal environmental impact.[13–15] Laccases (1.10.3.2, p-diphenol: dioxygen oxidoreductases), a type of oxidative enzyme containing four copper atoms in the active site, could oxidize a broad range of phenolic compounds[16,17] The mechanism for laccase-induced treatment involves the oxidation of pollutants to free radicals or quinones that subsequently undergo polymerization and partial precipitation. However, free laccases are very sensitive to pH and temperature, and their applications present some drawbacks related to their limited stability, difficult recovery, and reusability, which results in high operational costs.[18–20]

Alternatively, immobilization of enzymes in or on membranes has been considered an effective way to avoid the aforementioned limitations. Numerous studies have been dedicated to immobilizing laccases onto various supports. Lante et al.[21] successfully adsorbed laccases onto polyethersulphone membranes by recirculating enzyme solution through. Hou et al.[22] covalently immobilized laccases onto the TiO_2 sol-gel coated polyvinylidene fluoride (PVDF) membrane, where nearly 80% of the original laccase activity was preserved. Costa et al.[17] efficiently immobilized laccases over polysulfone membranes blended with functionalized carbon nanotubes. However, the enzyme loadings of each strategy above were relatively low due to the limited active sites of the support.

Regarding this, electrospun nanofibrous membranes (EFMs) can be one of the options. The ultrafine nanofibers with diameters ranging from a few nanometers to several micrometers obtained by electrospinning show their unique advantages benefit from high porosity and specific surface area, diverse choices of spinning materials, low cost, and various methods for further modifications.[23–25] Xu et al.[26] used nano-copper incorporated polyacrylonitrile (PAN)/PVDF EFMs as carrier materials, and the enzyme showed significantly better performance on 2,4,6-trichlorophenol removal. Interestingly, EFMs are also used as sorbents in various organic pollutant extraction[23,27,28]. However, the subsequent treatment for the adsorbed contaminants is still a huge dilemma. Therefore, thin-film composite NFMs will be a considerable material, providing a platform combining biocatalytic reactions with membrane separation as adsorbed and sedimentary contaminants separated by the active layer of the composite membrane provide an enriched substrate environment for enzymes. In return, enzymes immobilized on the fibers degrade the pollutants limiting the membrane fouling and prolonging the usage of membrane modules.

To achieve this, we employed a novel enzyme immobilization strategy to build a biocatalytic membrane reactor with high enzymatic activity, degradation performance, and long-time usage. For this purpose, PAN, with good stability and mechanical properties, was chosen as the primary material for electrospinning[29]. Besides, β-cyclodextrin (β-CD) was employed as an additive material as its remarkable adsorption property on protein and pollutants resulting from its cone-shaped structure and unique hydrophilicity.[27] In order to introduce functional groups into the polymer fibers, several steps of functionalization and modification were applied. Activity and stability of the immobilized enzyme were examined under different immobilization process parameters (e.g., pH and temperatures). The enzyme-based material was then employed in the membrane filtration to remove two commonly detected pharmaceuticals, mefenamic acid (MFA) and diclofenac (DCF).

2. Materials and methods

2.1. Chemicals and materials

Laccase from *Trametes versicolor* (EC 1.10.3.2, ≥0.5 U/mg), β-cyclodextrin (β-CD), 2,2'-azino-bis(3-ethyl-benzothiazoline-6-sulfonic acid: ABTS), diclofenac (DCF), mefenamic acid (MFA), polyacrylonitrile (PAN, Mw 150,000), piperazine (PIP), trimesoyl chloride (TMC), hydroxylamine hydrochloride, glutaraldehyde (GA, 50 wt.% in H_2O), sodium acetate (NaOAc), acetic acid (HAc), methanol (HPLC grade, 99.9%), ethanol absolute (99.8%), hexane (99.8%), (3-Aminopropyl)triethoxysilane (APTES, 99%), N, N-dimethylacetamide (DMAc, 99%) were obtained from Sigma-Aldrich.

2.2. Experimental procedures

Figure 1. illustrates the main process of laccase-immobilized NFMs production, including electrospinning, surface functionalization, laccase immobilization, and interfacial polymerization.

The laccase-immobilized membrane and a thin-film composite membrane were transferred into a membrane cell for membrane performance.

2.2.1. Preparation of electrospun nanofiber membranes(NFMs).

The spinning solution of PAN NFMs contained 7 wt% of PAN in DMAc, and the solution of PAN/ β-CD NFMs was prepared by adding 3.5 g PAN, and 1.5 g of β-CD was added to 45 g DMAc. Both solutions were stirred overnight at room temperature before the electrospinning. The electrospinning was carried out by a needle-based electrospinner (NS+, Inovenso, Turkey), corporate with a precision air Conditioner (NS AC150, Elmarco, Czech Republic). The solution was filled in a 10 mL syringe and fed through a stainless steel needle with an inner diameter of 0.8 mm at a constant rate of 0.7 mL/min. The spinning voltage and tip-to-collector distance were applied to 13.7 kV and 15 cm, respectively. The temperature and relative humidity were set at 25 °C and 30 %. The electrospun PAN and PAN/β-CD nanofibers were collected on a siliconized paper set with a constant speed of 100 rpm, and the acquired nanofibers were then stored in a vacuum oven for two h at 40 °C to clear up the solvent completely.

2.2.2. Surface modification of PAN/ β-CD NFMs

The surface of PAN/ β-CD NFMs was modified by following two steps:

i) **Amidoxime synthesis** was achieved by immersing 0.32 g PAN/β-CD NFMs in 100 mL 0.15 M hydroxylamine aqueous solution at 65 °C for two h. The pH value of the solution was adjusted to 7 by the addition of Na_2CO_3. The obtained NFMs, labeled as M-AO, were washed with distilled water three times and subsequently vacuum-dried overnight at 40 °C.

ii) **Silanization treatment** was performed by immersing obtained M-AO in 100 ml of 10 % (w/w) APTES ethanol solution at 70 °C for two hours. The resulting NFMs were washed with distilled water three times and vacuum-dried overnight at 40°C.

The PAN, PAN/β-CD, amidoxime treated PAN/β-CD, and silanized PAN/β-CD NFMs are labeled as M1, M2, M3, and M4 NFMs, respectively.

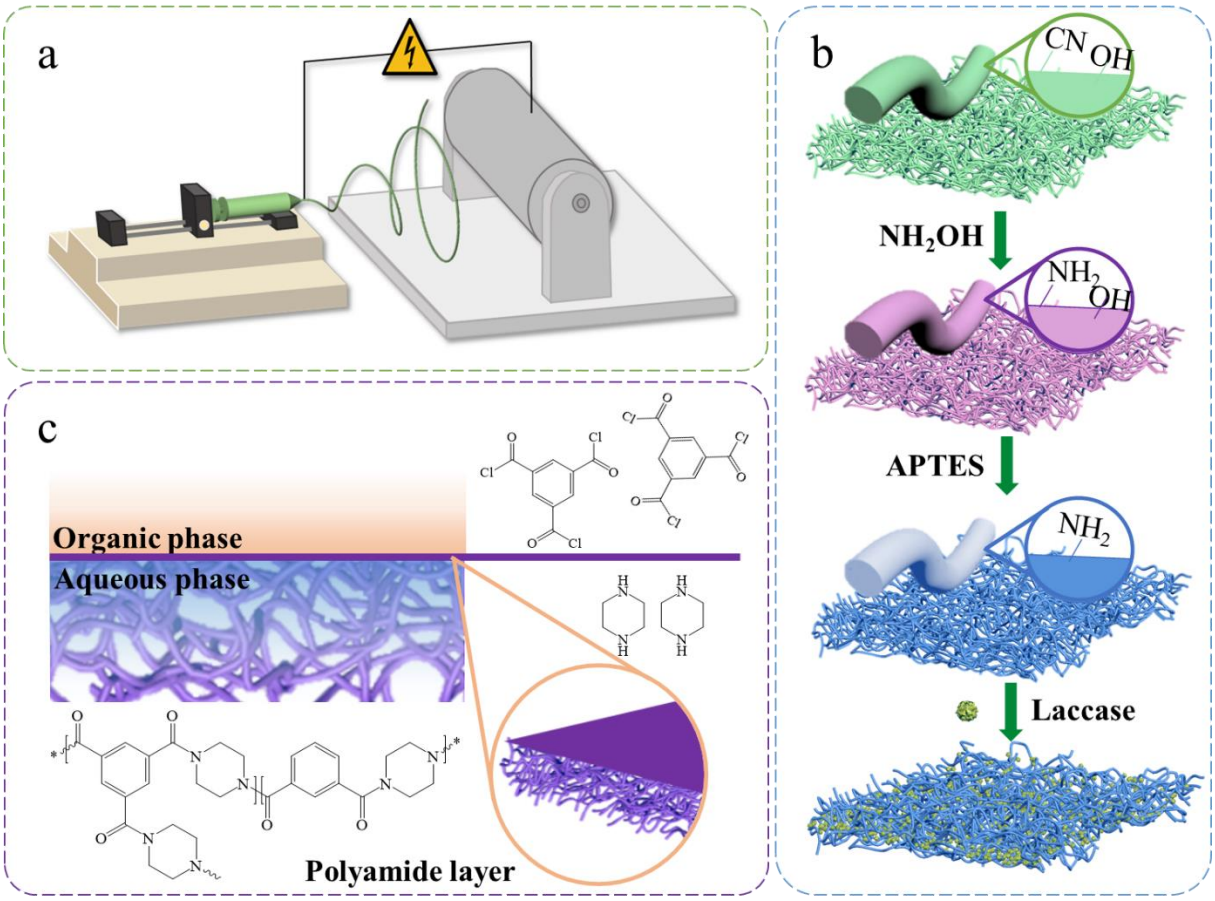

Figure 3.1 1 Schematic illustration of needle-based electrospinning a), enzyme immobilization b), and thin-film composite membrane fabrication.

2.2.3. Preparation of thin-film composite membrane

The thin-film composite membrane was prepared by interfacial polymerization of polyamide onto the electrospun PAN NFMs. The PAN NFMs were firstly soaked in PIP aqueous solutions with different concentrations for 5 min. Subsequently, the membrane was placed on the glass plate, and the excess aqueous solution was gently removed with an air knife. Nest, the membrane was immersed in a 0.4% (w/w) TMC hexane solution for 1 min and dried by an air-knife for 15 seconds to remove the excess organic solution. The resulting membrane was cured at different temperatures

for 5 min to further carry out the polymerization reaction. Finally, the detached membrane from the glass plate was washed and stored in Miliq H_2O.

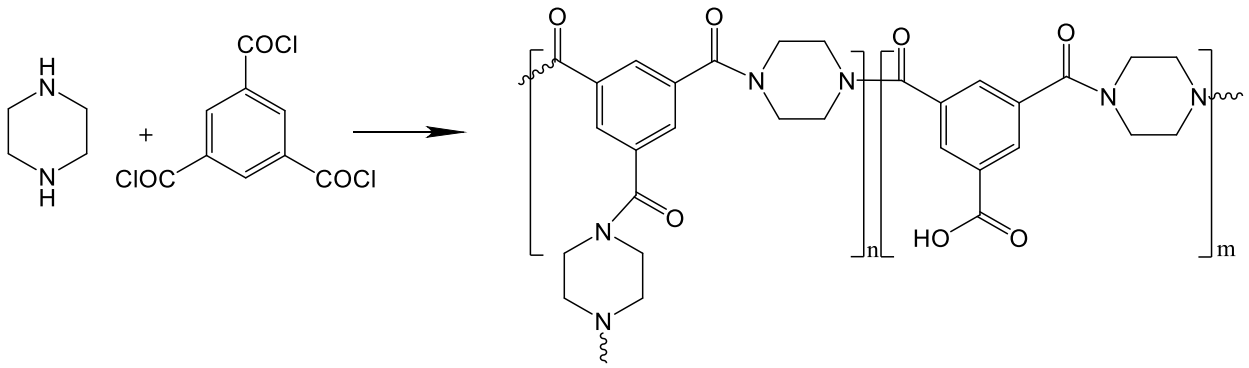

Figure 2. Interfacial polymerization reaction

2.2.4. Laccase immobilization and enzyme assays

Laccase immobilization on the modified NFMs was performed as described in our previous work. With minor modifications. Briefly, each modified membrane (36 cm^2) was immersed in a 5 mg mL^{-1} (by weight) laccase solution in 50 mM NaOAc buffer, pH 4.5, and incubated for one hour at 25 °C, and subsequently transferred to 4 °C for 24 h. Next, the laccase immobilized membrane was washed three times with the same buffer and stored at 4 °C. NFMs for enzyme assays were cut before the immobilization. The laccase activity in the initial immobilization bath, the residual after immobilization, and the wash fractions were determined spectrophotometrically using ABTS as the substrate. Specifically, 10 μL enzyme stock or 0.25 cm^2 of the laccase-immobilized membrane was added to 0.5 mM ABTS solution in 20 mM NaOAc buffer, pH 4.5, and the reaction mixture (300 μL) was incubated in a microtitre plate for 10 min after a 30-second rotary agitation at 25 °C, and the absorbance at 420 nm was monitored continuously.

Subsequently, the effect of pH on laccase activity was evaluated by testing both the free and immobilized enzyme prepared in 20 mM NaOAc at pH 3.5-6.5 and monitoring the absorbance at 420 nm at 25 °C. Furthermore, a thermal inactivation assay at 40, 50, and 60°C was performed to

investigate the stability of both the free and immobilized enzymes. An Eppendorf tube containing 980 μl NaOAc buffer (50 mM) was preheated for 5 min. 20 μl of 5 mg ml^{-1} enzyme solution (by weight) was added to the preheated buffer solution and incubated at a selected temperature. Then, 100 μl aliquots were collected at 10, 20, 30, 60, 90, and 120 min and stored on ice. Next, the residual activity was assayed using the standard assay described above at 25 °C. For the immobilized enzyme, three pieces of immobilized fibers were assayed before heating, and the same fiber was washed thoroughly. Thereafter, the washed fiber was incubated in a water bath at the same temperature for 10 min, stored on ice, and assayed for the remaining activity. This was repeated with new pieces of fibers at 20, 30, 60, 90, and 120 min.

2.2.6. Membrane performance on pharmaceutical degradation

To investigate the catalytic membrane performance of the thin-film composite membrane set, cross-flow membrane filtration was conducted, as shown in **Figure S1-2**. The active membrane area was 26 cm^2, and a gear pump was used to recirculate the retentate solution. 450 mL pharmaceutical mixture (with 1 mg L^{-1} of each pharmaceutical) in Miliq H_2O, including mefenamic acid and diclofenac, was used as a feed solution. The pressure applied in the cross-flow filtration was set as 2 bar. Duplicate samples were taken at different reaction times and filtered through 0.2 μm PTFE filters into 2 mL vials. Subsequently, acetonitrile was added as a quenching reagent.

2.3. Characterization and analytical procedures

2.3.1. Characterization of NFMs.

The microstructure of the electrospun NFMs and thin-film composite membrane were analyzed by field emission scanning electron microscopy (Quanta FEG 250, FEI, USA) at an accelerating

voltage of 5 kV. The chemical structure of each NFM was analyzed by Fourier transform infrared spectroscopy-Attenuated Total Reflectance (FTIR-ATR, Bruker, Germany).

2.3.2. Determination of enzyme loading and activity.

The protein concentrations in solutions were determined by the Bradford method on a microplate reader (Synergy H1, Agilent Technologies, USA). The amount of immobilized enzyme (m) was calculated as:

$$m = (C_0 - C)V - \sum C_w V_w \quad (1)$$

where C_0, C_w, and C represent the enzyme concentrations [μg mL^{-1}] in the initial stock, washing buffer, and residue solution, respectively, V and V_w are volumes of the enzyme solution and washing buffer (mL). Free enzyme activity (A_{free}), [U mL^{-1}], the laccase-immobilized fiber activity in terms of membrane weight ($A_{fiber,w}$), [U g^{-1}_{fiber}], and area ($A_{fiber,a}$), [U m^{-2}], were obtained as:

$$A_{free} = \frac{\alpha \times V_{Total}}{V_{Enzyme} \times \varepsilon \times d} \quad (2)$$

$$A_{fiber,w} = \frac{\alpha \times V_{Total}}{M_{fiber} \times \varepsilon \times d} \quad \text{or} \quad A_{fiber,a} = \frac{\alpha \times V_{Total}}{A_{fiber} \times \varepsilon \times d} \quad (3)$$

$$SA_{free} = \frac{A_{free}}{C_{free}} \quad (4)$$

where V_{Total}, V_{Enzyme} are the volume of total assay and enzyme solution, [μL], M_{fiber} is the mass of tested membrane [g], A_{fiber} is the area of the tested membrane [g], α is the absorbance per minute (determined by linear regression) at 420 nm [min^{-1}], d is the light path of the assay [cm], and ε represents the molar absorption coefficient of ABTS at 420 nm, 36,000 $M^{-1} \cdot cm^{-1}$. One unit of enzyme activity [U] was defined as the amount of enzyme which converts 1 μmol of substrate per minute under the assay conditions.

2.3.4. Determination of EPs degradation efficiency

The concentrations of EPs were analyzed by High-Performance Liquid Chromatography–Triple Quadrupole Mass Spectrometry (1290 Infinity II-6470 LC-QQQ, Agilent Technologies). The conversion efficiency (*D*) was calculated as follows:

$$D = \frac{C_{\mathrm{EP}_0} - C_{\mathrm{EP}}}{C_{\mathrm{EP}_0}} \times 100\% \quad (6)$$

where C_{EP0} and C_{EP} are the EP concentrations in solutions before and after degradation experiments.

2.3.5. Separation performance of membranes

A laboratory-scale cross-flow membrane filtration system was used to characterize the separation performance of thin-film composite membranes. The water flux (J) was calculated using the following equation:

$$J = \frac{V}{A\Delta t} \quad (8)$$

where *V* is the volume of permeate water, [L]; *A* is the effective area of the membrane, [m^2]; and *Δt* is the permeation time, [h].

3. Result and discussion

3.1. Membrane morphology and chemical structure

Figure 3.2A-D depicts the morphology of M1, M2, M3, and M4 NFMs. With the addition of β-CD, M2 NFMs compared with M1 NFMs, a slight decrease in fiber diameter was noticed. Surface-treated M3 and M4 NFMs maintained a smooth and uniform structure in a fiber diameter distribution at 450 ± 130 nm, 450 ± 130 nm, 465 ± 120 nm, and 452 ± 159 nm correspondingly. The addition of β-CD, amidoxime treatment, and silanization did not change the surface morphology of the NFMs.

The chemical structures and compositions of PAN/ β-CD nanofibers were characterized by FTIR-ATR. **Figure 3G** presents FTIR spectra of M1, M2, M3, and M4 NFMs. The prominent peaks of PAN at 2243, 2925, and 1452 cm^{-1} can be ascribed to the stretching vibrations of cyano groups (−C≡N)[30] and the stretching and bending vibrations of methylene groups (−CH_2−), respectively. Characteristic peaks for β-CD were observed at 1628 cm^{-1}, 1152 cm^{-1}, 1078 cm^{-1}, and 1031 cm^{-1}, assigning to bending vibration of hydroxyl groups (O−H), stretching vibrations of glycosidic linkage (C−O−C), stretching vibrations of C−C bond, and stretching vibrations of C−H bonds from cyclodextrin ring[31]. A new peak formed on M3 NFMs at 1597 cm^{-1}, corresponding to C−N stretching bonds, and weakened cyano groups at 2243 cm^{-1}, indicated that some cyano groups were converted into –$C(NH_2)$=NOH groups[32]. After the silanization, absorption peaks at about 1050 cm^{-1} corresponding to Si–O–C and Si–O–Si were observed, probably due to the long chain of the Si–O–Si network originating from APTES molecules.

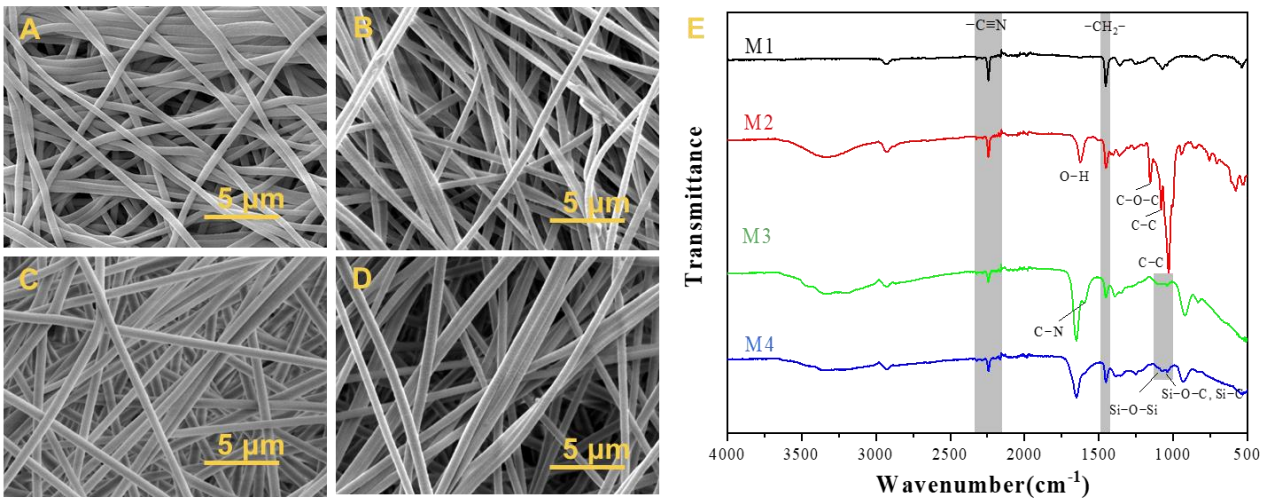

Figure 3. A-D) SEM image of M1, M2, M3, and M4 NFMs. E) FTIR-ATR spectrum of M1, M2, M3, and M4 NFMs.

Figure 4 shows the surface and cross-section of the TFC membrane. The thin nanofiber nonwoven matt with high porosity and low tortuosity reduced the severity of internal concentration

polarization. A continuous polyamide film was expected to adhere on top of the nanofiber matt, consistent with the results from **Figure 4A-D**. The nanofibers were partially embedded in the top layer, indicating a tight polyamide adhesion to the nanofibers. By tuning the conditions of interfacial polymerization, different morphologies of the polyamide layer were achieved. Ridge-and-valley structures were observed (**Figure 4A**). The formation of these structures was found to be related to the concentration of PIP monomers and temperatures of thermal treatment. With the decrease in the monomer concentration and thermal treatment temperature, the surface of the polyamide layer turned out to be smoother. The interfacial polymerization reaction between PIP and TMC is an exothermic reaction producing heat, which could vaporize organic solvent to promote the formation of hollow nodules. Honeycomb-shaped pores can be observed on the back of the polyamide selective layer with a ridge-and-valley structure (**Figure S3**). That is because the rapid-formed polyamide film interrupted the gas to escape from the interface side. The vapor instead releases to the substrates to unsealing the nanovoids[33,34]. From the cross-section image (**Figure 4E-F**), the polyamide layer and TFC membrane thicknesses were 155 ± 5 nm and 25 ± 1 μm, respectively.

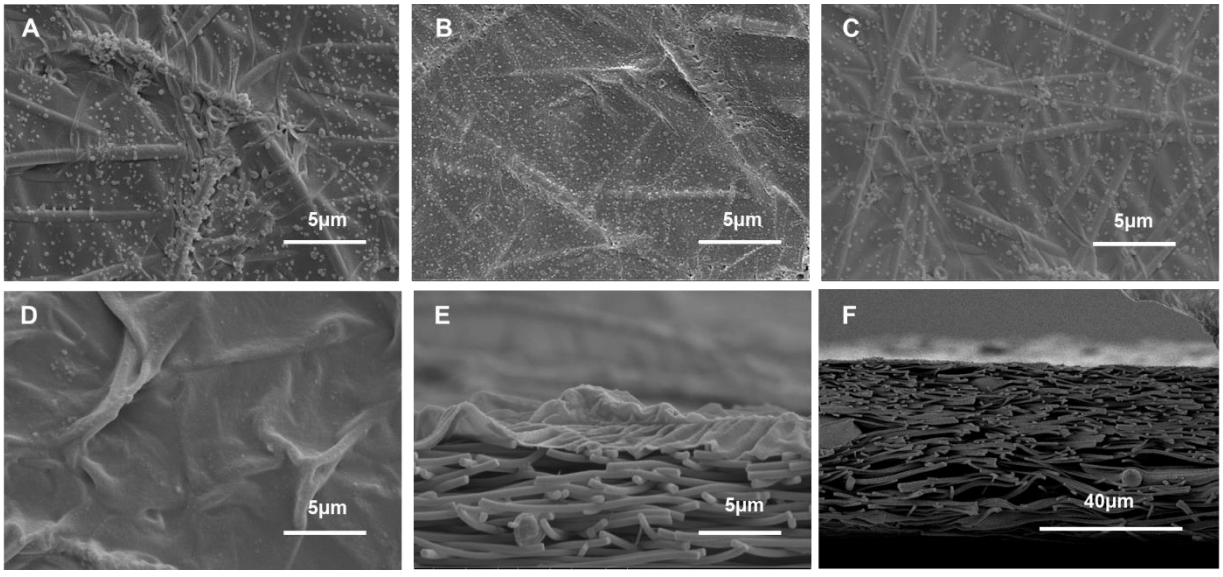

Figure 4. Surface morphology of TFC membranes prepared with different conditions: A) 1 wt% PIP solution, 70°C, B) 0.4 wt% PIP solution, 70°C, C) 0.4 wt%PIP solution, 60°C, D) 0.4 wt%PIP PIP solution, 55°C. Cross-section morphology of TFC membrane with different magnifications: E) ×10,000, F) ×1,000.

3.2. Optimization of laccase immobilization

Figure 4A shows the specific activity of biocatalytic membranes. It was observed that M3 NFMs exhibited the highest values in terms of unit weight and area of the membrane. The amidoxime reaction transferring cyano groups into hydroxyl groups and amine groups largely increased active sites for laccase immobilization. Similar findings were found in amidoxime-treated PAN NFMs[32]. However, after the salinization treatment, the specific activity of biocatalytic NFMs was decreased. The possible reason for the finding could be the self-aggregates of APTES, competing with the active sites with laccase. The amount of protein immobilized onto the fiber was difficult to quantify in M2-M4 NFMs, where the β-CD interfaces the Bradford and BCA reagent, which was also noticed in other studies[35]. Therefore, enzyme performance in this study was mainly focused on the apparent specific activities of fibers.

High enzyme activity of fiber (A_{fiber}) loss, correlated to the high protein load, is observed on M3 and M4 NFMs. Nonetheless, M3 NFMs exhibited the highest enzyme activity of fiber, corresponding to 8% of total activity, as described in **Figure 4B**. The decrease in activity observed may be due to the immobilized enzymes becoming crowded on the fibers, as indicated in **Figure 4C**. The activity of the fiber is preserved at 86% when the enzyme load is reduced by 50%, while the loss of activity declines from 70% to 62%. Excessive enzyme loading results in protein-protein interactions, which restrict the flexible stretching of enzyme conformation, leading to steric hindrance and enzyme inactivation[36]. Under molecular crowding conditions, the enzyme molecule

may find it challenging to adopt its optimal conformation for substrate binding and product release. Further reduction in enzyme load leads to a significant decline in fiber activity.

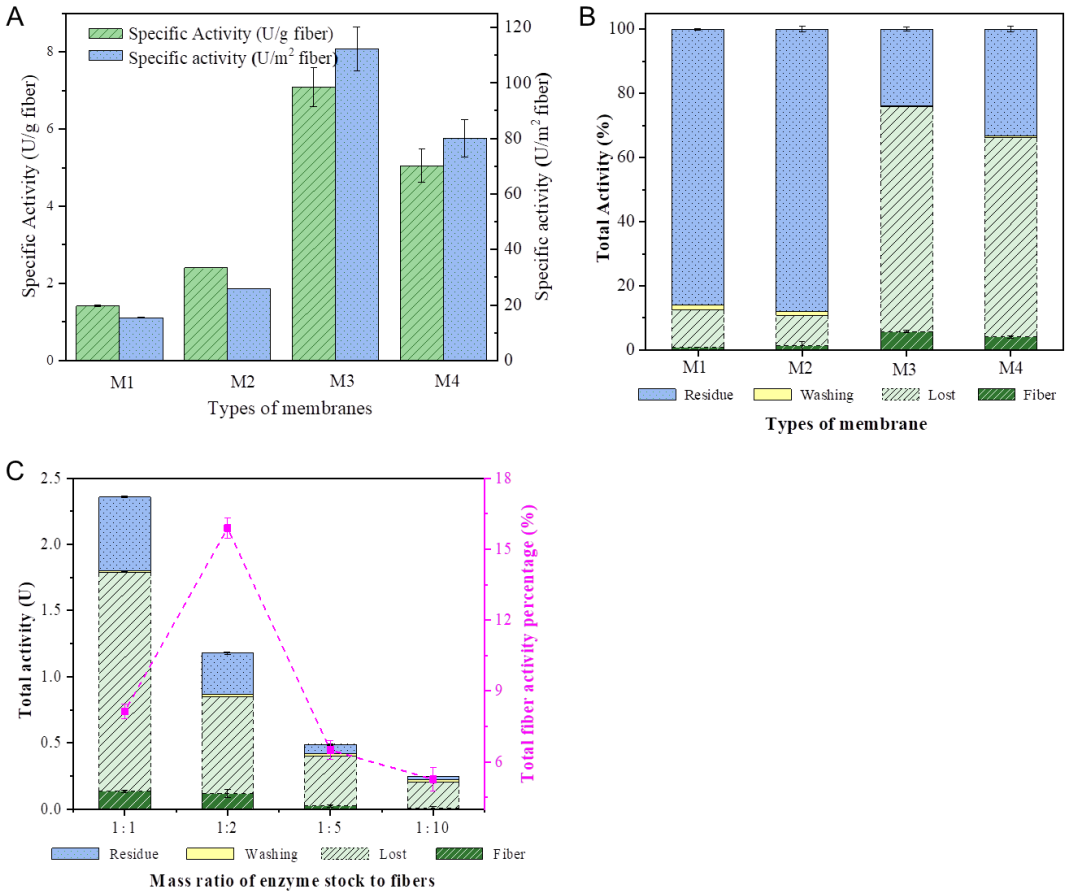

Figure 4 A) Specific activity of different fibers in terms of weight and area. B) Total residual enzyme activity in the residue solution, washing buffer, immobilized fibers, and the calculated lost activity with different NFMs. C) Total residual enzyme activity in the residue solution, washing buffer, immobilized fibers, and the calculated lost activity with different enzyme stock.

3.3. Stability of the immobilized laccase

The impact of pH on the relative activities of free and immobilized laccase on M3 NFMs is illustrated in **Figure 5A**. Immobilized laccase exhibited over 60% of its optimal activity across a wider pH range than the free enzyme, although the optimal pH values for both forms were identical at 4.5. These findings suggest that the immobilized laccase has better chemical stability than its

free form, as it can tolerate a neutral pH range, making it a promising candidate for enzymatic applications in water treatment. Meanwhile, **Figure 5B** shows the thermal inactivation kinetics for both free and immobilized laccase. A_0 and A indicate the initial and remaining enzyme activity of the free or immobilized enzyme. After 120 minutes of heating at 50 °C, the residual activity of the immobilized laccase was 67%, compared to 53% for the free laccase. These data suggest that immobilization enhances the thermal stability of laccase, consistent with the observation that immobilization enhances an enzyme's resistance to high temperatures.

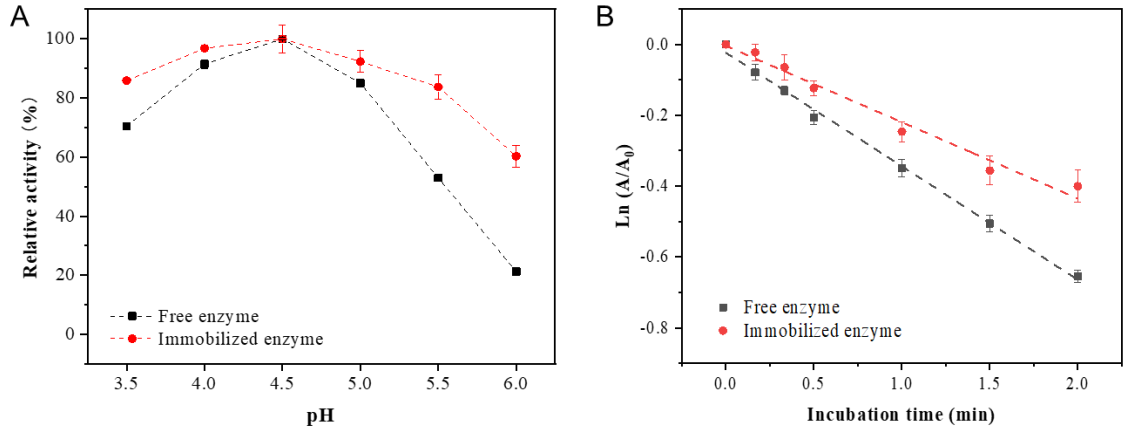

Figure 5 A) The pH stability of laccase-immobilized M3 NFMs and free laccase. B) Thermal inactivation kinetics of laccase-immobilized M3 NFMs and free laccase.

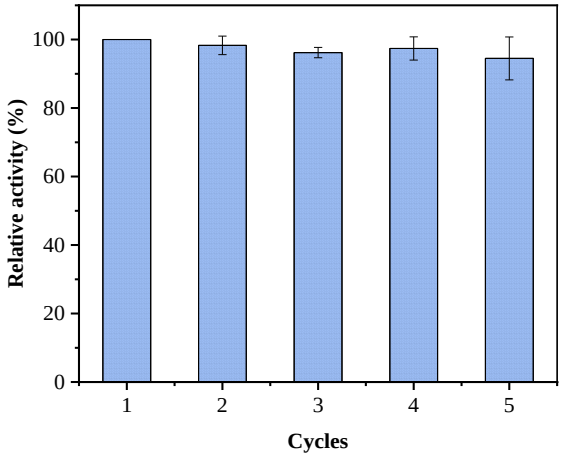

Figure 6 Relative activity of laccase-immobilized NFMs with recycling usage.

The recovery and reuse of catalysts are crucial benefits of enzyme immobilization. To assess the operational stability of the immobilized laccase over multiple cycles, the residual activity of the enzyme was measured after incubation with ABTS, as depicted in **Figure 6**. Remarkably, the immobilized enzyme retained up to 95% of its initial activity after undergoing five cycles of reuse, indicating its excellent operational stability.

3.4. Removal of emerging pollutants

The enzymatic membrane system was applied with a laccase-immobilized M3 membrane and a lab-made TFC membrane. The pharmaceutical depletion performance involved both separation and biocatalytic reaction. Both the concentrations of selected pharmaceuticals were measured in both retentate and permeate. The volume of the membrane performance was set at 450 mL. During the filtration process, the TFC membrane retained about 50% of pharmaceuticals. Therefore, as the feed tank volume decreased, the retained pharmaceuticals led to an increased concentration of both diclofenac (DCF) and mefenamic acid (MFA), as demonstrated in **Figure 7A.** The permeate flux of the TFC membrane was calculated at 17.96 ± 5.2 L m^{-2} h^{-1}.

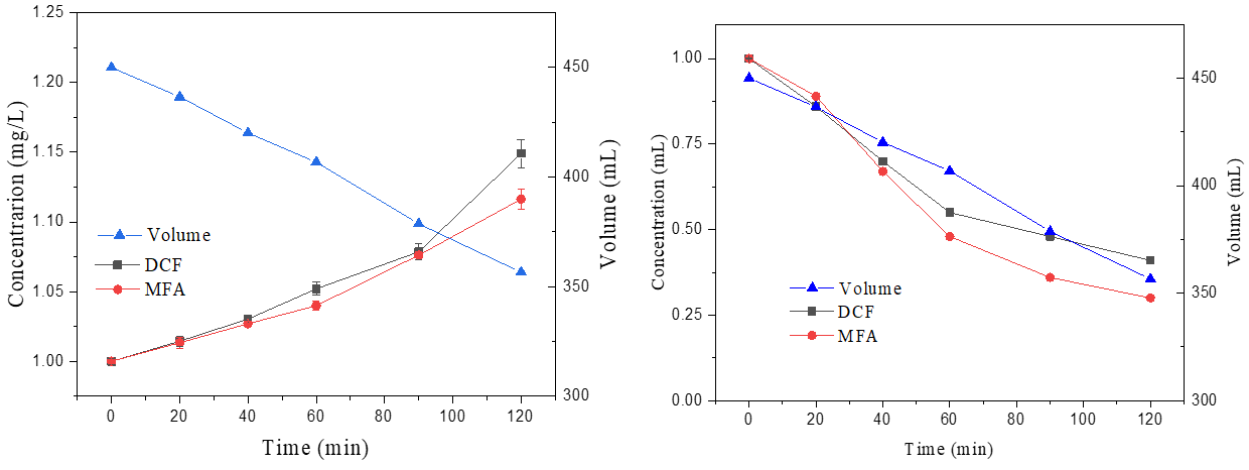

Figure 7 Pharmaceutical concentrations in the retentate A) with a TFC membrane, B) with a TFC and catalytic membrane.

Different from the performance of TFC membranes, the additional layer of a biocatalytic membrane decreased the concentrations of pharmaceuticals in the feed (retentate) side (**Figure 7B**). The immobilized laccase on the NFMs effectively reacted with the substrate molecules on the retentate side. Within two hours, the concentration of DCF and MFA reached 0.41 mg mL^{-1} and 0.3 mg mL^{-1} separately. Notably, the depletion of both DCF and MFA in the permeate by the TFC membrane side reached 52%, and 65%, separately. Higher depletion of pharmaceuticals was achieved by over 85%, largely improved by adding a biocatalytic membrane to the membrane system (**Figure 8**). Overall, the biocatalytic membrane system was able to remove pharmaceuticals effectively. However, this type of pharmaceutical depletion performance involves complex mechanisms, including biocatalytic reaction and membrane separation. As the biocatalytic membrane was kept exposed to the substrates, where the biocatalytic reaction continuously happened, the concentration of the substrate compounds on the retentate side was largely influenced by the performance scale and the contact time with the biocatalysts.

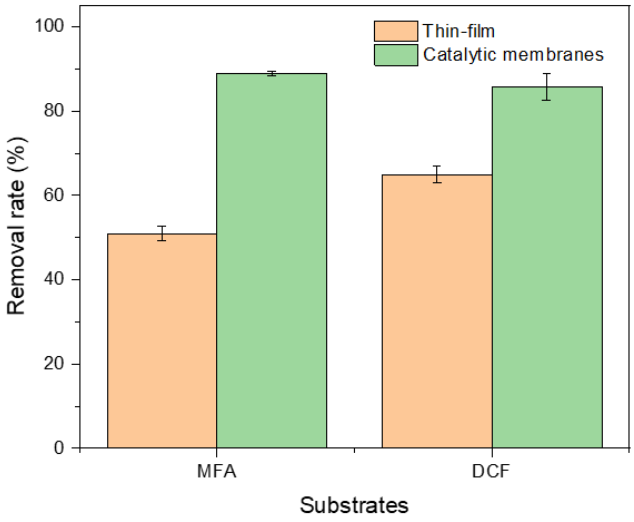

Figure 8 Pharmaceutical depletion in the permeate.

4. Conclusion

The immobilization of laccase onto functionalized PAN/β-CD NFMs was successfully achieved, and the potential of biocatalytic NFMs for pharmaceutical depletion was explored. The results indicate that the incorporation of β-cyclodextrin into the fibers and the introduction of –OH and $–NH_2$ functional groups onto the membrane surface can enhance the enzymatic activity of the membranes. Moreover, the immobilization process has been shown to improve the performance of the biocatalyst. The immobilized enzymes exhibit a broader range of pH and enhanced thermal tolerance, making them highly suitable for industrial applications. Additionally, the ability to recycle the biocatalyst provides an economic advantage over free enzymes, which are expensive to produce. The feasibility of using laccase immobilized membranes in filtration systems has been demonstrated by the high depletion efficiency achieved with two selected pharmaceuticals. Overall, our study highlights the tremendous potential of biocatalytic membrane systems in the removal of pharmaceuticals during wastewater treatment.

Declaration of competing interest

No conflict of interest exists.

Acknowledgment

This work was sponsored by the Novo Nordisk Foundation (NNF18OC0034918) and the Danish Research Council (Grant No. 8022-00237B). The authors would like to acknowledge the financial support from China Scholarship Council. The authors would like to thank Mikael Emil Olsson for the experimental support.

Reference

1. Taheran, M. *et al.* Membrane processes for removal of pharmaceutically active compounds (PhACs) from water and wastewaters. *Sci. Total Environ.* **547**, 60–77 (2016).
2. Baalbaki, Z. *et al.* Fate and mass balance of contaminants of emerging concern during wastewater treatment determined using the fractionated approach. *Sci. Total Environ.* **573**, 1147–1158 (2016).
3. Zhang, X. *et al.* Impacts of sulfadiazine on the performance and membrane fouling of a hybrid moving bed biofilm reactor-membrane bioreactor system at different C/N ratios. *Bioresour. Technol.* **318**, 124180 (2020).
4. Jelic, A. *et al.* Occurrence, partition and removal of pharmaceuticals in sewage water and sludge during wastewater treatment. *Water Res.* **45**, 1165–1176 (2011).
5. Verlicchi, P., Al Aukidy, M., Galletti, A., Petrovic, M. & Barceló, D. Hospital effluent: Investigation of the concentrations and distribution of pharmaceuticals and environmental risk assessment. *Sci. Total Environ.* **430**, 109–118 (2012).
6. Yu, Z., Peldszus, S. & Huck, P. M. Adsorption characteristics of selected pharmaceuticals and an endocrine disrupting compound-Naproxen, carbamazepine and nonylphenol-on activated carbon. *Water Res.* **42**, 2873–2882 (2008).
7. Baccar, R., Sarrà, M., Bouzid, J., Feki, M. & Blánquez, P. Removal of pharmaceutical compounds by activated carbon prepared from agricultural by-product. *Chem. Eng. J.* **211**–**212**, 310–317 (2012).
8. Klavarioti, M., Mantzavinos, D. & Kassinos, D. Removal of residual pharmaceuticals from aqueous systems by advanced oxidation processes. *Environment International* **35**, 402–417 (2009).
9. An, T. *et al.* Kinetics and mechanism of advanced oxidation processes (AOPs) in degradation of ciprofloxacin in water. *Appl. Catal. B Environ.* **94**, 288–294 (2010).
10. Ali, F., Khan, J. A., Shah, N. S., Sayed, M. & Khan, H. M. Carbamazepine degradation by UV and UV-assisted AOPs: Kinetics, mechanism and toxicity investigations. *Process Saf. Environ. Prot.* **117**, 307–314 (2018).
11. Yang, X., Flowers, R. C., Weinberg, H. S. & Singer, P. C. Occurrence and removal of pharmaceuticals and personal care products (PPCPs) in an advanced wastewater reclamation plant. *Water Res.* **45**, 5218–5228 (2011).
12. Acero, J. L., Benitez, F. J., Leal, A. I., Real, F. J. & Teva, F. Membrane filtration technologies applied to municipal secondary effluents for potential reuse. *J. Hazard. Mater.* **177**, 390–398 (2010).
13. Stadlmair, L. F., Letzel, T., Drewes, J. E. & Grassmann, J. Enzymes in removal of pharmaceuticals from wastewater: A critical review of challenges, applications and screening methods for their selection. *Chemosphere* **205**, 649–661 (2018).
14. Bilal, M., Adeel, M., Rasheed, T., Zhao, Y. & Iqbal, H. M. N. Emerging contaminants of high concern and their enzyme-assisted biodegradation – A review. *Environ. Int.* **124**, 336–353 (2019).

15. Chapman, J., Ismail, A. E. & Dinu, C. Z. catalysts Industrial Applications of Enzymes: Recent Advances, Techniques, and Outlooks. doi:10.3390/catal8060238

16. Majeau, J. A., Brar, S. K. & Tyagi, R. D. Laccases for removal of recalcitrant and emerging pollutants. *Bioresour. Technol.* (2010). doi:10.1016/j.biortech.2009.10.087

17. Costa, J. B. *et al.* Enhanced biocatalytic sustainability of laccase by immobilization on functionalized carbon nanotubes/polysulfone membranes. *Chem. Eng. J.* **355**, 974–985 (2019).

18. Luo, M. *et al.* Supported growth of inorganic-organic nanoflowers on 3D hierarchically porous nanofibrous membrane for enhanced enzymatic water treatment. *J. Hazard. Mater.* (2020). doi:10.1016/j.jhazmat.2019.120947

19. Ren, Z., Luo, J. & Wan, Y. Highly permeable biocatalytic membrane prepared by 3D modification: Metal-organic frameworks ameliorate its stability for micropollutants removal. *Chem. Eng. J.* (2018). doi:10.1016/j.cej.2018.04.203

20. Nisha, S., Karthick, A. & Gobi, N. A review on methods, application and properties of immobilized enzyme. *Chem. Sci. Rev. Lett.* **1**, 148–155 (2012).

21. Lante, A., Crapisi, A., Krastanov, A. & Spettoli, P. Biodegradation of phenols by laccase immobilised in a membrane reactor. *Process Biochem.* **36**, 51–58 (2000).

22. Hou, J., Dong, G., Ye, Y. & Chen, V. Enzymatic degradation of bisphenol-A with immobilized laccase on TiO2 sol-gel coated PVDF membrane. *J. Memb. Sci.* (2014). doi:10.1016/j.memsci.2014.06.027

23. Kang, X. *et al.* The investigation of electrospun polymer nanofibers as a solid-phase extraction sorbent for the determination of trazodone in human plasma. *Anal. Chim. Acta* **587**, 75–81 (2007).

24. Sawicka, K., Gouma, P. & Simon, S. Electrospun biocomposite nanofibers for urea biosensing. *Sensors Actuators B Chem.* **108**, 585–588 (2005).

25. Pinto, S. C., Rodrigues, A. R., Saraiva, J. A. & Lopes-da-Silva, J. A. Catalytic activity of trypsin entrapped in electrospun poly(ε-caprolactone) nanofibers. *Enzyme Microb. Technol.* **79**–**80**, 8–18 (2015).

26. Xu, R., Cui, J., Tang, R., Li, F. & Zhang, B. Removal of 2,4,6-trichlorophenol by laccase immobilized on nano-copper incorporated electrospun fibrous membrane-high efficiency, stability and reusability. *Chem. Eng. J.* **326**, 647–655 (2017).

27. Khalil, A. M. & Schäfer, A. I. Cross-linked β-cyclodextrin nanofiber composite membrane for steroid hormone micropollutant removal from water. *J. Memb. Sci.* **618**, 118228 (2021).

28. Topuz, F., Holtzl, T. & Szekely, G. Scavenging organic micropollutants from water with nanofibrous hypercrosslinked cyclodextrin membranes derived from green resources. *Chem. Eng. J.* **419**, 129443 (2021).

29. Taheran, M. *et al.* Covalent Immobilization of Laccase onto Nanofibrous Membrane for Degradation of Pharmaceutical Residues in Water. *ACS Sustain. Chem. Eng.* **5**, 10430–10438 (2017).

30. Li, G. *et al.* Laccase immobilized on PAN/O-MMT composite nanofibers support for

substrate bioremediation: A: de novo adsorption and biocatalytic synergy. *RSC Adv.* **6**, 41420–41427 (2016).

31. Gao, Y., Li, G., Zhou, Z., Guo, L. & Liu, X. Supramolecular assembly of poly(β-cyclodextrin) block copolymer and benzimidazole-poly(ε-caprolactone) based on host-guest recognition for drug delivery. *Colloids Surfaces B Biointerfaces* **160**, 364–371 (2017).

32. Zhang, P., Wang, Q., Zhang, J., Li, G. & Wei, Q. Preparation of amidoxime-modified polyacrylonitrile nanofibers immobilized with laccase for dye degradation. *Fibers Polym.* **15**, 30–34 (2014).

33. Ma, X.-H. *et al.* Nanofoaming of Polyamide Desalination Membranes To Tune Permeability and Selectivity. *Environ. Sci. Technol. Lett.* **5**, 123–130 (2018).

34. Hu, D. *et al.* Constructing highly rough skin layer of thin film (nano) composite polyamide membranes to enhance separation performance: A review. *J. Appl. Polym. Sci.* **139**, e52692 (2022).

35. Rabilloud, T. Optimization of the cydex blue assay: A one-step colorimetric protein assay using cyclodextrins and compatible with detergents and reducers. *PLoS One* **13**, e0195755 (2018).

36. Boudrant, J., Woodley, J. M. & Fernandez-Lafuente, R. Parameters necessary to define an immobilized enzyme preparation. *Process Biochem.* **90**, 66–80 (2020).

Biodegradable Crosslinked Nanofibrous Membranes for Enzyme Immobilization and Transformation of Emerging Pollutants.

Dan Zhao[a], Tian Tian[b], Maria Louise Leth[c], Maher Abou Hachem[c], Claus Hélix-Nielsen[a, *], Wenjing (Angela) Zhang[a, *]

a. Department of Environmental and Resource Engineering, Technical University of Denmark, DTU, 2800 Kgs. Lyngby, Denmark

b. MOE Key Laboratory of Bioinorganic and Synthetic Chemistry, School of Chemistry, Sun Yat-sen University, Guangzhou, 510006 P. R. China

c. Department of Biotechnology and Biomedicine, Technical University of Denmark, DTU, 2800 Kgs. Lyngby, Denmark

[*] **Corresponding author:**

Dr. Wenjing (Angela) Zhang

Tel: (+45) 20352356; E-mail address: wen@env.dtu.dk

Dr. Claus Hélix-Nielsen

Tel: (+45) 45252228; E-mail address: clhe@env.dtu.dk

Abstract

Enzymatic membranes, integrating the benefits of membranes and enzymes, have gained attention in wastewater treatment. However, disposing of these plastic membranes is not environmentally sustainable. As a result, researchers have explored the use of biodegradable polymeric membranes as carriers for enzyme immobilization. One such material is β-cyclodextrin (β-CD), a natural compound derived from starch with a unique toroidal cavity with a hydrophobic interior and a hydrophilic exterior. These materials offer a high surface-to-volume ratio and biodegradability, making them a promising alternative. In this research, we have synthesized biodegradable crosslinked HP-β-CD NFMs to immobilize laccase. The β-cyclodextrin based nanofibers were characterized using FTIR and SEM to evaluate their structural and morphological properties. The crosslinked HP-β-CD NFMs were highly insoluble in various solvents, including water, ethanol, DMAc, n-Hexane, and toluene, indicating their potential in various applications. Laccase immobilization on the crosslinked HP-β-CD NFMs was achieved through adsorption and was found to remarkably enhance the stability of the enzyme, particularly with higher resistance towards neutral pH. The immobilized laccase on the crosslinked NFMs also showed potential for repeated use, with over 80% of initial activity maintained and effective in depleting >80% of two emerging pollutants (diclofenac and mefenamic acid) after three times of use. This is the first study to employ scalable insoluble biodegradable crosslinked HP-β-cyclodextrin NFMs as laccase carriers and highlights the promising potential of biodegradable NFMs for the treatment of emerging pollutants

Keywords: Laccase, Biodegradable membrane, Immobilization, Cyclodextrin polymer

Graphical Abstract

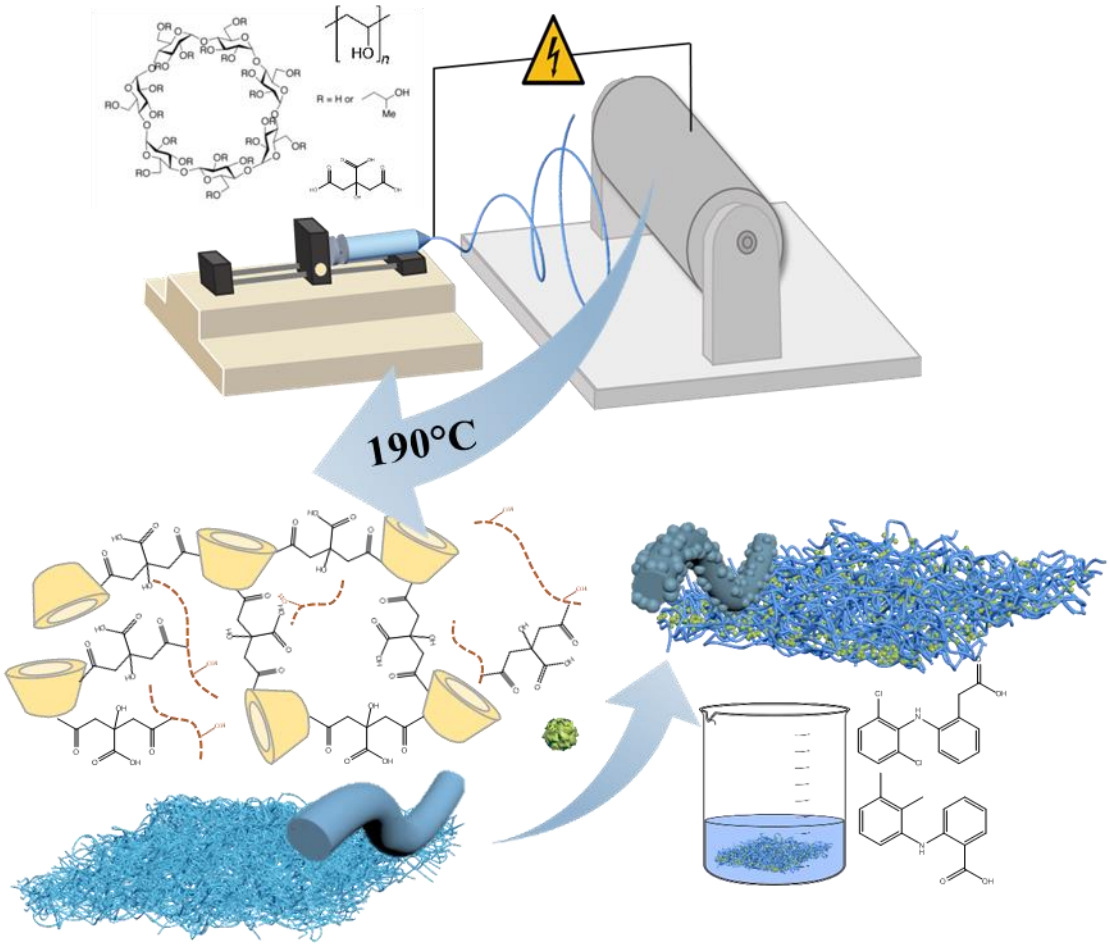

1. Introduction

Emerging pollutants (EPs), including distinct pharmaceuticals, personal care products, polycyclic aromatic hydrocarbons as well as pesticides, are persistent compounds in the environment at trace concentrations and exposure to these EPs might have detrimental effects on both environment and human beings [1–4]. The usage of these compounds has been increasing considerably; however, there are no guidelines or standards regarding the disposal and discharge of EPs in existing wastewater treatment plants (WWTPs) at present [5]. Efforts to address these emerging concerns have been applied, e.g., EP removal during water treatment, such as activated sludge adsorption [6] and membrane filtration [7]. However, even though a high EP adsorption on activated sludge and membrane filtration is accomplished, further treatment is required in both cases, including post-treatment of enriched EPs in the sludge and retentate of the membrane process. Therefore, a green and environmentally friendly process chemically transforms the pollutants, making further treatment of concentrated pollutants a necessity.

Enzymatic electrospun membranes where biocatalysts are embedded or immobilized have drawn significant attention. Among known biocatalysts, laccases (benzenediol: oxygen oxidoreductase, EC 1.10.3.2) are the most promising group for industrial application due to their broad activity on substrates that includes synthetic dyes, chlorinated phenolics, and polycyclic aromatic hydrocarbons [8–10]. The high specific area of the nanofibers largely improves the enzyme immobilization yields. Apart from increasing the surface area, another strategy is to enhance the electron transfer rate between substrates and laccase, thereby increasing the catalytic efficacy of the immobilized enzymes [11–13]. Furthermore, spacers that tether the enzyme to the membrane surface [14,15], conferring higher flexibility and possibly active site accessibility, are commonly employed in enzyme immobilization. Spacers such as glutaraldehyde, ethylenediamine,

hexamethylenediamine, and poly(ethylene glycol) have been shown to provide high relative activity compared to conjugation directly to the support [16,17]. Notably, the durability of biocatalytic membranes is largely limited by enzyme catalytic performance. Therefore, contaminated biocatalytic membranes without catalytic activities are required to be taken into consideration. However, most enzyme carrier materials are non-degradable polymers, such as polyacrylonitrile, poly(vinylidene fluoride), and polystyrene, which may cause an extra burden to the environment by discharging the used polymeric membrane as plastic waste. Much effort has been applied to addressing the problem. Dan et al. [18] successfully developed flexible ceramic membranes as enzyme carrier materials. However, the complex fabrication processes involving high temperatures to eliminate polymeric sacrifice content possess high energy consumption. Another strategy to avoid plastic waste is to incorporate natural biodegradable compounds into the membranes, such as cellulose [19], chitosan [20], nano clay, and β-cyclodextrin (CD). Electrospun blend membranes of polyurethane, amidoxime polyacrylonitrile, and β-cyclodextrin have been developed as enzyme carriers and found high catalytic activity and resistance against the variations of temperature and pH value than the free laccase [21].

Inspired by the previous research, CD, a natural compound from starch possessing a unique toroidal cavity with a hydrophobic interior and hydrophilic exterior, has drawn our attention. This unique structure acts as a supramolecular complexation agent for a broad spectrum of molecules, ranging from small, poorly soluble drug molecules to large polymer chains forming pseudorotaxanes. CD polymers have attracted considerable research interest as such materials combine the benefits of a high surface-to-volume ratio and high functional CD content. CD polymers have been heavily utilized in environmental applications. One of the applications is to scavenge textile dyes and polycyclic aromatic hydrocarbons from water. The crosslinked CD

polymers demonstrated rapid scavenging of pollutants with a maximum adsorption capacity of 692 mg g^{-1} [22].

Herein, we designed insoluble biodegradable NFMs for enzyme immobilization to build a biocatalytic membrane reactor with efficient degradation performance. The biodegradable NFMs, utilizing HP-β-cyclodextrin as the primary material, citric acid as a crosslinker, and polyvinyl alcohol (PVA) as a spinning polymer, were fabricated by electrospinning followed by thermal crosslinking. The highly insoluble NFMs have a potential for laccase immobilization. This is the first study to employ scalable insoluble biodegradable crosslinked HP-β-cyclodextrin NFMs as laccase carriers for emerging contaminant transformation applications.

2. Materials and methods

2.1. Chemicals and materials

Laccase from *Trametes versicolor* (EC 1.10.3.2, ≥0.5 U mg^{-1}), sodium acetate (NaOAc), acetic acid (HOAc), 2,2'-azino-bis(3-ethyl-benzothiazoline-6-sulfonic acid: ABTS), poly(vinyl alcohol) (PVA, Mw 89,000~98,000 Da), hydroxypropyl-beta-cyclodextrin (HP-β-CD), citric acid, diclofenac (DCF) sodium salt, mefenamic acid (MFA) were purchased from Sigma-Aldrich. Milli-Q water (Millipore Milli-Q system; 18.2 MΩ cm resistance) was used during the experiments. Solvents used in this work are listed in **supporting material T1**.

2.2. Experimental procedures

2.2.1. Fabrication of electrospun HP-β-CD nanofiber membranes (NFMs)

Figure 1 illustrates the fabrication process of the crosslinked HP-β-CD NFMs. 100-150% (w/w) of HP-β-CD was dissolved in water, and 20% (w/w) of citric acid was added with respect to the HP-β-CD content. 10 g 5% (w/w) PVA was slowly added to the HP-β-CD solution. The mixed solution was homogenized by mixing for six hours at room temperature. The electrospinning was

carried out by a needle-based electrospinner (NS+, Inovenso, Turkey), corporate with a precision air Conditioner (NS AC150, Elmarco, Czech Republic). The solution was filled in a 10 mL syringe and fed through a stainless steel needle with an inner diameter of 0.8 mm at a constant rate of 0.8 mL/min. The spinning voltage and tip-to-collector distance were applied to 15.3 kV and 10 cm, respectively. The temperature and relative humidity were set at 25 °C and 30 %. The electrospun nanofibers were collected on aluminum foil set with a constant speed of 200 rpm, and the acquired nanofibers (HP-β-CD NFMs) were then stored in a vacuum oven for two hours at 40 °C to clear up the solvent completely. The fibers were heated in a vacuum oven at 140 °C, 170 °C, and 190°C for four hours to obtain the water-insoluble electrospun fibers for the thermal crosslinking. The crosslinked HP-β-CD membranes with different conditions are listed in **Table 1**.

	M_{PVA} (g)	$M_{HP\text{-}\beta\text{-}CD}$ (g)	M_{CA} (g)	Temperature[a]
C1-140	0.5	15	3	140
C2-140	0.5	10	2	140
C3-140	1	10	2	140
C1-170	0.5	15	2	170
C2-170	0.5	10	2	170
C3-170	1	10	2	170
C1-190	0.5	15	2	190
C2-190	0.5	10	2	190
C3-190	1	10	2	190

a refers to the temperature of thermal crosslinking

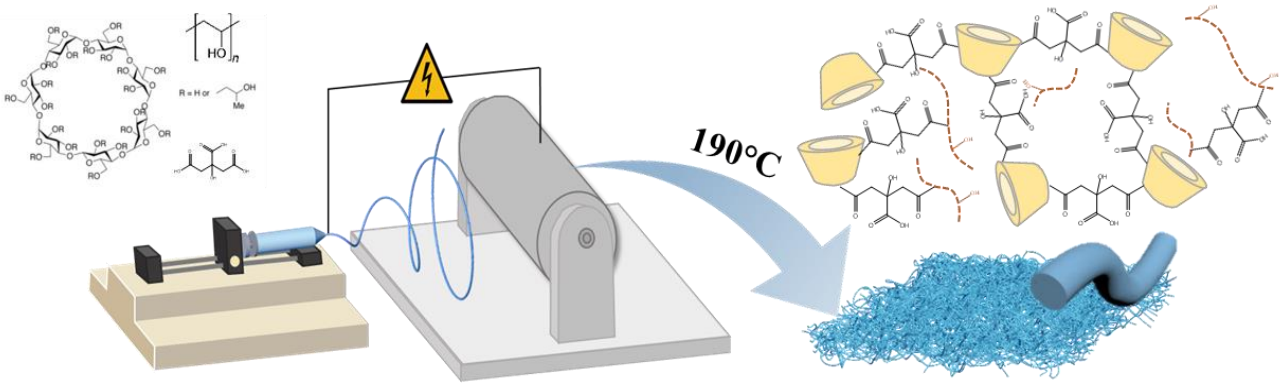

Figure 1 Schematic illustration of crosslinked HP-β-CD membranes fabrication.

125

126 2.2.3. Laccase immobilization and enzyme assays

127 Laccase immobilization on the modified NFMs was performed as described by Lee et al.[23] with
128 minor modifications. Briefly, the membrane (36 cm^2) was immersed in a 5 mg mL^{-1} (by weight)
129 laccase solution in 50 mM NaOAc buffer, pH 4.5 and incubated for one h at 25 °C, and
130 subsequently transferred to 4 °C for 2, 6, 12, and 24 h. Next, the laccase immobilized membrane
131 was washed three times with the same buffer and stored at 4 °C. NFMs for enzyme assays were
132 cut before the immobilization. The laccase activities in the initial immobilization bath, the residual
133 after immobilization, and the wash fractions were determined spectrophotometrically using ABTS
134 as the substrate. Specifically, 10 μL enzyme stock or 0.25 cm^2 of the laccase-immobilized
135 membrane was added to 0.5 mM ABTS solution in 20 mM NaOAc buffer, pH 4.5, and the reaction
136 mixture (300 μL) was incubated in a microtitre plate for 10 min after a 30-second rotary agitation
137 at 25 °C, and the absorbance at 420 nm was monitored continuously.

138 Subsequently, the effect of pH on laccase activity was evaluated by testing both the free and
139 immobilized enzyme prepared in 20 mM NaOAc at pH 3.5-6.5 and monitoring the absorbance at
140 420 nm at 25 °C. Furthermore, a thermal inactivation assay was performed to investigate the
141 stability of both the free and immobilized enzymes. An Eppendorf tube containing 980 μl NaOAc
142 buffer (50 mM) was preheated at 50°C for 5 min. 20 μl of 5 mg ml^{-1} enzyme solution (by weight)
143 was added to the preheated buffer solution and incubated at 50 °C. Then, 100 μl aliquots were
144 collected at 10, 20, 30, 60, 90, and 120 min and stored on ice. Next, the residual activity was
145 assayed using the standard assay described above at 25 °C. For the immobilized enzyme, three
146 pieces of immobilized fibers were assayed before heating, and the same fiber was washed
147 thoroughly. Thereafter, the washed fiber was incubated in a water bath at 50 °C for 10 min, stored

148 on ice, and assayed for the remaining activity. This was repeated with new pieces of fibers at 20,
149 30, 60, 90, and 120 min.
150 2.2.4. EPs degradation by free enzyme and laccase-immobilized membranes
151 To investigate the catalytic performance of laccase immobilized crosslinked HP-β-CD membranes,
152 a 250 mL EP mixture (with 200 μg L^{-1} of each EP) in Miliq H_2O, including mefenamic acid and
153 diclofenac, was used as feed solution in a batch study. The active membrane area was 36 cm^2.
154 Duplicate samples were taken at different reaction times, filtered through 0.2 μm PTFE filters into
155 2 mL vials. Subsequently, acetonitrile was added as a quenching reagent.
156 **2.3. Characterization and analytical procedures**
157 2.3.1. Characterization of NFMs.
158 The microstructure of the electrospun fibers was analyzed by field emission scanning electron
159 microscopy (Quanta FEG 250, FEI, USA) at an accelerating voltage of 5 kV. The chemical
160 structure of each NFM was analyzed by Fourier transform infrared spectroscopy-Attenuated Total
161 Reflectance (FTIR-ATR, Bruker, Germany).
162 2.3.2. Solubility Test of Crosslinked HP-β-CD membranes
163 For the solubility experiment, squares of 6 cm^2 of the fiber mats were immersed in deionized water.
164 After 24 h, the fiber mats were removed from the deionized water and placed in a vacuum oven to
165 dry until constant weight. The insoluble fraction (%), water uptake (WU), and in-plane swelling
166 ratio (SR) were determined as follows:
167 $$\text{Insoluble fraction}(\%) = \frac{W_i}{W_0} \times 100\% \quad (1)$$
168 $$\text{WU} = \frac{W_a - W_d}{W_d} \quad (2)$$
169 $$\text{SR} = \frac{L_a - L_d}{L_d} \quad (3)$$

Where W_0, W_i were defined as the fiber weight of initial and after drying, [mg]; W_a, W_d were defined as the weight of wet and dry fibers, [mg]; L_a and L_d were the lengths of the wet and dry membranes, [cm]

Additionally, the solvent resistance of the fibers was demonstrated by immersing the fibers into various solvents for 24 h. The effect of pH on crosslinked NFMs was evaluated by immersing the fibers at different pH of an aqueous 1 mM NaCl solution. The pH of the KCl solution was adjusted to 4.5, 7, and 9 by adding either 50 mM HCl or NaOH.

2.3.2. Determination of enzyme activity.

The enzyme activity (A) of enzyme solution (A_{free}) or fiber (A_{fiber}) was calculated from the initial slope of the obtained absorbance versus the time curve (Abs_{420} min^{-1}). One unit of enzyme activity (U) was defined as the amount of enzyme which converts 1 μmol of ABTS per minute under the assay conditions (μmol min^{-1}).

$$A = \frac{\alpha \times V_{\mathrm{Total}}}{\varepsilon \times d} \quad (4)$$

where V_{Total} is the volume of total assay and enzyme solution (μL), α is the absorbance per minute at 420 nm, determined by linear regression (min^{-1}), d is the light path of the assay, estimated by assay volume, and the single well area of the microplate (cm), and ε represents the molar absorption coefficient of ABTS at 420 nm, 36,000 $M^{-1} \cdot cm^{-1}$.

The specific activity of the enzyme immobilized fiber (SA_{fiber}) were defined as the enzyme activity of fiber per weight of support membrane (U g^{-1} fiber).

$$SA_{\mathrm{fiber}} = \frac{A_{\mathrm{fiber}}}{M_{\mathrm{fiber}}} \quad (5)$$

where M_{fiber} is mass of tested fibers, [g].

2.3.4. Determination of EPs degradation efficiency

The concentrations of EPs were analyzed by High-Performance Liquid Chromatography–Triple Quadrupole Mass Spectrometry (1290 Infinity II-6470 LC-QQQ, Agilent Technologies). The conversion efficiency (*D*) was calculated as:

$$D = \frac{C_{\mathrm{EP}_0} - C_{\mathrm{EP}}}{C_{\mathrm{EP}_0}} \times 100\% \quad (5)$$

where C_{EP0} and C_{EP} are the EP concentrations in solutions before and after degradation experiments.

3. Result and discussion

3.1. Membrane morphology and chemical structure

Figure 1 depicts the morphology of pristine and crosslinked HP-β-CD NFMs with different ratios of PVA and HP-β-CD. **Figure 1A-B** exhibited the morphology of C1 NFMs with the highest content of HP-β-CD. The membrane consisted of a large number of beads and particles, but barely any fiber structures were observed. The possible reason for beads and particle formation during the electrospinning could be the high viscosity of the solution and an extremely low ratio of PVA. With the decrease of HP-β-CD content and increase of PVA, enhancing the electrospinnability of the solution, smooth and uniform nanofibers were observed in both C2 NFMs and C3 NFMs, as shown in **Figure C** and **Figure E**. Both fibers were noticed with a ribbon structure instead of cylinder structure. The fiber diameters of C3 NFMs were 1.6 times increased than that of C2 NFMs. After the thermal crosslinking treatment at 190°C, both pristine C2 and C3 NFMs maintained intact fiber structures but with a slight decrease in the fiber diameters from 883 ± 58 to 850 ± 103 nm and 1418 ± 188 to 1413 ± 182 nm, separately. The fiber distribution on pristine and crosslinked C2 and C3 NFMs is depicted in **Figure S2**.

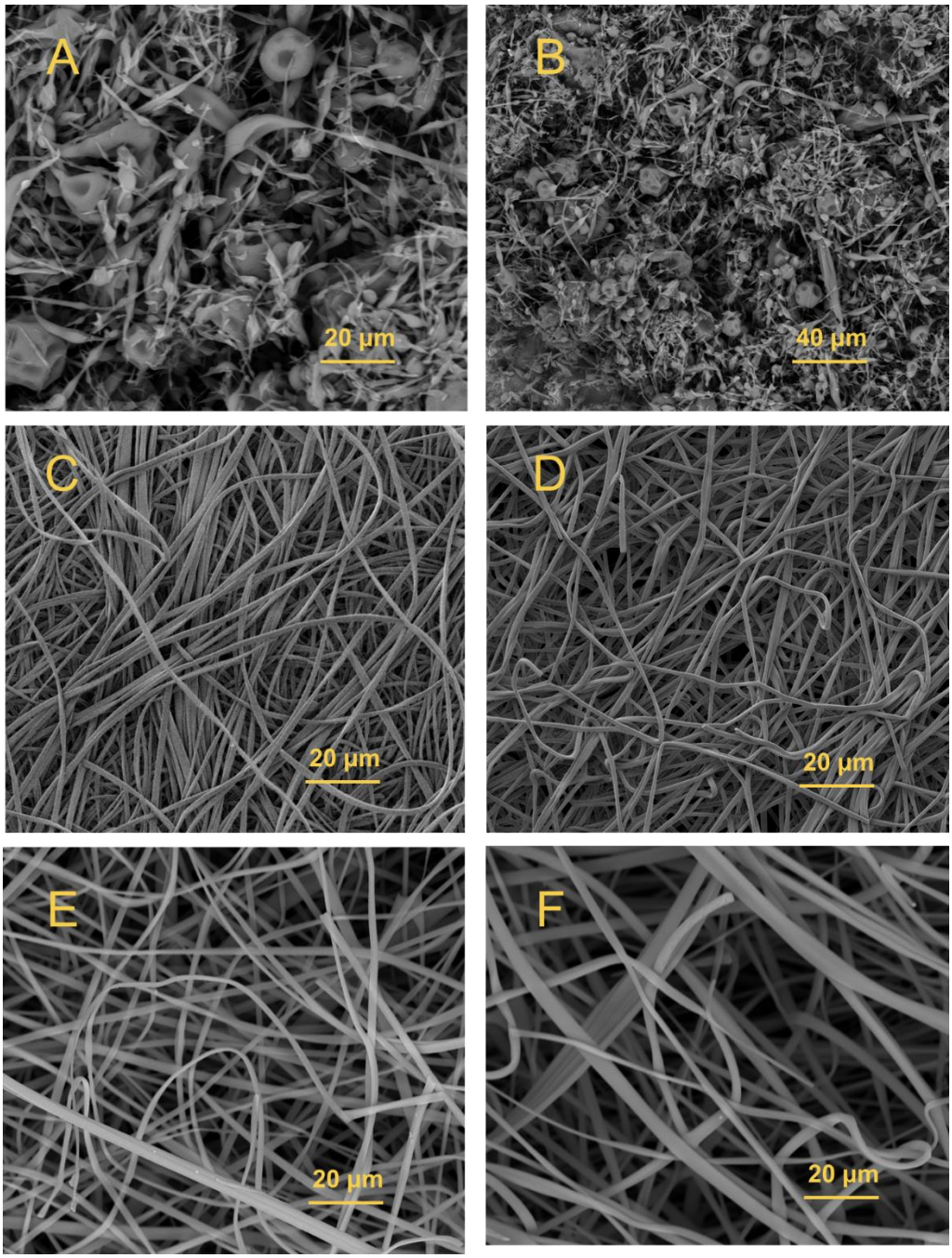

Figure 2 SEM images of A, B) pristine C1 NFMs with different magnifications. C, D) pristine C2 NFMs and crosslinked C2-190 NFMs, E, F) C3 NFMs and crosslinked C3-190 NFMs

The stability of crosslinked HP-β-CD NFMs was found to be influenced mainly by the pH of the aqueous solution. **Figure 3** depicts the morphology difference after treating the C2-190 NFMs in aqueous solutions with different pH values.

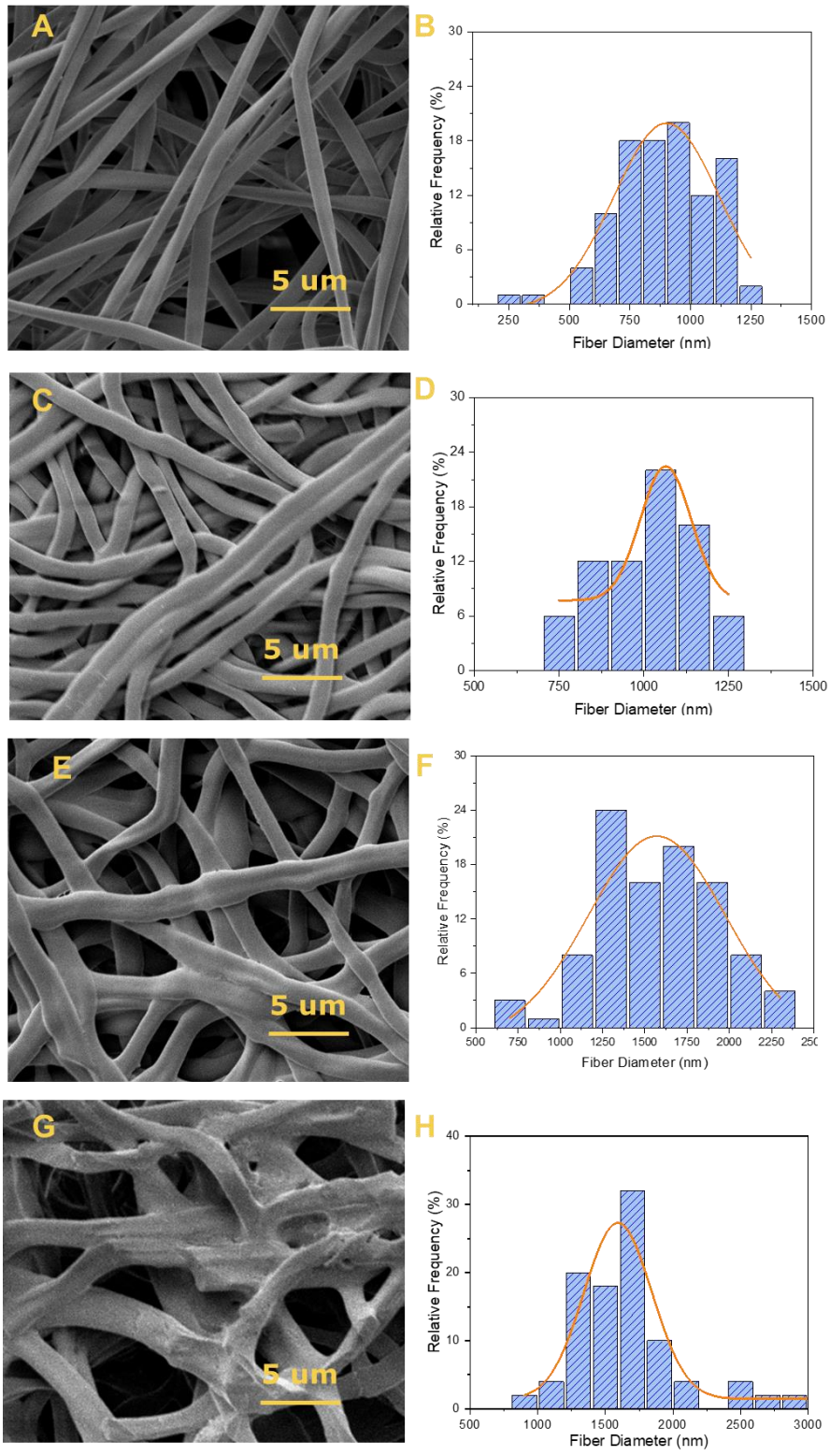

Figure 3 Morphology and fiber diameter distribution histograms of C2-190 NFMs treated in aqueous solutions with different pH values: A, B) Untreated; C, D) pH = 4.5; E, F) pH = 7; and G, H) pH = 9.

Notably, pH values play a significant role in fiber diameters. After immersing the fibers in the different aqueous solutions for 24 h, the diameters of the fibers were found to have various degrees of swelling, and it turned out that with the increase of pH values, the swelling degree of fiber diameter was increased consistently. The fiber diameter distribution treated in pH 4.5, 7, and 9, compared with the pristine C2-190 NFMs (850 ± 103 nm), was 1065 ± 75 nm, 1570 ± 406 nm, and 1593 ± 251 nm. In addition, another finding is that in an alkaline solution, defects and edges were observed. The fibers tended to aggregate together, indicating the poor resistance of the fibers in the alkaline condition.

FTIR was used to investigate the possible chemical bond formation and secondary interactions, indicating the differences between the electrospun fibers before and after the thermal crosslinking process. As depicted in **Figure 3**, in the spectra of pristine HP-β-CD NFMs, the −OH vibration band in alcohol groups between 3000-3600 cm^{-1} and asymmetric and symmetric streching bands of $-CH_2$ were observed at 2982 cm^{-1} and 2926 cm^{-1}, respectively. C–O–C vibration streching bands at 1156 cm^{-1}, C−O streching bands at 1032 cm^{-1} and were observed. The characteristic peaks at 951, 1032, and 1156 cm^{-1} were observed. The peak at 945 cm^{-1} is due to the R-1,4-bond skeleton vibration of β-CD, and the peak at 1032 cm^{-1} corresponds to the antisymmetric glycosidic va(C–O–C) vibrations. The peak at 1156 cm^{-1} corresponds to the C–H vibration. Similar absorption bands were also seen in the crosslinked NFMs. The degree of crosslinking was determined from the absorbance ratio (A 1082/A 1033) in this region of the spectrum. After thermal treatment, an increase of about 6% was observed in the A 1082/A 1033 ratio for crosslinked HP-β-CD NFMs when compared to pristine NFMs. FTIR analysis revealed the shift of a characteristic corresponding to the symmetric stretching bands of $-CH_2$ at 2916 cm^{-1} and C =

O stretching vibration of the crosslinker at 1720 cm^{-1}, whereas the pristine HP-β-CD showed at 2922 cm^{-1} and 1735 cm^{-1} (**Figure 4B-C**).

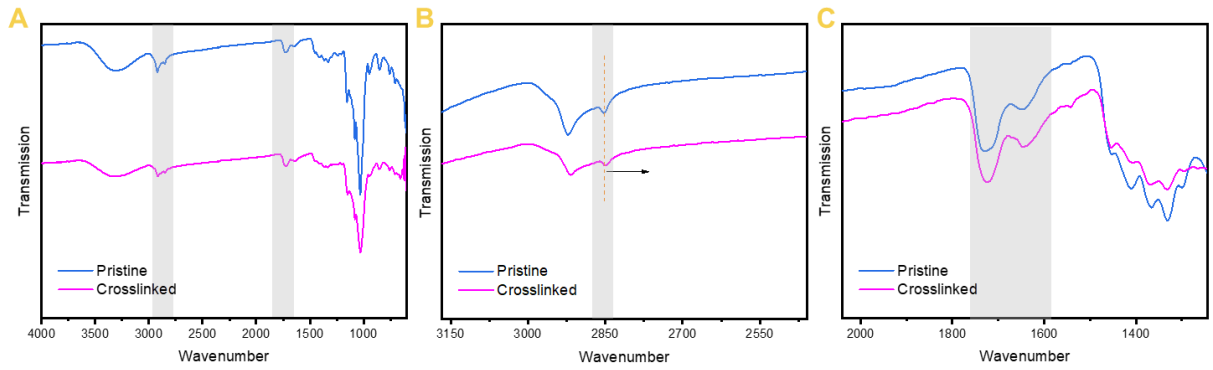

Figure 4 A) FTIR-ATR spectrum of pristine and crosslinked HP-β-CD NFMs. B) Enlargement of wavenumber region from 3150 to 2550 cm^{-1}. C) Enlargement of wavenumber region from 2000 to 1400 cm^{-1}.

3.2. Solubility of Crosslinked HP-β-CD NFMs

The swelling behavior of the crosslinked films was observed by the change in film area after being wetted with 1mM NaCl aqueous solution for 24 h. **Table 2** lists the water intake, insoluble fractions, and in-plane swelling ratio of different HP-β-CD NFMs. Notably, the insoluble fraction of NFMs was largely influenced by the temperature of thermal crosslinking. The increase in temperature intensifies the crosslinking degree of the HP-β-CD and citric acid. The insoluble fraction of the crosslinked C2-170 NFMs and C2-190 NFMs increased from 82.3% to 86%.

Table 2. Water uptake, in-plane swelling ratio, and insoluble fraction of different HP-β-CD NFMs.

	pH	Temperature (°C)	WU	SR	Insoluble fraction (%)
C2 NFMs	7	170	2.1	0.05	82.3
	4.5	190	3.3	0.04	86.7
	7	190	2.3	0.04	86.0
	9	190	4.6	0.07	81.8
C3 NFMs	7	170	2.2	0.05	80.1
	4.5	190	3.0	0.04	83.8
	7	190	2.3	0.04	84.2
	9	190	4.9	0.06	80.3

Similarly, the same trend of increase in the insoluble fraction of the crosslinked C3 NFMs was observed, but the value was slightly lower than crosslinked C2 NFMs. The change in pH values influenced the swelling ratio and water uptake of crosslinked NFMs. In accordance with the result of fiber diameter, both crosslinked C2 and C3 NFMs exhibited the highest water uptake and in-plane swelling ratio, indicating poor resistance to the alkaline solutions. Overall, C2-190 NFMs were the best candidates considering the insoluble fractions.

The solubility of C2-190 NFMs in different solvents was investigated, as shown in **Figure 5**. The crosslinked nanofibers strongly resist various solvents, including DMAc, DMSO, and ACN, indicating a strong potential use of these NFMs in the industrial industry.

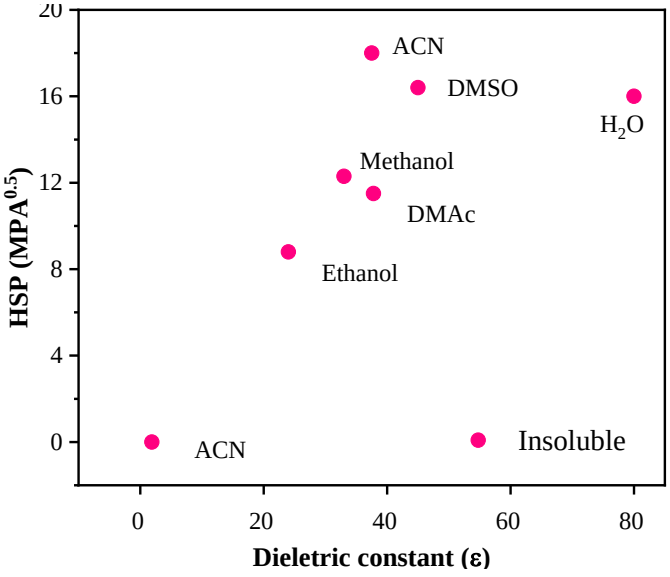

Figure 5. Solubility test for C2 NFMs in various solvents.

3.2. Optimization of immobilization

Enzyme activity is a crucial parameter to evaluate the support materials and immobilization performance. In order to optimize the activity of biocatalytic NFMs, the reaction time and mass ratio of enzyme to fibers were adjusted. **Figure 6.** exhibits total residual enzyme activity in the

residue solution, washing buffer, immobilized fibers, and the calculated lost activity with different immobilization times. High enzyme activity of fiber (A_{fiber}) loss is observed, correlated to the reaction time between laccase and NFMs. The highest enzyme activity of fiber was achieved to 0.0012 U g^{-1}fiber after a 12-hour reaction time. Nevertheless, the highest enzyme activity of fiber only corresponded to 3% of total activity, as described in **Figure 6A**. One of the possible reasons could be attributed to the crosslinked materials, where unreacted citric acid could be released from the fibers, resulting in a pH shift in the residue solution. The high activity loss may be correlated to crowding of immobilized enzymes on the fibers, which is consistent with the results in **Figure 6B**. Fiber maintains 56% of the activity while the enzyme load is reduced by 50%, while activity losses decline from 78% to 73%. Further reduction of enzyme load led to a significant loss of fiber activity. Therefore, optimizing the reaction time is essential to maximize the yield of immobilization active enzyme per membrane mass in this study.

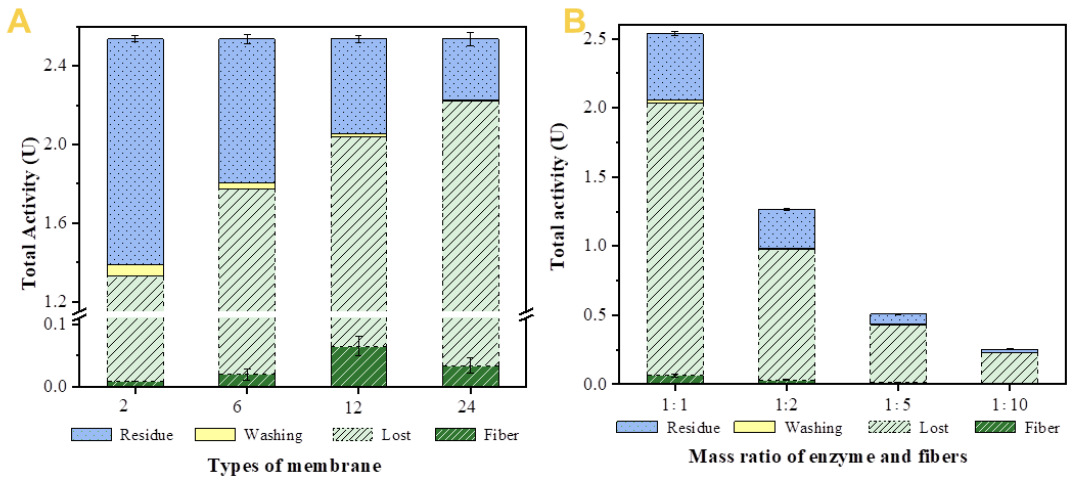

Figure 6. A) Total residual enzyme activity in the residue solution, washing buffer, immobilized fibers, and the calculated lost activity with different immobilization times. B) Total residual enzyme activity in the residue solution, washing buffer, immobilized fibers, and the calculated lost activity with different enzyme stock.

3.3. Stability of the immobilized laccase

Recovering and reusing the catalysts is one of the advantages of enzyme immobilization. In order to elucidate this, laccase immobilized C2-190 NFMs were repeatedly incubated with ABTS, and the catalytic activity was measured and the results are illustrated in **Figure 7a**. The fibers maintained over 80% of initial activity after three-time testing. However, only around 60% of the initial activity of the immobilized enzyme was retained after five cycles of reuse. A possible explanation could be the loss of fiber fractions washed off and left in the washing solution, leading to a sharp drop in fiber activity during the fierce washing process. The results demonstrated that laccase immobilized on NFMs offers high operational stability but the poor mechanical properties limit the potential use of NFMs.

Figure 7B shows the effect of pH on the relative activities of free and immobilized laccase on C2-190 NFMs. The optimum pH values of the free and immobilized laccase were 4.5 and 5.0, correspondingly. This apparent pH shift to a higher value, in accordance with the literature [24,25] can be explained by the acidic crosslinkers in the NFMs resulting to the surface of the support more acidic than the buffer solution. Enzyme immobilization resisted enzyme denaturing that the immobilized laccase maintained more than 30% of its optimum activity at a higher range of pH values. Similar observations were noticed for laccase immobilized on PAN/O-MMT composite nanofiberss, and the optimum pH was found to be 3.0 for free laccase as compared to 3.5 for immobilized laccase [24].

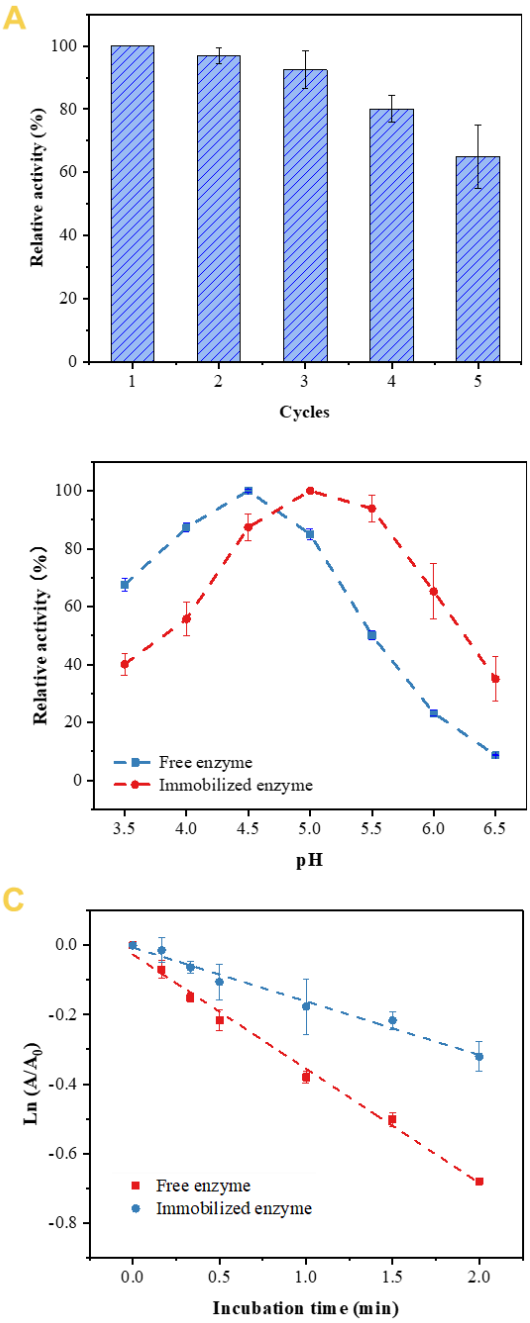

Figure 7. A) Relative activity of laccase-immobilized NFMs with recycling usage. B) The pH stability of Lac-C2-190 NFMs and free laccase. C) Thermal inactivation kinetics of Lac-C2-190 NFMs and free laccase.

With regard to thermal stability, thermal inactivation kinetics for free and immobilized laccase was studied (**Figure 7C)**. A_0 and A refer to the initial and remaining activity of the free or immobilized enzyme. The residual activity of immobilized laccase was 72.5 ± 3.1% as compared to 50.7 ± 0.4% for free laccase after heating for 120 min at 50 °C. Thermal inactivation data were modeled with first-order kinetics, with coefficients of Determination (COD) of 0.99 and 0.98 for free and immobilized laccase, respectively. The thermal inactivation rate constant (k_{inact}) decreased two-fold for the immobilized enzyme (0.15 h^{-1}) as compared to the free laccase (0.33 h^{-1}), which corresponds to an increase in the half-time of thermal inactivation ($t_{1/2}$) at 50 °C from 2.1 h to 4.3 h. These data revealed improved thermal stability of the immobilized laccase compared to the free form, which is consistent with the observation that the enzyme's resistance to high temperatures is greatly increased by immobilization [18,26].

3.4. Removal of emerging pollutants

The occurrence of EPs is commonly found in wastewater treatment plants (WWTPs) effluent at concentrations ranging from low ng L^{-1} to a few μg L^{-1}. The occurrence of DCF and MFA are found in a range of 3.04−411 ng L^{-1} and 3.65−13.9 ng L^{-1} separately in the effluents of the WWTPs [27]. However, the extremely low concentration of the EPs challenges both the detection and catalytic performance of the biocatalytic materials. Therefore, our study focuses on removing EPs by the enzymatic reaction, which is considered a post-treatment process. **Figure 8A-B** depicts the EPs depletion by crosslinked C2-190 NFMs and lac-C2-190 NFMs. The pristine NFMs have shown about 18% and 57% of depletion outcomes on DCF and MFA due to the adsorption properties within three hours. After the enzyme immobilization, the biocatalytic membranes notably largely enhanced the depletion outcomes, where 60% of DCF and 89% of MFA were effectively transformed.

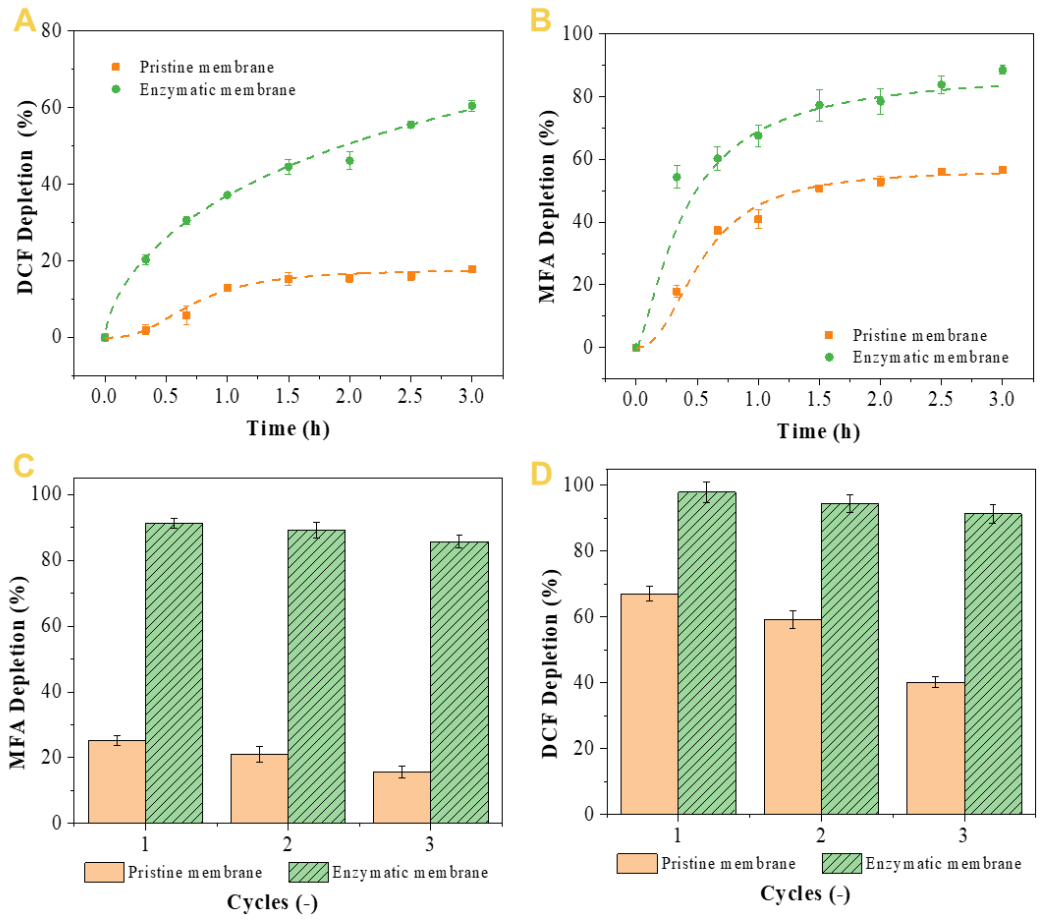

Figure 8. Membrane depletion efficiency of A) DCF, B) MFA; Depletion effi-ciency of reused membrane of C) DCF, D) MFA. Pristine membrane refers to C2-190 NFMs; Enzymatic membrane refers to Lac-C2-190 NFMs.

Additionally, the reusability of lac-C2-190 NFMs for EPs removal was tested. As illustrated in **Figure 8C-D**, immobilized laccase displayed stable performance for DCF and MFA; up to 90% of the initial depletion efficiency was retained three times of reuse on both compounds. A slight decrease in depletion efficiency of DCF and MFA was noticed as the active sites of immobilized laccase may be covered by the reaction products and inhibited during repeated use of the membranes, which would lead to lower activity.

4. Conclusion

We have successfully produced crosslinked β-cyclodextrin NFMs that are biodegradable. These membranes possess high insolubility and can resist different solvents such as water, ethanol, DMAc, and n-hexane, indicating that they have potential applications in various fields. We also investigated the catalytic activities of immobilized laccase using these NFMs as enzyme carriers. The results showed that the immobilized laccase had better stability compared to the free enzyme, particularly with higher resistance towards neutral pH, making it suitable for industrial applications. However, we need to consider some aspects before applying these NFMs, particularly their high water uptake and swelling ratio, which suggest that batch reactors with full contact with substrate compounds may be more appropriate than fixed membrane modules. These biodegradable NFMs offer a solution to the environmental issue of disposing of contaminated polymeric modules as plastic waste. Overall, our study demonstrates the promising potential of biodegradable NFMs for pollutant treatment.

Declaration of competing interest

No conflict of interest exists.

Acknowledgment

This work was sponsored by the Novo Nordisk Foundation (NNF18OC0034918) and the Danish Research Council (Grant No. 8022-00237B). The authors would like to acknowledge the financial support from China Scholarship Council. The authors would like to thank Mikael Emil Olsson and Kai Tang for the experimental support.

Reference

[1] C.G. Daughton, T.A. Ternes, Pharmaceuticals and personal care products in the environment: Agents of subtle change?, Environ. Health Perspect. 107 (1999) 907–938. doi:10.1289/ehp.99107s6907.

[2] M. Taheran, S.K. Brar, M. Verma, R.Y. Surampalli, T.C. Zhang, J.R. Valero, Membrane processes for removal of pharmaceutically active compounds (PhACs) from water and wastewaters, Sci. Total Environ. 547 (2016) 60–77. doi:10.1016/j.scitotenv.2015.12.139.

[3] R. Morsi, M. Bilal, H.M.N. Iqbal, S.S. Ashraf, Laccases and peroxidases: The smart, greener and futuristic biocatalytic tools to mitigate recalcitrant emerging pollutants, Sci. Total Environ. 714 (2020) 136572. doi:10.1016/J.SCITOTENV.2020.136572.

[4] A. Zenker, M.R. Cicero, F. Prestinaci, P. Bottoni, M. Carere, Bioaccumulation and biomagnification potential of pharmaceuticals with a focus to the aquatic environment, J. Environ. Manage. 133 (2014) 378–387. doi:10.1016/J.JENVMAN.2013.12.017.

[5] L. Wiest, A. Gosset, A. Fildier, C. Libert, M. Hervé, E. Sibeud, B. Giroud, E. Vulliet, T. Bastide, P. Polomé, Y. Perrodin, Occurrence and removal of emerging pollutants in urban sewage treatment plants using LC-QToF-MS suspect screening and quantification, Sci. Total Environ. 774 (2021) 145779. doi:10.1016/j.scitotenv.2021.145779.

[6] Z. Baalbaki, T. Sultana, T. Maere, P.A. Vanrolleghem, C.D. Metcalfe, V. Yargeau, Fate and mass balance of contaminants of emerging concern during wastewater treatment determined using the fractionated approach, Sci. Total Environ. 573 (2016) 1147–1158. doi:10.1016/j.scitotenv.2016.08.073.

[7] J.L. Acero, F.J. Benitez, A.I. Leal, F.J. Real, F. Teva, Membrane filtration technologies applied to municipal secondary effluents for potential reuse, J. Hazard. Mater. 177 (2010) 390–398. doi:10.1016/j.jhazmat.2009.12.045.

[8] M. Bilal, S.S. Ashraf, D. Barceló, H.M.N. Iqbal, Biocatalytic degradation/redefining "removal" fate of pharmaceutically active compounds and antibiotics in the aquatic

environment, Sci. Total Environ. 691 (2019) 1190–1211. doi:10.1016/j.scitotenv.2019.07.224.

[9] A.T. Martínez, F.J. Ruiz-Dueñas, S. Camarero, A. Serrano, D. Linde, H. Lund, J. Vind, M. Tovborg, O.M. Herold-Majumdar, M. Hofrichter, C. Liers, R. Ullrich, K. Scheibner, G. Sannia, A. Piscitelli, C. Pezzella, M.E. Sener, S. Kılıç, W.J.H. van Berkel, V. Guallar, M.F. Lucas, R. Zuhse, R. Ludwig, F. Hollmann, E. Fernández-Fueyo, E. Record, C.B. Faulds, M. Tortajada, I. Winckelmann, J.A. Rasmussen, M. Gelo-Pujic, A. Gutiérrez, J.C. del Río, J. Rencoret, M. Alcalde, Oxidoreductases on their way to industrial biotransformations, Biotechnol. Adv. 35 (2017) 815–831. doi:10.1016/j.biotechadv.2017.06.003.

[10] F. Christopher, The structure and function of fungal laccase, Microbiology. 140 (1994) 19.

[11] R.J. Lopez, S. Babanova, Y. Ulyanova, S. Singhal, P. Atanassov, Improved interfacial electron transfer in modified bilirubin oxidase biocathodes, ChemElectroChem. 1 (2014) 241–248. doi:10.1002/celc.201300085.

[12] Y. Dai, J. Yao, Y. Song, X. Liu, S. Wang, Y. Yuan, Enhanced performance of immobilized laccase in electrospun fibrous membranes by carbon nanotubes modification and its application for bisphenol A removal from water, J. Hazard. Mater. 317 (2016) 485–493. doi:10.1016/j.jhazmat.2016.06.017.

[13] J.B. Costa, M.J. Lima, M.J. Sampaio, M.C. Neves, J.L. Faria, S. Morales-Torres, A.P.M. Tavares, C.G. Silva, Enhanced biocatalytic sustainability of laccase by immobilization on functionalized carbon nanotubes/polysulfone membranes, Chem. Eng. J. 355 (2019) 974–985. doi:10.1016/J.CEJ.2018.08.178.

[14] C. Chen, W. Sun, H. Lv, H. Li, Y. Wang, P. Wang, Spacer arm-facilitated tethering of laccase on magnetic polydopamine nanoparticles for efficient biocatalytic water treatment, Chem. Eng. J. 350 (2018) 949–959. doi:10.1016/J.CEJ.2018.06.008.

[15] M. Maryšková, I. Ardao, C.A. García-González, L. Martinová, J. Rotková, A. Ševců, Polyamide 6/chitosan nanofibers as support for the immobilization of Trametes versicolor laccase for the elimination of endocrine disrupting chemicals, Enzyme Microb. Technol. 89 (2016) 31–38. doi:10.1016/J.ENZMICTEC.2016.03.001.

[16] O. Celikbicak, G. Bayramoglu, M. Yilmaz, G. Ersoy, N. Bicak, B. Salih, M.Y. Arica, Immobilization of laccase on hairy polymer grafted zeolite particles: Degradation of a model dye and product analysis with MALDI–ToF-MS, Microporous Mesoporous Mater. 199 (2014) 57–65. doi:10.1016/J.MICROMESO.2014.08.003.

[17] J. Sun, C. Wang, Y. Wang, S. Ji, W. Liu, Immobilization of carbonic anhydrase on polyethylenimine/dopamine codeposited membranes, J. Appl. Polym. Sci. 136 (2019) 1–9. doi:10.1002/app.47784.

[18] D. Zhao, M.L. Leth, M. Abou Hachem, I. Aziz, N. Jančič, T. Luxbacher, C. Hélix-Nielsen, W. Zhang, Facile fabrication of flexible ceramic nanofibrous membranes for enzyme immobilization and transformation of emerging pollutants, Chem. Eng. J. 451 (2023) 138902.

[19] P. Sathishkumar, S. Kamala-Kannan, M. Cho, J.S. Kim, T. Hadibarata, M.R. Salim, B.-T. Oh, Laccase immobilization on cellulose nanofiber: The catalytic efficiency and recyclic application for simulated dye effluent treatment, J. Mol. Catal. B Enzym. 100 (2014) 111–120. doi:10.1016/J.MOLCATB.2013.12.008.

[20] L. Lu, M. Zhao, Y. Wang, Immobilization of laccase by alginate-chitosan microcapsules and its use in dye decolorization, World J. Microbiol. Biotechnol. 23 (2007) 159–166. doi:10.1007/s11274-006-9205-6.

[21] D. Wu, Q. Feng, T. Xu, A. Wei, H. Fong, Electrospun blend nanofiber membrane consisting of polyurethane, amidoxime polyarcylonitrile, and B-cyclodextrin as high-performance carrier/support for efficient and reusable immobilization of laccase, Chem. Eng. J. (2018). doi:10.1016/j.cej.2017.08.129.

[22] F. Topuz, T. Holtzl, G. Szekely, Scavenging organic micropollutants from water with nanofibrous hypercrosslinked cyclodextrin membranes derived from green resources, Chem. Eng. J. 419 (2021) 129443. doi:10.1016/j.cej.2021.129443.

[23] K.H. Lee, C.S. Ki, D.H. Baek, G.D. Kang, D.-W. Ihm, Y.H. Park, Application of electrospun silk fibroin nanofibers as an immobilization support of enzyme, Fibers Polym. 6 (2005) 181–185.

[24] G. Li, A.G. Nandgaonkar, K. Lu, W.E. Krause, L.A. Lucia, Q. Wei, Laccase immobilized on PAN/O-MMT composite nanofibers support for substrate bioremediation: A: de novo adsorption and biocatalytic synergy, RSC Adv. 6 (2016) 41420–41427. doi:10.1039/c6ra00220j.

[25] Y. Dai, J. Niu, J. Liu, L. Yin, J. Xu, In situ encapsulation of laccase in microfibers by emulsion electrospinning: Preparation, characterization, and application, Bioresour. Technol. 101 (2010) 8942–8947. doi:10.1016/J.BIORTECH.2010.07.027.

[26] A. Leonowicz, J.M. Sarkar, J.-M. Bollag, Improvement in stability of an immobilized fungal laccase, 1988.

[27] S. Aydin, M.E. Aydin, A. Ulvi, Monitoring the release of anti-inflammatory and analgesic pharmaceuticals in the receiving environment, Environ. Sci. Pollut. Res. 26 (2019) 36887–36902. doi:10.1007/s11356-019-06821-4.

Supplementary Material for:

Biodegradable Crosslinked Nanofibrous Membranes for Enzyme Immobilization and Transformation of Emerging Pollutants.

Dan Zhao[a], Tian Tian[b], Maria Louise Leth[c], Maher Abou Hachem[c], Claus Hélix-Nielsen[a, *], Wenjing (Angela) Zhang[a, *]

a. Department of Environmental and Resource Engineering, Technical University of Denmark, DTU, 2800 Kgs. Lyngby, Denmark

b. MOE Key Laboratory of Bioinorganic and Synthetic Chemistry, School of Chemistry, Sun Yat-sen University, Guangzhou, 510006 P. R. China

c. Department of Biotechnology and Biomedicine, Technical University of Denmark, DTU, 2800 Kgs. Lyngby, Denmark

[*] **Corresponding author:**

Dr. Wenjing (Angela) Zhang

Tel: (+45) 20352356; E-mail address: wen@dtu.dk

Dr. Claus Hélix-Nielsen

Tel: (+45) 45252228; E-mail address: clhe@dtu.dk

Text S1. Materials

Table S1. Solvent properties

	Emerging pollutants	**HSP[a]**	**ε[b]**	**Supplier**
1	H_2O	16	80	-
2	Acetonitrile (ACN)	18	37.5	Sigma-Aldrich
3	*n*-hexane	0.0	1.89	Sigma-Aldrich
4	Dimethylacetamide (DMAc)	11.5	37.8	Sigma-Aldrich
5	Dimethyl sulfoxide (DMSO)	16.4	45	Sigma-Aldrich
6	Ethanol	8.8	24	Sigma-Aldrich
7	Methanol	12.3	33	Sigma-Aldrich

a refers to the Hansen Solubility Parameter

b refers to the dieletric constant

Text S2. Water treatment of HP-β-CD and cross-linked NFMs.

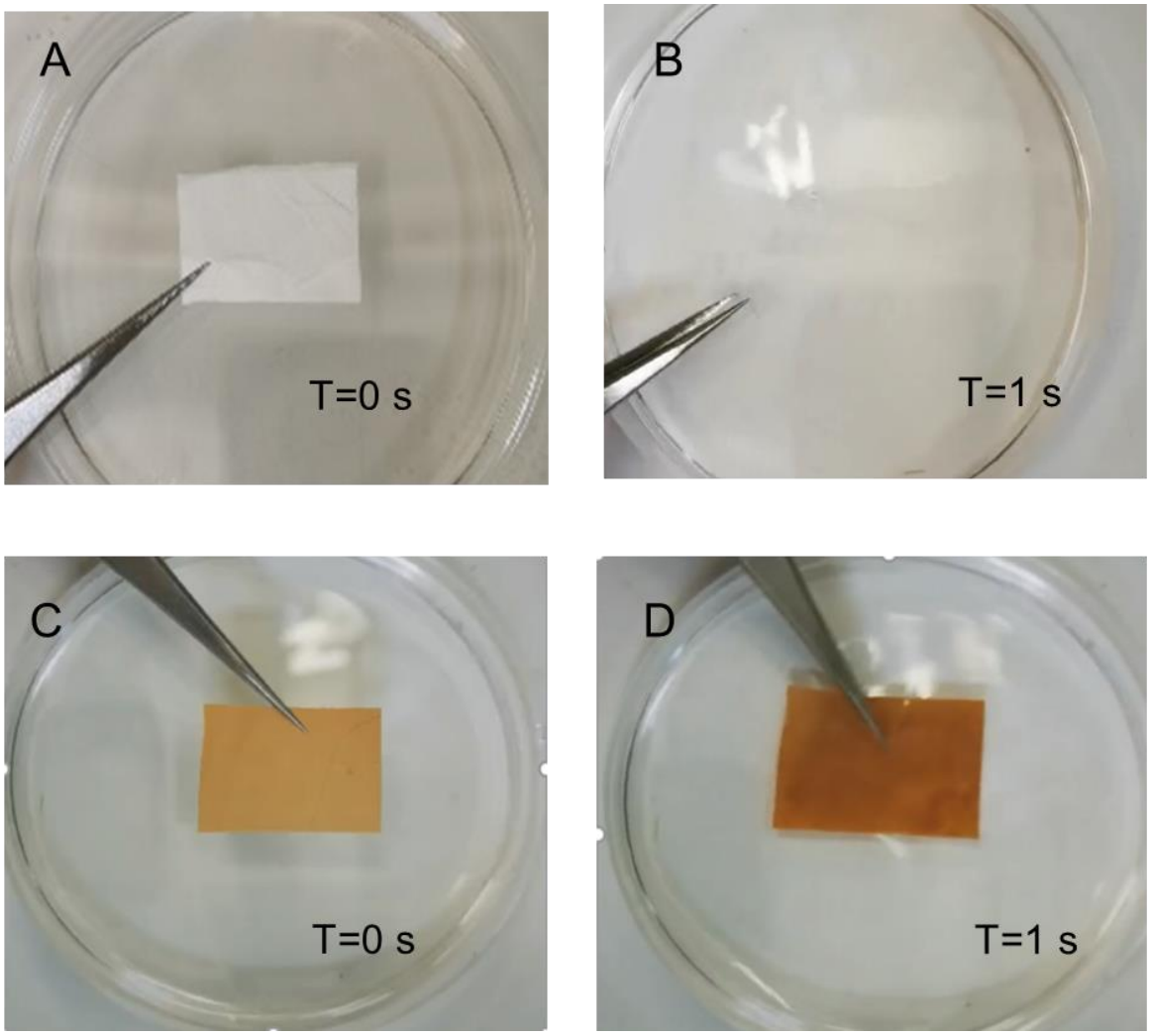

Figure S1. Optical images of A-B) HP-β-CD in contact with H_2O; C-D) Cross-linked NFMs in contact with H_2O

Text S3. Thermal inactivation kinetics

The thermal inactivation data for free and immobilized laccase was plotted for zero (residual activity versus time), first (natural logarithm of the residual activity versus time) and second-order (reciprocal activity versus time). The rate constant k_{inact} [h^{-1}] for first-order thermal inactivation was determined from the slope of the inactivation time:

$$ln\left(\frac{A_t}{A_0}\right) = -k_{inact}t \quad (1)$$

$$t_{0.5} = \frac{ln(2)}{k_{inact}} \quad (2)$$

Where At is the residual activity that remains after heating the enzyme for time t, and A_0 is the initial enzyme activity before heating. The half-time of thermal inactivation ($t_{0.5}$) was determined by equation S2.

Text S4. Fiber distribution of pristine and crosslinked nanofibers.

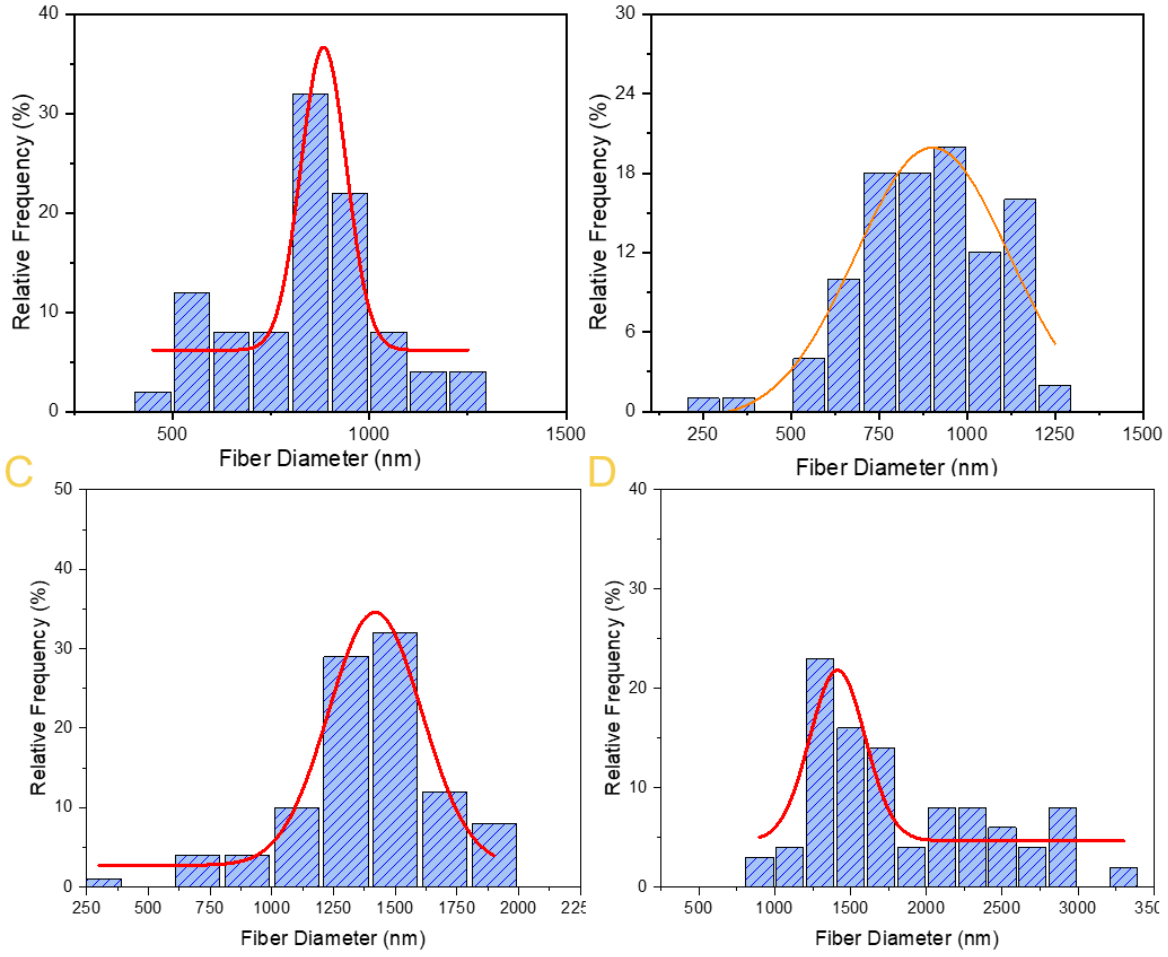

Figure S2. Fiber diameter distribution of :A, B) pristine C2 NFMs and crosslinked C2-190 NFMs, C, D) C3 NFMs and crosslinked C3-190 NFMs

Chemical Engineering Journal 451 (2023) 138902

Contents lists available at ScienceDirect

Chemical Engineering Journal

journal homepage: www.elsevier.com/locate/cej

Facile fabrication of flexible ceramic nanofibrous membranes for enzyme immobilization and transformation of emerging pollutants

Dan Zhao [a], Maria Louise Leth [b], Maher Abou Hachem [b], Iram Aziz [c], Natalija Jančič [d], Thomas Luxbacher [d,e], Claus Hélix-Nielsen [a,*], Wenjing Zhang [a,*]

[a] Department of Environmental and Resource Engineering, Technical University of Denmark, DTU, 2800 Kgs. Lyngby, Denmark
[b] Department of Biotechnology and Biomedicine, Technical University of Denmark, DTU, 2800 Kgs. Lyngby, Denmark
[c] Department of Chemistry and Chemical Engineering, Lahore University of Management Sciences, 54792 Lahore, Pakistan
[d] Faculty of Chemistry and Chemical Engineering, University of Maribor, 2000 Maribor, Slovenia
[e] Anton Paar GmbH, 8054 Graz, Austria

ARTICLE INFO

Keywords:
Laccase
Flexible ceramic membranes
Immobilization

ABSTRACT

Biocatalytic nanofibrous membranes, integrating the benefits of membranes and enzymes, have drawn attention in wastewater treatment because of their efficient catalytic performance and operational catalytic stability. However, these membranes are typically polymeric membranes, and their fate as plastic waste is not considered environmentally sustainable. By contrast, ceramic-based membranes are considered more environmental-friendly due to their low-risk recycling and disposal procedures, but the brittleness of these membranes limits their implementation. Here, we report the fabrication of high flexibility SiO_2 biocatalytic nanofiber membranes (NFMs) and their previously unreported application in emerging pollutant bioremediation. We used a commercial laccase (EC 1.10.3.2) as a model biocatalyst to evaluate the impact of different strategies to improve the catalytic properties of the NFMs in terms of enzyme load and apparent activity per membrane weight. Enzyme immobilization with the co-deposition of polydopamine (PDA) and polyethyleneimine (PEI) resulted in the best immobilization yield (57.9 ± 0.5 %) and apparent activity of 6.4 ± 1.1 U g^{-1} membrane. Compared to the free enzyme, the fabricated bio-catalytic membranes maintained 80 % of residual activity after five cycles. In addition, the membranes exhibited > 95 % depletion of the five emerging pollutants diclofenac, mefenamic acid, benzefabrite, bicalutamide, and clarithromycin. The successful fabrication of flexible biocatalytic ceramic membranes holds promise as a new technological platform for sustainable wastewater treatment and brings novel insights into a previously less explored realm of membrane applications.

1. Introduction

Emerging pollutants (EPs) are persistent compounds in the environment at trace concentrations, and exposure to these EPs might have detrimental effects on both environment and human beings [1,2]. These recalcitrant compounds, including distinct pharmaceuticals, personal care products, polycyclic aromatic hydrocarbons as well as pesticides, escape degradation by higher organisms to bioaccumulate and/or to exert toxic effects in terrestrial and aquatic ecological systems [3]. The usage of these compounds has been increasing considerably; however, there are no guidelines or standards regarding the disposal and discharge of EPs in existing wastewater treatment plants (WWTPs) at present [4]. Efforts to address these emerging concerns have been applied, such as EP removal during water treatment by activated sludge adsorption [5]. However, current WWTPs have not been designed for the efficient removal of EPs at low concentrations. Even though a high EP adsorption on activated sludge is accomplished, further treatment is required to prevent enriched EPs in the sludge from eventually entering the environment through landfills or as fertilizer.

The transformation of pollutants catalyzed by enzymes is considered an environmental-friendly and highly efficient way of water treatment [6]. However, the feasibility of enzyme applications with enzyme in the free form suffers from high enzyme prices and irreversible enzyme inactivation, e.g., due exposure to denaturing conditions. The aforementioned problems can be mitigated by immobilizing enzymes in/on various supports such as membrane materials. Membranes applied in

* Corresponding authors.
E-mail addresses: clhe@dtu.dk (C. Hélix-Nielsen), wenz@dtu.dk (W. Zhang).

https://doi.org/10.1016/j.cej.2022.138902
Received 10 July 2022; Received in revised form 24 August 2022; Accepted 26 August 2022
Available online 30 August 2022

filtration [7] offer a promising strategy for EP capture, but it requires further chemical treatment of concentrated pollutants as a necessity for their disposal. Biocatalytic membranes with embedded or immobilized biocatalysts merge the benefits of bioremediation and membrane separation and markedly facilitate the reuse of immobilized enzymes.

Among known biocatalysts, laccases (benzenediol: oxygen oxidoreductase, EC 1.10.3.2) are model commercial enzymes with broad substrate profile that includes synthetic dyes, chlorinated phenolics, and polycyclic aromatic hydrocarbons [8–10]. Several types [11,12] of laccase-immobilized membranes have been developed. These applications commonly utilize polymeric membranes as enzyme support which raises the environmental issue of discharging the contaminated membrane modulus as plastic waste after use. Ceramics are promising and potentially more sustainable alternatives considering their recyclability; however, most applications notably avoid utilizing ceramics as membrane materials due to their high production cost, complex fabrication schemes, and brittleness that deteriorates their performance compared to polymers [13]. To overcome the rigidness and brittleness of ceramics fabricated by common procedures, including hot-die casting, isostatic pressing, extrusion, and grouting, researchers have successfully produced flexible ceramics via needle-based electrospinning combined with a sol–gel process [14], followed by calcination [15]. Subsequent studies have revealed that ceramic nanofibers with high length-to-diameter (L D^{-1}) ratios could alter the crystal size to enlarge the grain boundaries, reducing crack propagation and thus softening and reinforcing the fibrous materials. [16].The superior flexibility of ceramic membrane has promoted applications in battery separators [17] and oil separation [15], but not in emerging pollutant transformation to our knowledge.

Herein, we developed a facile reinforcement fabrication strategy for flexible ceramic membranes and immobilized a model enzyme to generate biocatalytic membranes by one-step co-deposition of polydopamine (PDA) and polyethyleneimine (PEI). This is the first study to employ scalable biocatalytic ceramic membranes with superior flexibility and high catalytic efficiency for emerging pollutant transformation applications.

2. Materials and methods

2.1. Chemicals and materials

Laccase from *Trametes versicolor* (EC 1.10.3.2, ≥0.5 U mg^{-1}), sodium acetate (NaOAc), acetic acid (HOAc), 2,2′-azino-bis(3-ethyl-benzothiazoline-6-sulfonic acid: ABTS), tetraethyl orthosilicate (TEOS), poly (vinyl alcohol) (PVA, Mw 89,000 ~ 98,000 Da), phosphoric acid, dopamine hydrochloride, sodium (meta) periodate, tris(hydroxymethyl) aminomethane (Tris), (3-Aminopropyl)triethoxysilane (APTES, 99 %), polyethylenimine (branched, Mw ~ 800 Da by light scattering), ethanol absolute (99.8 %), acetonitrile (anhydrous, 99.8 %) were obtained from Sigma-Aldrich. 20 EPs are listed in **Table S1** of the Supporting information.

2.2. Experimental procedures

2.2.1. Fabrication of electrospun SiO_2 nanofiber membranes (NFMs)

10 g of 10 % (w/w) PVA sol solution was slowly added to 30 g of silica gel with a mass composition of tetraethyl orthosilicate (TEOS): H_3PO_4: H_2O = 1:0.007:1, and the composite solution was stirred for another 6 h before electrospinning. The electrospinning was applied by a continuous needle-less system (NS LAB, Elmarco, Czech Republic), corporate with a precision air Conditioner (NS AC150, Elmarco, Czech Republic) which generated electrospun nanofibers by a wire electrode. The composite solution was filled in a spinning carriage at a speed of 100 mm s^{-1}. The spinning voltage and tip-to-support distance were applied to 37 kV and 17 cm, respectively. The temperature and relative humidity of electrospinning were set as 25 °C and 25 %. Then, the fibers were collected on a siliconized paper set with a speed of 5 mm min^{-1}. The precursor nanofibers were calcined at 800 °C for 2 h with a series of heat-up rates (5 °C min^{-1} to 250 °C, followed by 1 °C min^{-1} to 450 °C and 5 °C to 800 °C).

2.2.2. Surface functionalization of SiO_2 NFMs

Three approaches were applied to functionalize the surface of SiO_2 NFMs:

i) **Silanization treatment** was performed by immersing 0.16 g of SiO_2 NFMs in 200 mL of 10 % (w/w) APTES ethanol solution at 70 °C for 2 h.
ii) **Dopamine coating** was to dip 0.16 g of SiO_2 NFMs in 200 mL 10 mM Tris buffer, 2 g/L of dopamine hydrochloride, 5 mM $NaIO_4$, pH 8.5 for 12 h.
iii) **Co-deposition of polydopamine(PDA)/ polyethyleneimine (PEI)** was applied by soaking SiO_2 NFMs in a 1:1 (w/w) mixture of dopamine (2 g/L) and PEI for 12 h. Treated membranes were washed with water and vacuum dried overnight at 40 °C.

The resulting NFMs were designated as SiO_2-SA, SiO_2-PD, and SiO_2-PE, respectively.

2.2.3. Laccase immobilization and enzyme assays

Laccase immobilization on the modified NFMs was performed as described by Lee et al.[18] with minor modifications. Briefly, the membrane (64 cm^2) was immersed in a 5 mg mL^{-1} (by weight) laccase solution in 50 mM NaOAc buffer, pH 4.5, incubated for 1 h at 25 °C, and subsequently transferred to 4 °C for 24 h. Next, the laccase immobilized membrane was washed three times with the same buffer and stored at 4 °C. The resulting biocatalytic NFMs were designated as Lac- SiO_2-SA, Lac-SiO_2-PD, and Lac-SiO_2-PE NFMs, respectively. For enzyme assays, the NFMs (2 cm^2) were cut into 8 pieces and immersed in 5 mg mL^{-1} laccase solution (50 mM NaOAc buffer, pH 4.5). The activity of the free laccase in the initial immobilization bath and the residual activity after immobilization, as well as the activities of the fibrous membrane with immobilized enzyme and the wash fractions, were determined spectrophotometrically using ABTS as the substrate. Specifically, 10 μL laccase solution or 0.25 cm^2 of the laccase-immobilized membrane was added to 0.5 mM ABTS solution in 20 mM NaOAc buffer, pH 4.5, and the reaction mixture (300 μL) was incubated in a microtitre plate for 10 min after a 30-second agitation at 25 °C. The absorbance at 420 nm was monitored continuously.

Subsequently, the effect of pH on laccase activity was evaluated by testing both the free and immobilized enzyme prepared in 20 mM NaOAc at pH 3.5–6.5 and monitoring the absorbance at 420 nm at 25 °C. Furthermore, a thermal-irreversible inactivation assay was performed to investigate the stability of both the free and immobilized enzymes. An Eppendorf tube containing 980 μL 50 mM NaOAc buffer was preheated at 50 °C for 5 min. 20 μL of 5 mg ml^{-1} enzyme solution in 50 mM NaOAc buffer was added to the preheated buffer solution and incubated at 50 °C. Then, 100 μL aliquots were collected at 10, 20, 30, 60, 90, and 120 min and stored on ice. Next, the residual activity was assayed using the standard assay described above at 25 °C. For the immobilized enzyme, 6x3 pieces of enzyme-immobilized fibers (as a technical triplicate for six measurements) were assayed before heating, and the same fiber pieces were washed thoroughly. Thereafter, the washed fibers were incubated in a water bath at 50 °C for 10, 20, 30, 60, 90, and 120 min, stored on ice, and assayed for the remaining activity.

2.2.4. Eps transformation by free enzyme and laccase-immobilized membranes

The free laccase activity was screened against a panel of 20 EPs to identify substrates converted by the enzyme. In short, 150 μL of 1.5 μM laccase was incubated with 200 μg L^{-1} of each EP in 50 mM NaOAc buffer, pH 4.5, in 3 mL total reaction volume for 24 h at room temperature. After the screening, to further investigate catalytic membrane

performance, dead-end membrane filtration was conducted in a batch stirred cell (Amicon Model 8400, Millipore), as shown in Fig. S1. In order to control the same flux of the filtration, all the membranes were assembled with a commercial microfiltration membrane (MFG2, Alfa Laval, Denmark) in the testing cell. The volume of the stirred cell is 400 mL with an internal membrane diameter of 7.6 cm. An aqueous solution containing five EPs (bicalutamide, mefenamic acid, diclofenac, clarithromycin, and bezafibrate), prepared in Milli-Q-H_2O, was pumped through the membranes at 0.25 bar. For cycling mode, 500 mL synthetic EP solution was cumulatively pumped through the membrane during each cycle, and between the adjacent cycles, the membrane was washed thoroughly by Milli-Q-H_2O. Functionalized SiO_2 NFMs without laccase assembled with MFG2 were tested under the same conditions as the control experiment.

Additionally, we carried the transformation reaction of the model EP, diclofenac, by laccase-immobilized NFMs. Diclofenac transformation was carried out in a 500 mL borosilicate glass beaker at room temperature. 20.48 mg of laccase-immobilized NFMs (64 cm^2) were soaked in freshly prepared 300 mL of 200 μg L^{-1} diclofenac solution in Milli-Q-H_2O under vigorous stirring. Duplicate samples were taken at different reaction times and filtered through 0.2 μm PTFE filters into 2 mL vials. Subsequently, acetonitrile was added as a quenching reagent.

2.3. Characterization and analytical procedures

2.3.1. Characterization of SiO_2 NFMs

The microstructure of the electrospun fibers was analyzed by field emission scanning electron microscopy (Quanta FEG 250, FEI, USA) at an accelerating voltage of 5 kV. A laser confocal scanning microscopy (TCS SP5, Leica, Germany) was used to observe the presence and distribution of the enzyme on the NFMs. Laccase was previously labeled with fluorescein isothiocyanate (FITC) by mixing 100 mg of laccase and 10 μg FITC in sodium carbonate buffer solution (50 mM, pH 8.8) at 4 °C for 1 h in the dark and then dialyzed to remove residual FITC by gel filtration. Thereupon, labeled laccase was immobilized on the SiO_2 NFMs as described above (Section 2.2.3). The excitation and emission wavelengths of FITC were 492 and 518 nm, respectively. The chemical structure of each NFMs was analyzed by Attenuated Total Reflectance-Fourier transform infrared spectroscopy (ATR-FTIR, Bruker, Germany). The zeta potential of the SiO_2 NFMs was determined at different pH of an aqueous 1 mM KCl solution by the streaming potential method (SurPASS 3, Anton Paar, Austria). The NFMs were ground gently to obtain coarse granular particles, which were inserted into a sample holder for powder samples. A continuously decreasing pressure gradient was applied to the aqueous test solution between both ends of the granular powder sample, and the streaming potential was recorded simultaneously. The slope of the linear dependence of streaming potential on pressure difference was converted to the zeta potential using the classical Smoluchowski equation. The pH of the KCl solution was adjusted automatically by adding either 50 mM HCl or KOH.

2.3.2. Determination of enzyme loading and activity

The protein concentrations in solutions were determined by the Bradford method (Fig. S2 of the Supporting information) on a microplate reader (Synergy H1, Agilent Technologies, USA). The total amount (m) of the immobilized enzyme (μg) was calculated as:

$$m = (C_0 - C_r)V - \sum C_w V_w \tag{1}$$

where C_0, C_w, and C_r represent the enzyme concentrations (μg mL^{-1}) in the initial stock, washing buffer, and residual solution, respectively, V and V_w are volumes (mL) of the enzyme solution and washing buffer.

The enzyme activity (A) of enzyme solution (A_{free}) or fiber (A_{fiber}) was calculated from the initial slope of the obtained absorbance versus the time curve (Abs_{420} min^{-1}). One unit of enzyme activity (U) was defined as the amount of enzyme which converts 1 μmol of ABTS per minute under the assay conditions (μmol min^{-1}).

$$A = \frac{\alpha \times V_{Total}}{\varepsilon \times d} \tag{2}$$

where V_{Total} is the volume of total assay and enzyme solution (μL), α is the absorbance per minute at 420 nm, determined by linear regression (min^{-1}), d is the light path of the assay, estimated by assay volume, and the single well area of the microplate (cm), and ε represents the molar absorption coefficient of ABTS at 420 nm, 36,000 $M^{-1}{\cdot}cm^{-1}$.

The specific activity of free enzyme (SA_{free}) was defined as the enzyme activity of enzyme solution per weight of free enzyme (U mg^{-1} enzyme). The specific activities of the immobilized enzyme (SA_{imm}) and fiber (SA_{fiber}) were defined as the enzyme activity of fiber per weight of immobilized enzyme (U mg^{-1} enzyme) and support membrane(U g^{-1} fiber) separately.

$$SA_{free} = \frac{A_{free}}{M_{free}} \tag{3}$$

$$SA_{imm} = \frac{A_{fiber}}{M_{imm}} \tag{4}$$

$$SA_{fiber} = \frac{A_{fiber}}{M_{fiber}} \tag{5}$$

where M_{free}, is the amount of free enzyme in the assay (mg). M_{imm} and M_{fiber} are the amount of immobilized enzyme on tested fiber (mg) and the mass of tested fibers (g).

2.3.3. Determination of kinetic parameters

The Michaelis–Menten kinetic apparent parameters of free and immobilized enzymes were determined by calculating the specific activity of free and immobilized enzymes using ABTS with different concentrations from 0.1 to 5 mM. The values of the kinetic parameters were determined graphically from the non-linear regression of the Michaelis–Menten kinetics:

$$v = V_{max}\frac{[S]}{K_m + [S]} \tag{6}$$

$$\frac{1}{V} = \frac{K_m}{V_{max}[S]} + \frac{1}{V_{max}} \tag{7}$$

where v is the initial reaction rate, [S] is the substrate concentration, V_{max} is the apparent maximum rate of the bio-catalyst. K_m [mM] is the apparent Michaelis–Menten constant.

2.3.4. Determination of EPs depletion efficiency

The concentrations of EPs were analyzed by High-Performance Liquid Chromatography–Triple Quadrupole Mass Spectrometry (1290 Infinity II-6470 LC-QQQ, Agilent Technologies). The depletion efficiency (D) was calculated as.

$$D = \frac{C_{EP_0} - C_{EP}}{C_{EP_0}} \times 100\% \tag{8}$$

where C_{EP0} and C_{EP} are the EP concentrations in solutions (μg L^{-1}) before and after the membrane process.

3. Result and discussion

3.1. Membrane morphology, flexibility, and chemical structure

Fig. 1a shows the manufacturing scheme of flexible SiO_2 NFMs. Specifically, a metastable silica sol containing TEOS and PVA was subject to rapid stretching and solidification due to solvent evaporation to generate the precursor NFs during the electrospinning process. Fig. 1b depicts a smooth and uniform morphology of precursor NFs. The addition of PVA solution enhanced the silica sol electrospinnability, and a

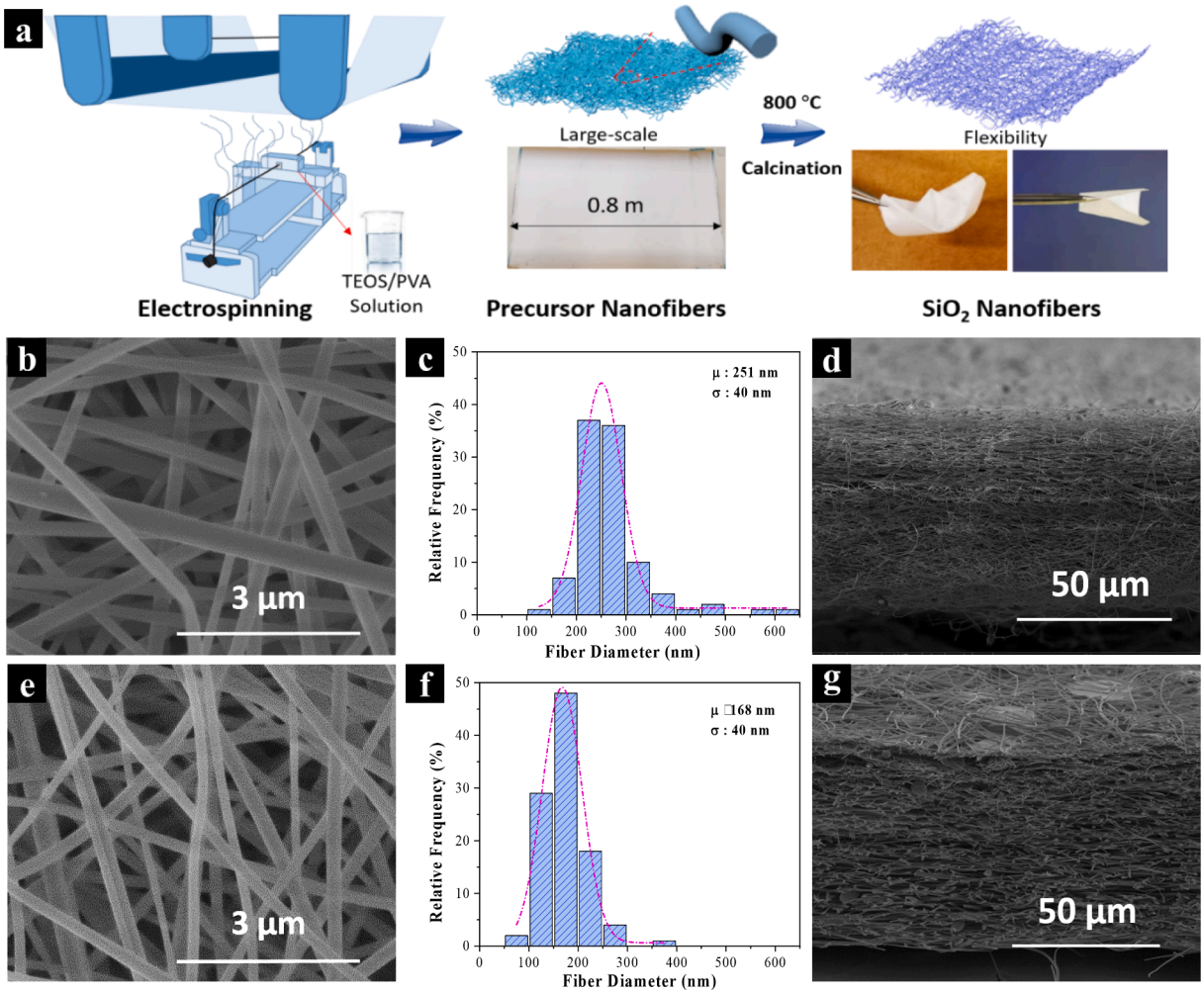

Fig. 1. a) A large-scale electrospun fibrous membrane (NFMs) production by needle-less electrospinning of tetraethyl orthosilicate (TEOS)/poly(vinyl alcohol) (PVA) solution, followed by a calcination process. b, e) SEM image of precursor nanofibers and calcined SiO_2 nanofibers. c, f) Fiber diameter distribution of the precursor nanofibers and calcined SiO_2 nanofibers. μ and σ refer to weighted arithmetic mean of fiber diameter and standard deviation, respectively. d, e) Cross-section SEM image of precursor nanofiber membrane and calcined SiO_2 nanofiber membrane.

narrow fiber diameter distribution was obtained (251 ± 40 nm, Fig. 1c), and the thickness of the precursor NFMs was 60.0 ± 0.8 μm (Fig. 1d). In the following calcination step, the PVA and TEOS in precursor NFs decomposed in the air, accompanied by SiO_2 grain growth. After calcination at 800 °C, PVA was sacrificed to leave the flexible SiO_2 NFs. As depicted in Fig. 1e, the calcined fibers appear shrunken in diameter without obvious fractures resulting in a narrower fiber diameter distribution (168 ± 40 nm, Fig. 1f), while the calcined NFMs thickness remained unchanged compared to precursor NFs (Fig. 1g). Notably, compared with the brittleness of common ceramic membranes, the obtained SiO_2 NFMs in our work remained intact after multiple deformations, including folding, twisting, bending, and kneading without any damage (**Fig. S3**). The flexibility of NFMs enables further modification and engineering of the membrane, such as functionalization and module design.

To further functionalize the NFMs surface, we tested silanization, dopamine coating, and co-deposition of PDA and PEI to introduce amine groups onto the SiO_2 nanofiber surface, as represented in Fig. 2a. The covalent attachment of functional organosilanes to silica and glass supports has proven to be efficient in immobilizing antibodies and cellular receptors in biosensors and adhesion layers in many applications [19]. The surface morphology of SiO_2-SA revealed the presence of thin films between fibers. Compared with silanization, both dopamine coating and co-deposition approaches introduced particles onto the fiber surfaces, which increased the roughness of the nanofiber (Fig. 2b-d). It is possible that the rapid self-polymerization of dopamine aggregates on the fiber. In the co-deposition process, the addition of PEI altered the formation of PDA aggregates. As a result, a relatively uniform surface of SiO_2-PE was obtained with a 1:1 mass ratio DA: PEI and a coating time of 12 h (**Fig. S4**). It has been reported that PEI establishes covalent bonding with the phenyl group of dopamine, thereby preventing the PDA from self-aggregation, which impacts the composition and morphology of the NFMs [20]. Weight losses of dry SiO_2-SA, SiO_2-PD, and SiO_2-PE were measured after the calcination at 800 °C to 0.9 ± 0.2 %, 13.2 ± 3.7 %, and 10.6 ± 0.7 %, respectively.

FTIR was used to investigate the possible chemical bond formation and secondary interactions, indicating the differences between the electrospun fibers before and after surface functionalization. Hydrogen bonding, protonation of the amine on the silica surface, and covalent bonding mainly contribute to the interaction between APTES and SiO_2[21]. As depicted in Fig. 2e, for the pristine SiO_2 membrane, the absorption peaks at 804 cm^{-1} were attributed to the bending vibration of the Si–O bond and two strong bands at 1083 cm^{-1} and 1147 cm^{-1} to asymmetrical Si–O–Si vibrations. A new band was observed as a significant change in SiO_2-SA at 922 cm^{-1}, corresponding to Si–O and the amino groups, attributed to the APTES conjugation [22]. It is well known that PDA exhibited good adhesion to various materials via covalent and non-covalent interactions. Electronic interaction between

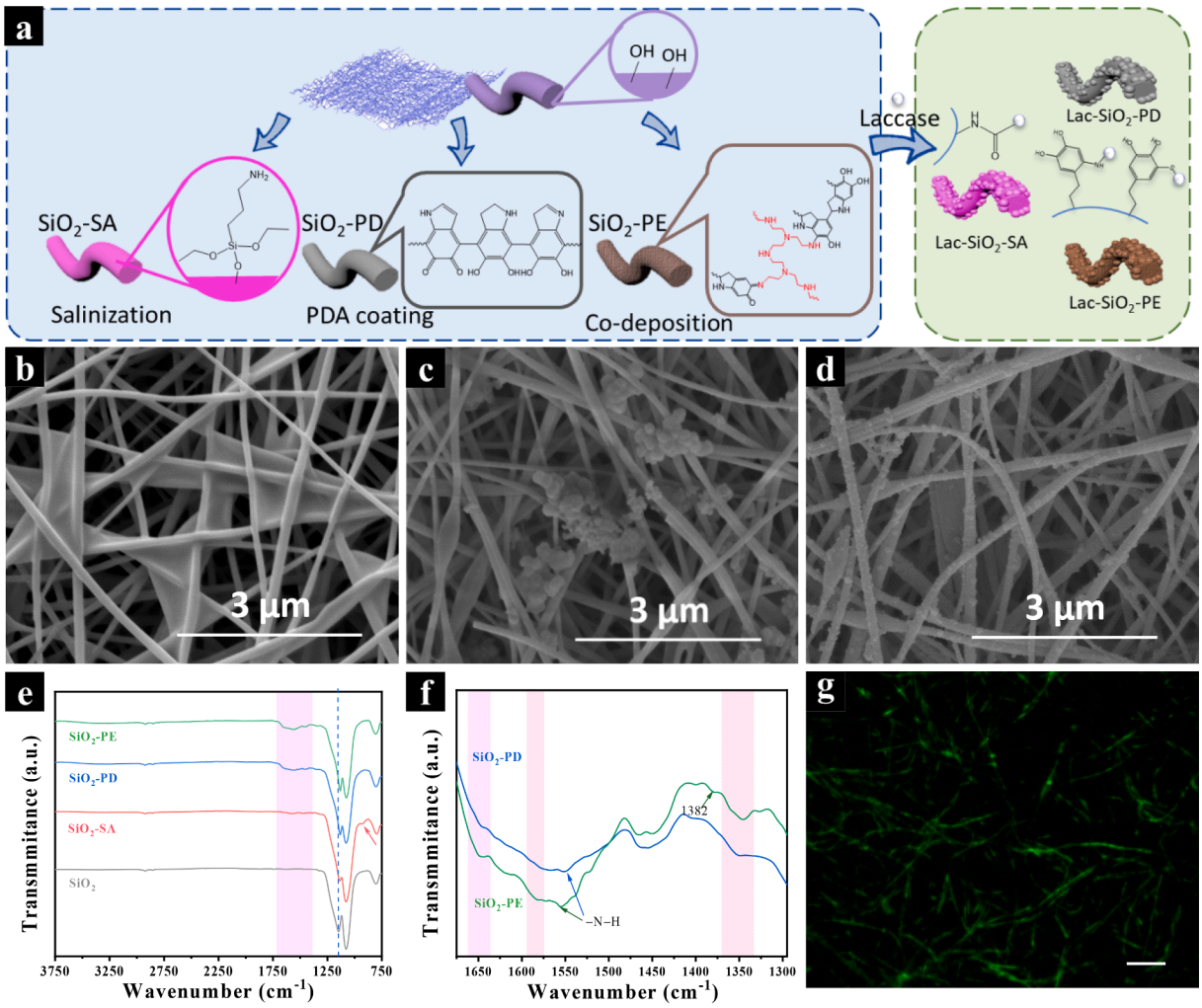

Fig. 2. a) Schematics of fibrous membrane functionalization and laccase immobilization. b-d) SEM images of SiO_2-SA, SiO_2-PD, and SiO_2-PE nanofibers. e-f) ATR-FTIR spectra of selected NFMs. g) A laser confocal scanning microscopy (LCSM) image of Lac-SiO_2-PE. The green fluorescence signal is from fluorescence-labeled enzymes. The scale of the unlabeled bar is 10 μm. (For interpretation of the references to colour in this figure legend, the reader is referred to the web version of this article.)

PDA and SiO_2 was demonstrated.[23] PEI is strongly adsorbed onto the negatively charged silanol groups of SiO_2 via electrostatic interactions.[24] Due to the planar cyclic and aromatic parts, the spectrum of SiO_2-PD and SiO_2-PE is composed of peaks between 2000 and 1300 cm^{-1} corresponding to NH and CN deformation modes (δNH and δCN). The characteristic shoulder peak of PDA in both spectra at 1351 cm^{-1} is assigned to indole ring CNC stretching, highlighted in Fig. 2f. The presence of the indole features supports the melanin-like structures containing 5,6-dihydroxyindole/5,6-indolequinone units that exist in both membranes [25]. A characteristic peak at 1382 cm^{-1} attributed to the CH_2 bending confirmed the successful grafting of PEI onto the membrane. Bands around 1648, 1589, and 1552 cm^{-1} were observed in both spectrums, corresponding to the deformation of primary amine groups [26], bending vibration of N—H bonds, and the stretching vibration of the secondary amine groups [27]. The absorption intensity of both peaks was stronger for SiO_2-PE than for SiO_2-PD, which further confirmed the incorporation of the PEI into the membrane surface. The introduction of PEI increased the amine groups' proportion to the membrane surface for enzyme immobilization. In order to visualize the distribution of immobilized laccase on SiO_2-PE NFMs, laccase (fitc-lac) was fluorescence-labeled before the immobilization, and confocal laser scanning microscopy was employed. As shown in Fig. 2g, the ultrafine fiber emits green fluorescence under excitation light, and it is evident that the laccase molecules could be uniformly distributed onto the fiber surfaces during the immobilization.

3.2. Optimization of immobilization

3.2.1. Surface charge effect on protein loading

The enzyme immobilization capacity was altered with different NFMs (Fig. 3a). Pristine SiO_2 and SiO_2-PD NFMs could achieve 24.9 % and 30 % of the total protein to be immobilized onto the fibers. Surprisingly, the protein immobilization yield of SiO_2-SA NFMs decreased to 7 %; by contrast, SiO_2-PE NFMs instead could hold 57.9 % of protein bonded onto the surface. The distinct difference between membranes could be ascribed to the divergent surface charge values of both membrane and enzyme. The theoretical isoelectric point of laccase from *Trametes versicolor* is 5.7 (ProtParam Tool). Fig. 3b shows the zeta potential, which is a metric of the net surface charge, as a function of pH for each SiO_2 NFM in a 1 mM KCl solution. Pristine SiO_2 NFMs were negatively charged within a broad pH range from 3.3 to 7.0. Laccases are physically adsorbed onto the surface due to the electrostatic attraction and hydrogen bonding where silica acts as donors [28]. However, these non-covalent interactions between silica and enzymes are typically weak and reversible. The immobilized laccase was desorbed and leached out from the SiO_2 pristine NFMs, which is why proteins can be detected in the washing buffers.

By contrast, a sharp increase in the zeta potential of SiO_2-SA NFMs

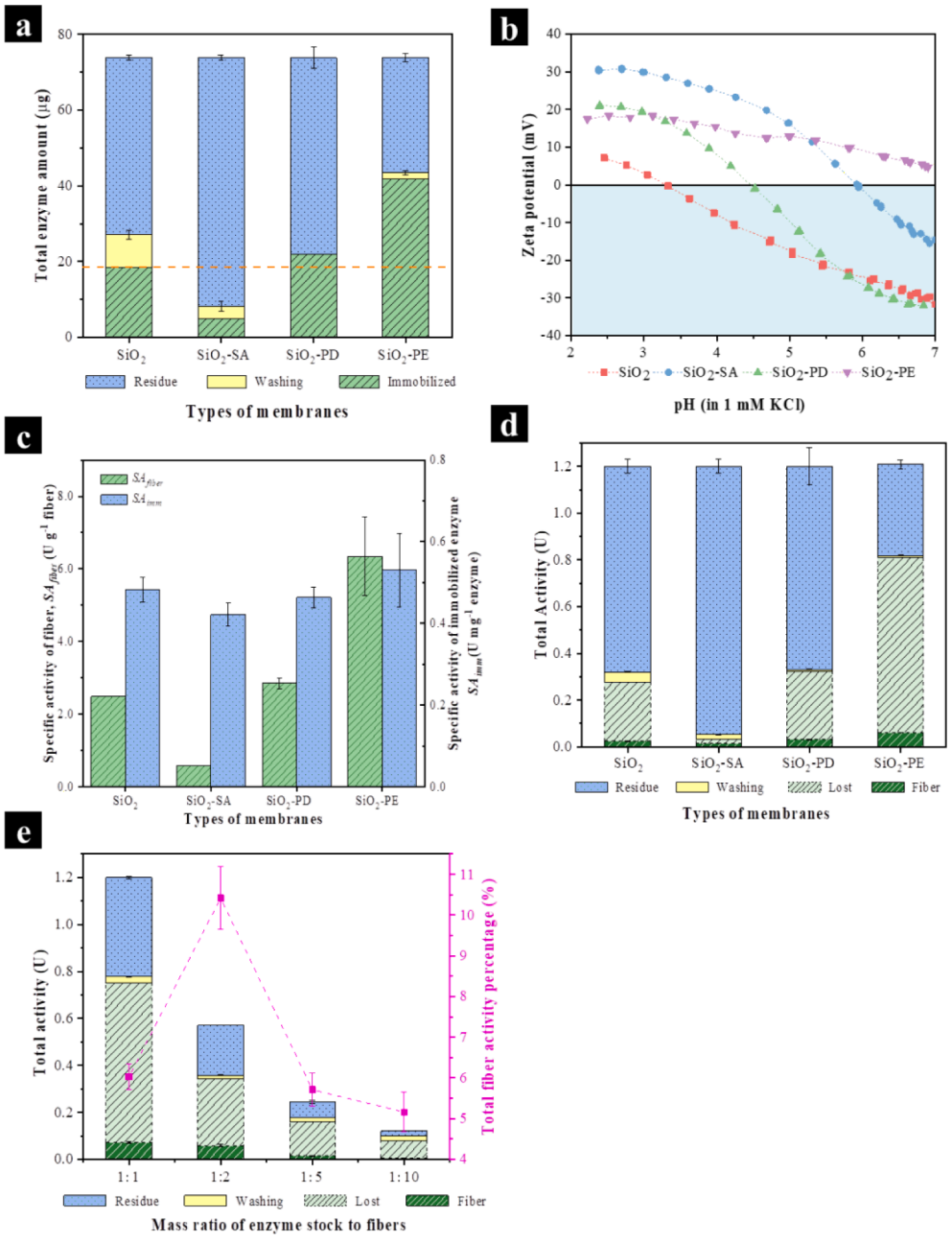

Fig. 3. a) Enzyme amount distribution in immobilization solution after immobilization (residue solution), washing buffers and immobilized fiber during the immobilization b) Zeta potential as a function of pH for fibrous membranes at 1 mM KCl ionic strength. The intersection of the horizontal solid line with the curves depicts the isoelectric point of each fibrous membrane. c) Specific activity of fiber (SA_{fiber}) and specific activity of immobilized laccase (SA_{imm}) on different fibrous membranes. d) Total enzyme activity of residue solution, washing buffer, immobilized fibers and calculated activity lost. Mass ratio of enzyme stock to membrane was set as 1:1 during the immobilization process. e) Total residual enzyme activity in the residue solution, washing buffer, immobilized fibers, the calculated lost activity. The total fiber activity proportion with different enzyme stock to membrane mass ratio is shown as a scatter plot. The data are the arithmetic mean ± standard deviation of two independent replicates.

(+20 mV) was observed and may explain the noticeable drop in protein loading due to repulsion between the strong positive charge of the membrane surface and enzymes. Amine groups grafted through PDA coating and co-deposition likewise introduced a positive charge to the membranes. With similar immobilization capacity, SiO_2-PD NFMs exhibited a neutral charge at pH 4.5. Besides physical adsorption, covalent binding between support materials and laccase molecules manifests during the immobilization process. The catechol groups of PDA can efficiently react with thiol and amine group of laccase *via* Schiff [29] and Michael addition reactions [11]. With the addition of the PEI, +12 mV zeta potential value was measured at pH 4.5, while the highest immobilization yield was achieved due to the smaller diameter range of particle aggregates, especially compared with PDA coating. The fine and evenly distributed particles increased the roughness and thereby the surface area accessible for laccase immobilization. This unique surface topography with a higher specific area further enhanced the immobilized enzyme capacity on SiO_2-PE NFMs. Similar findings that modulate the microstructure of the surface have been reported to modify the immobilization outcome. [30,31].

3.2.2. *Optimization of enzyme activity*

In addition to the protein concentration, enzyme activity is a crucial parameter in evaluating the support materials and immobilization performance. According to the definition in Section 2.3.2, the specific activities of the immobilized enzyme (SA_{imm}) and fiber (SA_{fiber}) were defined as the enzyme activity of fiber per weight of immobilized enzyme (U mg^{-1} enzyme) and support membrane(U g^{-1} fiber) separately. As depicted in Fig. 3**c**, SiO_2-PE NFMs exhibited the highest values on the specific activity of fiber, as more enzymes were immobilized on the same weight of membrane pieces. Besides the specific activity of immobilized enzymes, the functionalized NFMs demonstrated slight differences. SiO_2-PE NFMs modified by the co-deposition method exhibited the best immobilization performance considering both enzyme load and activity. Apparent kinetic parameters for the free and

immobilized laccase (Lac-SiO_2-PE NFMs), V_{max}, and K_m are listed in Table 1. The increase of K_m value also indicated lower accessibility or affinity of the substrate to the active sites of the immobilized enzyme.

The specific activity of the immobilized enzyme (0.53 ± 0.09 U mg^{-1}) was much lower than that of free laccase (16.13 ± 0.26 U mg^{-1}), which is not uncommon for immobilized enzymes due to a range of factors such as reduced enzyme flexibility[11], and/or conformational changes[32] or unfolding associated with the immobilization as well as crowding as will be discussed below. In addition, Fig. 3d depicts the distribution of activity along the immobilization process, including initial enzyme stock, washing buffers, and residual solution, which shows fiber-dependent changes in enzyme activity distribution. High enzyme activity of fiber (A_{fiber}) loss, correlated to the high protein load, is observed on SiO_2-PE NFMs. Nonetheless, this membrane type exhibited the highest enzyme activity of fiber (0.06 U), corresponding to 6 % of total activity. A possible reason for the decrease in activity, despite the high protein load, may be the crowding of immobilized enzymes on the fibers. An optimization experiment on different relative enzyme loads provided support to this hypothesis. As shown in Fig. 3e, fiber maintains 80 % of the activity when the enzyme load is reduced by 50 %, while activity losses decline from 56 % to 47 %. Further reduction of enzyme load, however, led to a significant loss of fiber activity. Therefore, optimizing the enzyme load on the fiber is important to maximize the yield of immobilization active enzyme per membrane mass.

3.3. Stability of the immobilized laccase

Fig. 4a shows the effect of pH on the relative activities of free and immobilized laccase on SiO_2-PE. Immobilized laccase maintained>40 % of its optimum activity within a broader pH range than the free enzyme. The optimum pH value of the free and immobilized laccase were 4.5 and 4.0, respectively. This apparent pH shift might be due to the higher charge density of SiO_2-PE NFMs that changes the electrostatics in the microenvironment around the enzyme. Similar observations were noticed for laccase immobilized on bacterial microcrystalline cellulose, and the optimum pH was found to be 3.5 for free laccase as compared to 2.5 for immobilized laccase [33].

With regard to thermal stability, thermal inactivation kinetics for free and immobilized laccase was studied (Fig. 4b). A_0 and A refer to the initial and remaining enzyme activity of the free or immobilized enzyme. The residual activity of the immobilized laccase was 82.4 ± 1.2 % as compared to 53.0 ± 0.01 % for the free laccase after heating for 120 min at 50 °C. Thermal inactivation data were modeled with first-order kinetics, with coefficients of determination (COD) of 0.99 and 0.98 for free and immobilized laccase, respectively. The thermal inactivation rate constant (k_{inact}) decreased threefold for the immobilized enzyme (0.1 h^{-1}) as compared to the free laccase (0.3 h^{-1}), which corresponds to an increase in the half-time of thermal inactivation ($t_{1/2}$) at 50 °C from 2.3 h to 6.9 h. These data revealed improved thermal stability of the immobilized laccase compared to the free form, which is consistent with the observation that the enzyme's resistance to high temperatures is greatly increased by immobilization [34].

One of the essential advantages of enzyme immobilization is

Table 1
Apparent activity and kinetic parameters of free and immobilized laccase.

	Specific activity (U mg^{-1}enzyme)	K_m (mM)[a]	V_{max} (U mg^{-1} enzyme)[b]
Free laccase	16.13 ± 0.26	0.13 ± 0.01	14.97 ± 0.07
Lac-SiO_2-PE	0.53 ± 0.09	2.35 ± 0.72	0.56 ± 0.19

a K_m [mM] is the apparent Michaelis–Menten constant; b V_{max} is the apparent maximum rate of the bio-catalyst.

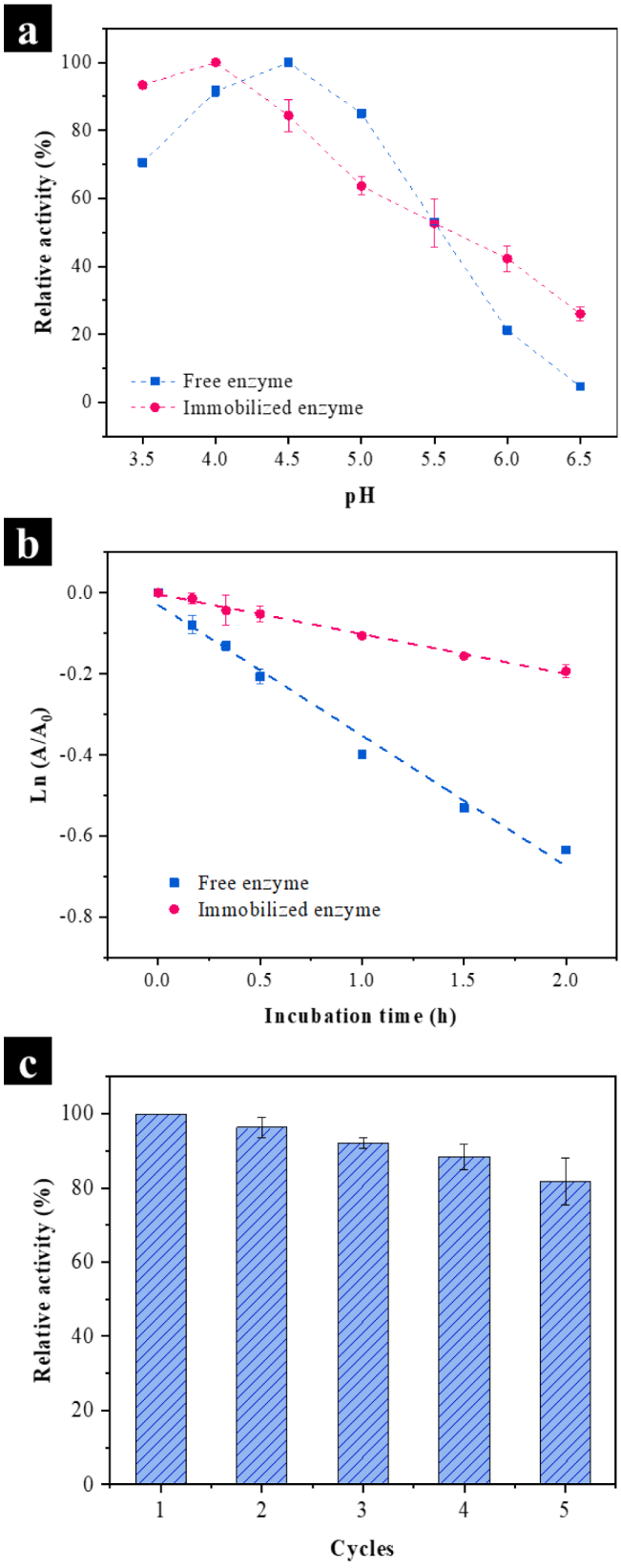

Fig. 4. a) The pH stability of Lac-SiO_2-PE NFMs and free laccase. b) Thermal inactivation kinetics of Lac-SiO_2-PE NFMs and free laccase. Enzyme solution and Lac-SiO_2-PE pieces (in 50 mM acetate buffer, pH 4.5) were incubated at 50 °C for 2 h. c) Relative activity of Lac-SiO_2-PE NFMs with recycling usage. A and A_0 refer to remaining and initial activity of free or immobilized enzyme. Values were arithmetic mean ± standard deviation of two independent replicates.

recovering and reusing the catalysts. In order to probe the operational stability over cycles of use, the residual activity of immobilized laccase was repeatedly measured following incubation with ABTS, and the results are illustrated in Fig. 4c. Up to 80 % of the initial activity of the immobilized enzyme was retained after five cycles of reuse. The loss of relative activity could be due to the irreversible inactivation of the enzyme cycles of reuse. The loss of relative activity could be due to the irreversible inactivation of the enzyme.

3.4. Removal of emerging pollutants

EPs are found in wastewater treatment plants (WWTPs) effluent at concentrations ranging from low ng L^{-1} to a few μg L^{-1} [35]. The occurrence of EPs and their removal has become a research focus in wastewater treatment. Considering the extreme-low pollutant concentrations accompanied by massive throughput in real wastewater treatment plants, laccase-immobilized NFMs are considered a post-treatment process of wastewater after the filtration process, where most of the other pollutants are removed, and the EPs are concentrated. Therefore, we performed a series of experiments on high concentrated synthetic EP mixtures in Milli-Q-H_2O to gain insight into the performance of laccase and laccase-immobilized NFMs. 20 EPs, including antibiotics, analgesics, blood pressure regulators, antidepressants, anti-inflammatory, and anti-corrosions, have been screened by free laccase (**Fig. S5**). Five compounds were efficiently transformed by the free laccase (>60 % transformation). Lac-SiO_2-PE NFMs have revealed promising depletion outcomes (≥95 %) for all selected EPs (Fig. 5a), including diclofenac, one of the most recalcitrant components detected in aquatic media. Although the SiO_2-PE NFMs as a reference also showed selectivity on these contaminants, possibly due to the adsorption effect on the membrane, the complement of enzymatic NFMs further enhanced the transformation rates.

Notably, Lac-SiO_2-PE NFMs displayed stable performance for the selected EPs, with maintained transformation efficiency > 90 % after three times of reuse (Fig. 5b). The total depletion efficiency derives mainly from both enzyme biotransformation and adsorption. A slight decrease observed in depletion efficiency could be explained by decreasing the adsorption property of control membranes (**Fig. S6**). The depletion efficiency achieved by the control membranes decreased from 25.9 % to 15.5 % in the 3rd cycle. Another possible reason for the slight decrease in depletion efficiency can be membrane fouling, which is inevitable, especially for membrane systems treating wastewater with a high concentration of pollutants. After 3 cycles of use, the NFM was slightly compressed due to the applied pressure but maintained its porous microstructure (**Fig. S7**). However, due to the repeated exposure of the NFMs to a high concentration of emerging pollutants, we observed the accumulation of emerging pollutants and/or their transformation products on/between the nanofibers, which may influence the catalytic performance of the immobilized laccase. Therefore, a back-washing is suggested in-between the membrane process. In addition, a batch study with Lac-SiO_2 NFMs on the model EP Diclofenac was depicted in Fig. 5c. The transformation curve of diclofenac shows 90 % removal efficiency within an hour.

To further evaluate the performance of Lac-SiO_2 NFMs, Table 2 summarizes the enzymatic membrane performance of this work and similar studies from other enzyme carriers. Quantitative comparison of enzyme reusability is difficult due to the different scales and experimental conditions. Our study, as well as listed research, achieved to reuse of designed enzymatic membranes with high remaining activity. We attempt to apply lower substrate concentrations and filtration systems compared to previous research. However, the applied concentrations of EPs are relatively higher than values expected in hospital and WWTPs effluents. Taking the actual concentration of diclofenac into consideration[40], the amount of treated diclofenac in this study is equivalent to 173 L of hospital effluents and 243 L of WWTPs effluents. Thus biocatalytic membranes are to be considered a treatment process of

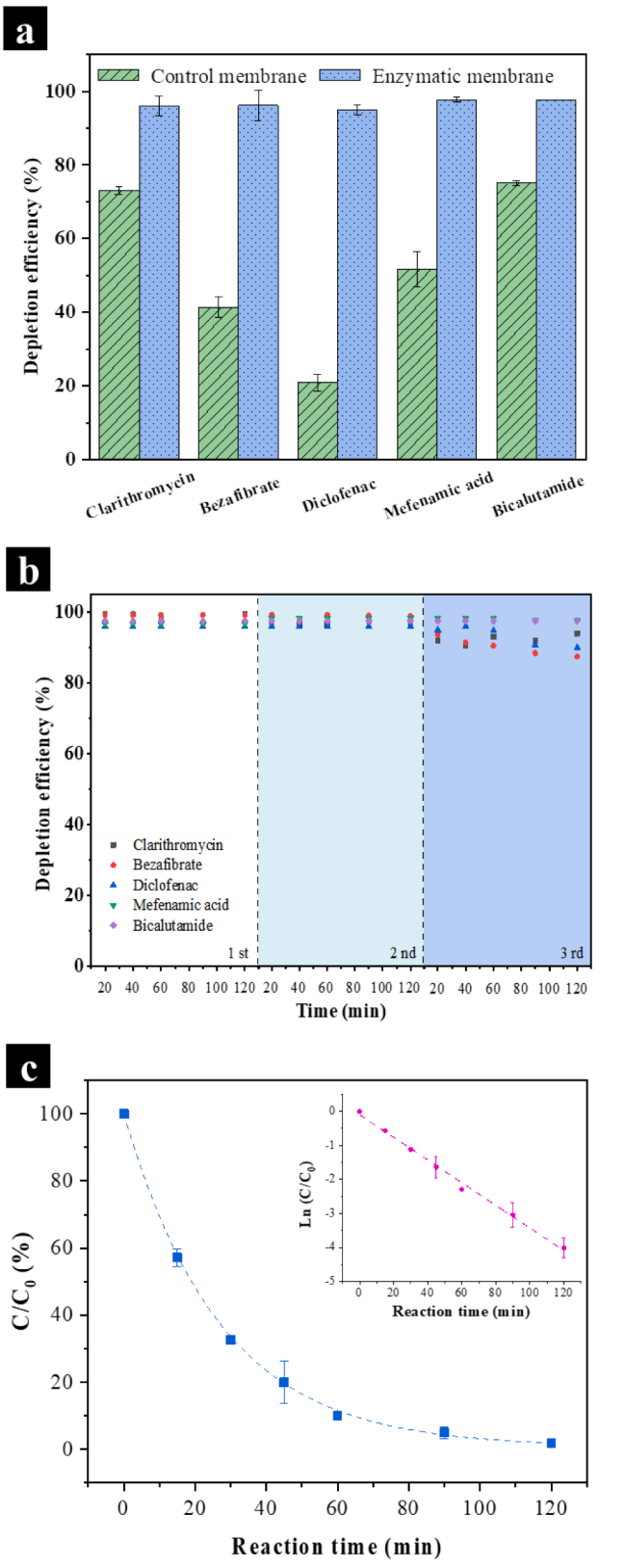

Fig. 5. Membrane performance on EPs removal. a) Depletion efficiency of 5 selected EPs by control membranes and lac-SiO_2 NFMs. b) Cycling performance of lac-SiO_2 NFMs in 5 selected EPs mixture. c) Diclofenac transformation efficiency (%) by Lac-SiO_2-PE NFMs in a batch study. The data are arithmetic mean ± standard deviation of two independent replicates.

Table 2
Performance of the immobilized laccase using various support materials.

Enzyme source	Support	Method	Yield (%)	Specific activity ($U\ g^{-1}_{membrane}$)	Target EPs	Operation	$C^{a}_{substrate}$	$V_{substrate}$ (mL)[b]	Support recyclability	Enzyme reusability	Depletion efficiency (%)	Ref.
Free Laccase from *Trametes versicolour*	–	–	–	–	Bicalutamide, mefenamic acid, diclofenac, clarithromycin, and bezafibrate	Batch	200 μg L^{-1}	300	–	No	–	This study
Laccase from *Trametes versicolour*	SiO_2-PE NFMs	Covalent bonding	57.9	6.4 ± 1.1	Bicalutamide, mefenamic acid, diclofenac, clarithromycin, and bezafibrate	Filtration	200 μg L^{-1}	500	Yes	Yes	> 95 %	This study
Laccase from *Trametes versicolour*	PES hollow fiber	Layer by layer assembly	20.32	–	Bisphenol	Dipping incubation	34.2 mg L^{-1}	50	No	Yes	92.1	[36]
Laccase from *Aspergillus oryzae*	CNTox-0.3-EN	Covalent bonding	89.8	12.7 ± 0.3	4-methoxyphenol	Batch	10 mgL^{-1}	20	No	Yes	85	[37]
Laccase from *Trametes versicolour*	PAN/PVdF/Cu NFMs	Covalent bonding	34.9	–	Bisphenol	Batch	5 mg L^{-1}	60	No	Yes	95.4	[38]
Laccase from *Pleurotus ostreatus*	Acrylic carriers (Purolite®)	Covalent bonding	80.5	5.34 ± 0.4	Bisphenol	Batch	0.5–10 mg L^{-1}	10	No	Yes	50–100	[39]

a $C_{substrate}$ initial substrate concentration.
b $V_{substrate}$ substrate volume is defined as the target pharmaceutical solution volume of a cycle.

wastewater using a concentrated wastewater stream.

4. Conclusion

We successfully immobilized laccase onto functionalized SiO_2 NFMs. Both the immobilization procedure and the properties of the immobilized support significantly impact biocatalyst loading and stability. The Lac-SiO_2-PE NFMs enabled a high protein load (57.9 ± 0.5 %), improved stability compared to the free enzyme, and most importantly, allowed for bio-catalyst recycling. The feasibility of applying laccase immobilized membranes into filtration systems has been demonstrated using five EPs with high depletion efficiency. Altogether, our work highlights the promising potential of Lac-SiO_2-PE NFMs in EPs removal in wastewater treatment. Our simple fabrication protocol of scalable and flexible ceramic membranes overcomes the key bottlenecks of conventional ceramic membranes, which are brittleness and complex production procedure. Finally, the implementation of flexible ceramics in membrane filtration addresses an environmental concern with discarding contaminated polymeric modulus via reuse of the biocatalytic membranes.

Declaration of Competing Interest

The authors declare that they have no known competing financial interests or personal relationships that could have appeared to influence the work reported in this paper.

Data availability

Data will be made available on request.

Acknowledgments

This work was sponsored by the Novo Nordisk Foundation (NNF18OC0034918) and the Danish Research Council (Grant No. 8022-00237B). The authors would like to acknowledge the financial support from China Scholarship Council. The authors would like to thank Song Wang, Mikael Emil Olsson, Kai Tang and Irena Petrinić for the experimental support.

Appendix A. Supplementary data

Supplementary data to this article can be found online at https://doi.org/10.1016/j.cej.2022.138902.

References

[1] C.G. Daughton, T.A. Ternes, Pharmaceuticals and personal care products in the environment: Agents of subtle change? Environ. Health Perspect. 107 (1999) 907–938, https://doi.org/10.1289/ehp.99107s6907.
[2] M. Taheran, S.K. Brar, M. Verma, R.Y. Surampalli, T.C. Zhang, J.R. Valero, Membrane processes for removal of pharmaceutically active compounds (PhACs) from water and wastewaters, Sci. Total Environ. 547 (2016) 60–77, https://doi.org/10.1016/j.scitotenv.2015.12.139.
[3] A. Zenker, M.R. Cicero, F. Prestinaci, P. Bottoni, M. Carere, Bioaccumulation and biomagnification potential of pharmaceuticals with a focus to the aquatic environment, J. Environ. Manage. 133 (2014) 378–387, https://doi.org/10.1016/J.JENVMAN.2013.12.017.
[4] L. Wiest, A. Gosset, A. Fildier, C. Libert, M. Hervé, E. Sibeud, B. Giroud, E. Vulliet, T. Bastide, P. Polomé, Y. Perrodin, Occurrence and removal of emerging pollutants in urban sewage treatment plants using LC-QToF-MS suspect screening and quantification, Sci. Total Environ. 774 (2021), 145779, https://doi.org/10.1016/j.scitotenv.2021.145779.
[5] Z. Baalbaki, T. Sultana, T. Maere, P.A. Vanrolleghem, C.D. Metcalfe, V. Yargeau, Fate and mass balance of contaminants of emerging concern during wastewater treatment determined using the fractionated approach, Sci. Total Environ. 573 (2016) 1147–1158, https://doi.org/10.1016/j.scitotenv.2016.08.073.
[6] M. de Cazes, R. Abejón, M.P. Belleville, J. Sanchez-Marcano, Membrane bioprocesses for pharmaceutical micropollutant removal from waters, Membranes (Basel). 4 (2014) 692–729, https://doi.org/10.3390/membranes4040692.
[7] J.L. Acero, F.J. Benitez, A.I. Leal, F.J. Real, F. Teva, Membrane filtration technologies applied to municipal secondary effluents for potential reuse,

J. Hazard. Mater. 177 (2010) 390–398, https://doi.org/10.1016/j.jhazmat.2009.12.045.
[8] M. Bilal, S.S. Ashraf, D. Barceló, H.M.N. Iqbal, Biocatalytic degradation/redefining "removal" fate of pharmaceutically active compounds and antibiotics in the aquatic environment, Sci. Total Environ. 691 (2019) 1190–1211, https://doi.org/10.1016/j.scitotenv.2019.07.224.
[9] A.T. Martínez, F.J. Ruiz-Dueñas, S. Camarero, A. Serrano, D. Linde, H. Lund, J. Vind, M. Tovborg, O.M. Herold-Majumdar, M. Hofrichter, C. Liers, R. Ullrich, K. Scheibner, G. Sannia, A. Piscitelli, C. Pezzella, M.E. Sener, S. Kılıç, W.J.H. van Berkel, V. Guallar, M.F. Lucas, R. Zuhse, R. Ludwig, F. Hollmann, E. Fernández-Fueyo, E. Record, C.B. Faulds, M. Tortajada, I. Winckelmann, J.A. Rasmussen, M. Gelo-Pujic, A. Gutiérrez, J.C. del Río, J. Rencoret, M. Alcalde, Oxidoreductases on their way to industrial biotransformations, Biotechnol. Adv. 35 (2017) 815–831, https://doi.org/10.1016/j.biotechadv.2017.06.003.
[10] F. Christopher, The structure and function of fungal laccase, Microbiology. 140 (1994) 19.
[11] C. Chen, W. Sun, H. Lv, H. Li, Y. Wang, P. Wang, Spacer arm-facilitated tethering of laccase on magnetic polydopamine nanoparticles for efficient biocatalytic water treatment, Chem. Eng. J. 350 (2018) 949–959, https://doi.org/10.1016/J.CEJ.2018.06.008.
[12] M. Maryšková, I. Ardao, C.A. García-González, L. Martinová, J. Rotková, A. Ševců, Polyamide 6/chitosan nanofibers as support for the immobilization of Trametes versicolor laccase for the elimination of endocrine disrupting chemicals, Enzyme Microb. Technol. 89 (2016) 31–38, https://doi.org/10.1016/J.ENZMICTEC.2016.03.001.
[13] S.P. Nunes, P.Z. Culfaz-Emecen, G.Z. Ramon, T. Visser, G.H. Koops, W. Jin, M. Ulbricht, Thinking the future of membranes: Perspectives for advanced and new membrane materials and manufacturing processes, J. Memb. Sci. 598 (2020), 117761, https://doi.org/10.1016/J.MEMSCI.2019.117761.
[14] S. Liu, H. Shan, S. Xia, J. Yan, J. Yu, B. Ding, Polymer Template Synthesis of Flexible SiO2Nanofibers to Upgrade Composite Electrolytes, ACS Appl. Mater. Interfaces. 12 (2020) 31439–31447, https://doi.org/10.1021/ACSAMI.0C06922/SUPPL_FILE/AM0C06922_SI_001.PDF.
[15] M. Guo, B. Ding, X. Li, X. Wang, J. Yu, M. Wang, Amphiphobic nanofibrous silica mats with flexible and high-heat-resistant properties, J. Phys. Chem. C. 114 (2010) 916–921, https://doi.org/10.1021/jp909672r.
[16] D. Han, S. Filocamo, R. Kirby, A.J. Steckl, Deactivating chemical agents using enzyme-coated nanofibers formed by electrospinning, ACS Appl. Mater. Interfaces. 3 (2011) 4633–4639, https://doi.org/10.1021/am201064b.
[17] P. Jing, M. Liu, P. Wang, J. Yang, M. Tang, C. He, Y. Pu, M. Liu, Flexible nonwoven ZrO2 ceramic membrane as an electrochemically stable and flame-resistant separator for high-power rechargeable batteries, Chem. Eng. J. 388 (2020), 124259, https://doi.org/10.1016/J.CEJ.2020.124259.
[18] K.H. Lee, C.S. Ki, D.H. Baek, G.D. Kang, D.-W. Ihm, Y.H. Park, Application of electrospun silk fibroin nanofibers as an immobilization support of enzyme, Fibers Polym. 6 (3) (2005) 181–185.
[19] D. Zhao, J.F. Kim, G. Ignacz, P. Pogany, Y.M. Lee, G. Szekely, Bio-Inspired Robust Membranes Nanoengineered from Interpenetrating Polymer Networks of Polybenzimidazole/Polydopamine, ACS Nano. 13 (2019) 125–133, https://doi.org/10.1021/acsnano.8b04123.
[20] D. Schaubroeck, L. Mader, P. Dubruel, J. Vanfleteren, Surface modification of an epoxy resin with polyamines and polydopamine: Adhesion toward electroless deposited copper, Appl. Surf. Sci. 353 (2015) 238–244, https://doi.org/10.1016/J.APSUSC.2015.06.114.
[21] B. Qiao, T.J. Wang, H. Gao, Y. Jin, High density silanization of nano-silica particles using γ-aminopropyltriethoxysilane (APTES), Appl. Surf. Sci. 351 (2015) 646–654, https://doi.org/10.1016/J.APSUSC.2015.05.174.
[22] K.R. Diaz-Galvez, N.G. Teran-Saavedra, A.J. Burgara-Estrella, D. Fernandez-Quiroz, E. Silva-Campa, M. Acosta-Elias, H.M. Sarabia-Sainz, M.R. Pedroza-Montero, J.A. Sarabia-Sainz, Specific capture of glycosylated graphene oxide by an asialoglycoprotein receptor: a strategic approach for liver-targeting, Specific capture of glycosylated graphene oxide by an asialoglycoprotein receptor: a strategic approach for liver-targeting 9 (18) (2019) 9899–9906.
[23] H.-P. Zhang, W. Han, J. Tavakoli, Y.-P. Zhang, X. Lin, X. Lu, Y. Ma, Y. Tang, Understanding interfacial interactions of polydopamine and glass fiber and their enhancement mechanisms in epoxy-based laminates, Compos. Part A Appl. Sci. Manuf. 116 (2019) 62–71.
[24] J. Kim, Q. Fu, K. Xie, J.M.P. Scofield, S.E. Kentish, G.G. Qiao, CO2 separation using surface-functionalized SiO2 nanoparticles incorporated ultra-thin film composite mixed matrix membranes for post-combustion carbon capture, J. Memb. Sci. 515 (2016) 54–62, https://doi.org/10.1016/J.MEMSCI.2016.05.029.
[25] R.A. Zangmeister, T.A. Morris, M.J. Tarlov, Characterization of Polydopamine Thin Films Deposited at Short Times by Autoxidation of Dopamine, Characterization of Polydopamine Thin Films Deposited at Short Times by Autoxidation of Dopamine 29 (27) (2013) 8619–8628.
[26] M. Tan, Y. Feng, H. Wang, L. Zhang, M. Khan, J. Guo, Q. Chen, J. Liu, Immobilized Bioactive Agents onto Polyurethane Surface with Heparin and Phosphorylcholine Group, Macromol. Res. 21 (2013) 541–549, https://doi.org/10.1007/s13233-013-1028-3.
[27] Y. Zhang, H. Zhang, Y. Li, H. Mao, G. Yang, J. Wang, Tuning the Performance of Composite Membranes by Optimizing PDMS Content and Cross-Linking Time for Solvent Resistant Nanofiltration, (2015). doi:10.1021/acs.iecr.5b01236.
[28] J.D. Cyran, M.A. Donovan, D. Vollmer, F.S. Brigiano, S. Pezzotti, D.R. Galimberti, M.P. Gaigeot, M. Bonn, E.H.G. Backus, Molecular hydrophobicity at a macroscopically hydrophilic surface, Proc. Natl. Acad. Sci. U. S. A. 116 (2019) 1520–1525, https://doi.org/10.1073/pnas.1819000116.
[29] Y. Liu, K. Ai, L. Lu, Polydopamine and its derivative materials: Synthesis and promising applications in energy, environmental, and biomedical fields, Chem. Rev. 114 (2014) 5057–5115, https://doi.org/10.1021/cr400407a.
[30] R. Awad, A. Haghighat Mamaghani, Y. Boluk, Z. Hashisho, Synthesis and characterization of electrospun PAN-based activated carbon nanofibers reinforced with cellulose nanocrystals for adsorption of VOCs, Chem. Eng. J. 410 (2021), 128412, https://doi.org/10.1016/j.cej.2021.128412.
[31] Z.-G. Wang, L.-S. Wan, Z.-M. Liu, X.-J. Huang, Z.-K. Xu, Enzyme immobilization on electrospun polymer nanofibers: An overview, J. Mol. Catal. B Enzym. 56 (2009) 189–195, https://doi.org/10.1016/J.MOLCATB.2008.05.005.
[32] F. Secundo, Conformational changes of enzymes upon immobilisation, Chem. Soc. Rev. 42 (2013) 6250, https://doi.org/10.1039/c3cs35495d.
[33] M. Bilal, J. Cui, H.M.N. Iqbal, Tailoring enzyme microenvironment: State-of-the-art strategy to fulfill the quest for efficient bio-catalysis, Int. J. Biol. Macromol. 130 (2019) 186–196, https://doi.org/10.1016/J.IJBIOMAC.2019.02.141.
[34] A. Leonowicz, J.M. Sarkar, J.-M. Bollag, Improvement in stability of an immobilized fungal laccase, Appl Microbiol Biotechnol 29 (2-3) (1988) 129–135.
[35] R. Morsi, M. Bilal, H.M.N. Iqbal, S.S. Ashraf, Laccases and peroxidases: The smart, greener and futuristic biocatalytic tools to mitigate recalcitrant emerging pollutants, Sci. Total Environ. 714 (2020), 136572, https://doi.org/10.1016/J.SCITOTENV.2020.136572.
[36] X. Li, Y. Xu, K. Goh, T.H. Chong, R. Wang, Layer-by-layer assembly based low pressure biocatalytic nanofiltration membranes for micropollutants removal, J. Memb. Sci. 615 (2020), 118514, https://doi.org/10.1016/J.MEMSCI.2020.118514.
[37] J.B. Costa, M.J. Lima, M.J. Sampaio, M.C. Neves, J.L. Faria, S. Morales-Torres, A.P. M. Tavares, C.G. Silva, Enhanced biocatalytic sustainability of laccase by immobilization on functionalized carbon nanotubes/polysulfone membranes, Chem. Eng. J. 355 (2019) 974–985, https://doi.org/10.1016/J.CEJ.2018.08.178.
[38] R. Xu, J. Cui, R. Tang, F. Li, B. Zhang, Removal of 2,4,6-trichlorophenol by laccase immobilized on nano-copper incorporated electrospun fibrous membrane-high efficiency, stability and reusability, Chem. Eng. J. 326 (2017) 647–655, https://doi.org/10.1016/j.cej.2017.05.083.
[39] K. Wlizło, J. Polak, J. Kapral-Piotrowska, M. Gr ˛ Az, R. Paduch, A. Jarosz-Wilkołazka, Influence of Carrier Structure and Physicochemical Factors on Immobilisation of Fungal Laccase in Terms of Bisphenol A Removal, (n.d.). doi: 10.3390/catal10090951.
[40] S. Aydin, M.E. Aydin, A. Ulvi, Monitoring the release of anti-inflammatory and analgesic pharmaceuticals in the receiving environment, Environ. Sci. Pollut. Res. 26 (2019) 36887–36902, https://doi.org/10.1007/s11356-019-06821-4.

Supplementary Material for:

Facile Fabrication of Flexible Ceramic Nanofibrous Membrane for Laccase Immobilization Targeting in Emerging Contaminants Removal.

Dan Zhao[a], Maria Louise leth[b], Maher Abou Hachem[b], Iram Aziz[c],, Natalija Jančič[d], Thomas Luxbacher[d, e], Claus Hélix-Nielsen[a, *], Wenjing (Angela) Zhang[a, *]

a. Department of Environmental and Resource Engineering, Technical University of Denmark, DTU, 2800 Kgs. Lyngby, Denmark

b. Department of Biotechnology and Biomedicine, Technical University of Denmark, DTU, 2800 Kgs. Lyngby, Denmark

c. Department of Chemistry and Chemical Engineering, Lahore University of Management Sciences, 54792 Lahore, Pakistan

d. Faculty of Chemistry and Chemical Engineering, University of Maribor, 2000 Maribor, Slovenia

e. Anton Paar GmbH, 8054 Graz, Austria

[*] **Corresponding author:**

Dr. Wenjing (Angela) Zhang

Tel: (+45) 20352356; E-mail address: wen@dtu.dk

Dr. Claus Hélix-Nielsen

Tel: (+45) 45252228; E-mail address: clhe@dtu.dk

Text S1. Materials

Table S1. Twenty common emerging pollutants

	Emerging pollutants	CAS Number	Molecular weight (g/mol)	Formula	Supplier
1	Ciprofloxacin	85721-33-1	331.34	$C_{17}H_{18}FN_3O_3$	Sigma-Aldrich
2	Clarithromycin	81103-11-9	747.95	$C_{38}H_{69}NO_{13}$	Sigma-Aldrich
3	Atenolol	29122-68-7	266.34	$C_{14}H_{22}N_2O_3$	Sigma-Aldrich
4	(±)-Metoprolol (+)-tartrate salt	56392-17-7	684.81	$(C_{15}H_{25}NO_3)_2\ C_4H_6O_6$	Sigma-Aldrich
5	Hydrochlorothiazide	58-93-5	297.74	$C_7H_8ClN_3O_4S_2$	Sigma-Aldrich
6	Sulfamethoxazole	723-46-6	253.28	$C_{10}H_{11}N_3O_3S$	Sigma-Aldrich
7	Bezafibrate	41859-67-0	361.82	$C_{19}H_{20}ClNO_4$	Sigma-Aldrich
8	Carbamazepine	298-46-4	236.27	$C_{15}H_{12}N_2O$	Sigma-Aldrich
9	Diclofenac sodium salt	15307-79-6	318.13	$C_{14}H_{11}Cl_2NNaO_2$	Sigma-Aldrich
10	Mefenamic acid	61-68-7	241.29	$C_{15}H_{15}NO_2$	Sigma-Aldrich
11	Citalopram Hydrobromide	59729-32-7	405.30	$C_{20}H_{21}FN_2O$ HBr	Sigma-Aldrich
12	Venlafaxine hydrochloride	99300-78-4	313.86	$C_{17}H_{27}NO_2$ HCl	Sigma-Aldrich
13	Sertraline hydrochloride	79559-97-0	342.69	$C_{17}H_{17}Cl_2N$ HCl	Sigma-Aldrich
14	Iomeprol	78649-41-9	777.09	$C_{17}H_{22}I_3N_3O_8$	Dr. Ehrenstorfer GmbH (germany)
15	Ketoprofen	22071-15-4	254.28	$C_{16}H_{14}O_3$	Sigma-Aldrich
16	Bicalutamide	90357-06-5	430.37	$C_{18}H_{14}F_4N_2O_4S$	Sigma-Aldrich
17	1H-Benzotriazole	95-14-7	119.12	$C_6H_5N_3$	Sigma-Aldrich
18	5-Chlorobenzotriazole	94-97-3	153.57	$C_6H_4ClN_3$	Sigma-Aldrich
19	5-Methyl-1H-benzotriazole	136-85-6	133.15	$C_7H_7N_3$	Sigma-Aldrich
20	Clofibric acid	882-09-7	214.65	$C_{10}H_{11}ClO_3$	Sigma-Aldrich

Text S2. Operation of dead-end filtration

The flow diagram of the dead-end filtration system with the ceramic membrane is shown in **Figure S1.**

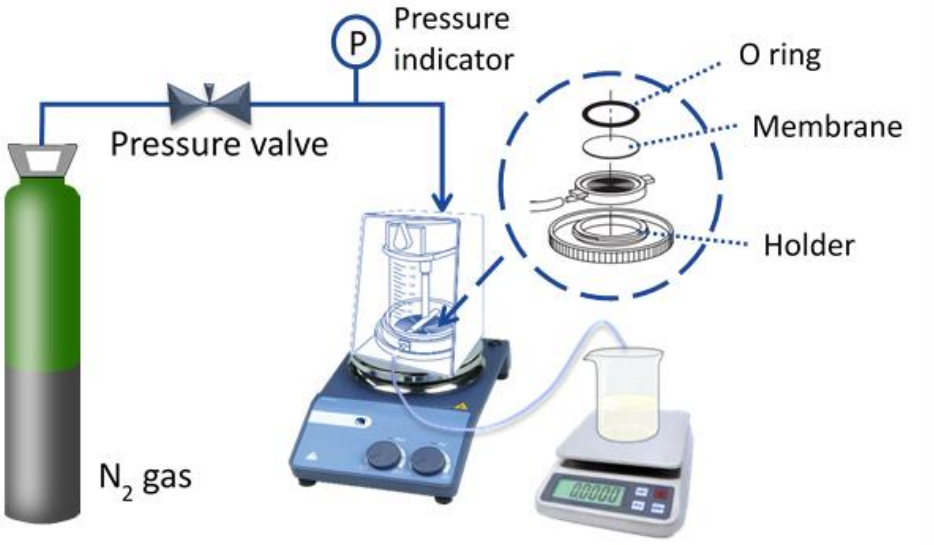

Figure S1. Dead-end filtration diagram

Text S3. Bradford assay

The Bradford assay was performed by mixing 20 μL of sample with 130 μL Pierce Coomassie plus assay reagent. After incubation 10 min at 25°C, the absorbancewas measured at 595 nm. The standard curve is shown as **Figure S2**

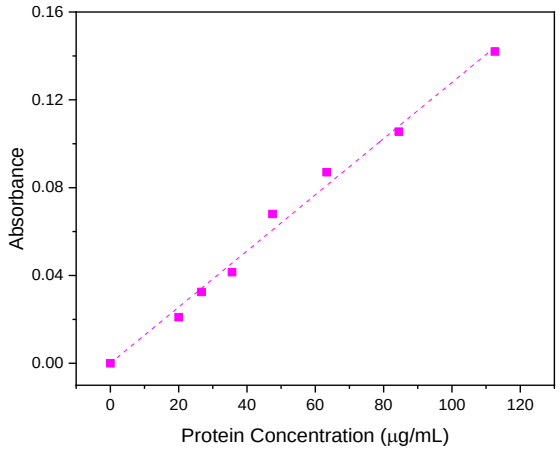

Figure S2. Standard curve for BSA

Text S4. Thermal inactivation kinetics

The thermal inactivation data for free and immobilized laccase was plotted for zero (residual activity versus time), first (natural logarithm of the residual activity versus time) and second-order (reciprocal activity versus time). The rate constant k_{inact} [h^{-1}] for first-order thermal inactivation was determined from the slope of the inactivation time:

$$ln\left(\frac{A_t}{A_0}\right) = -k_{inact}t \quad (1)$$

$$t_{0.5} = \frac{ln(2)}{k_{inact}} \quad (2)$$

Where At is the residual activity that remains after heating the enzyme for time t, and A_0 is the initial enzyme activity before heating. The half-time of thermal inactivation ($t_{0.5}$) was determined by equation S2.

Text S5. Determination of coating weight percentage

The weight percentages of coatings were determined according to the following equation:

$$C(\%) = \frac{Mc-M0}{M0} \times 100 \quad (3)$$

Where C(%) is the weight percentage of the coating, M_0 and Mc are the mass of NFMs before and after the coating process.

Text S6. The flexibility tests on SiO_2 NFMs

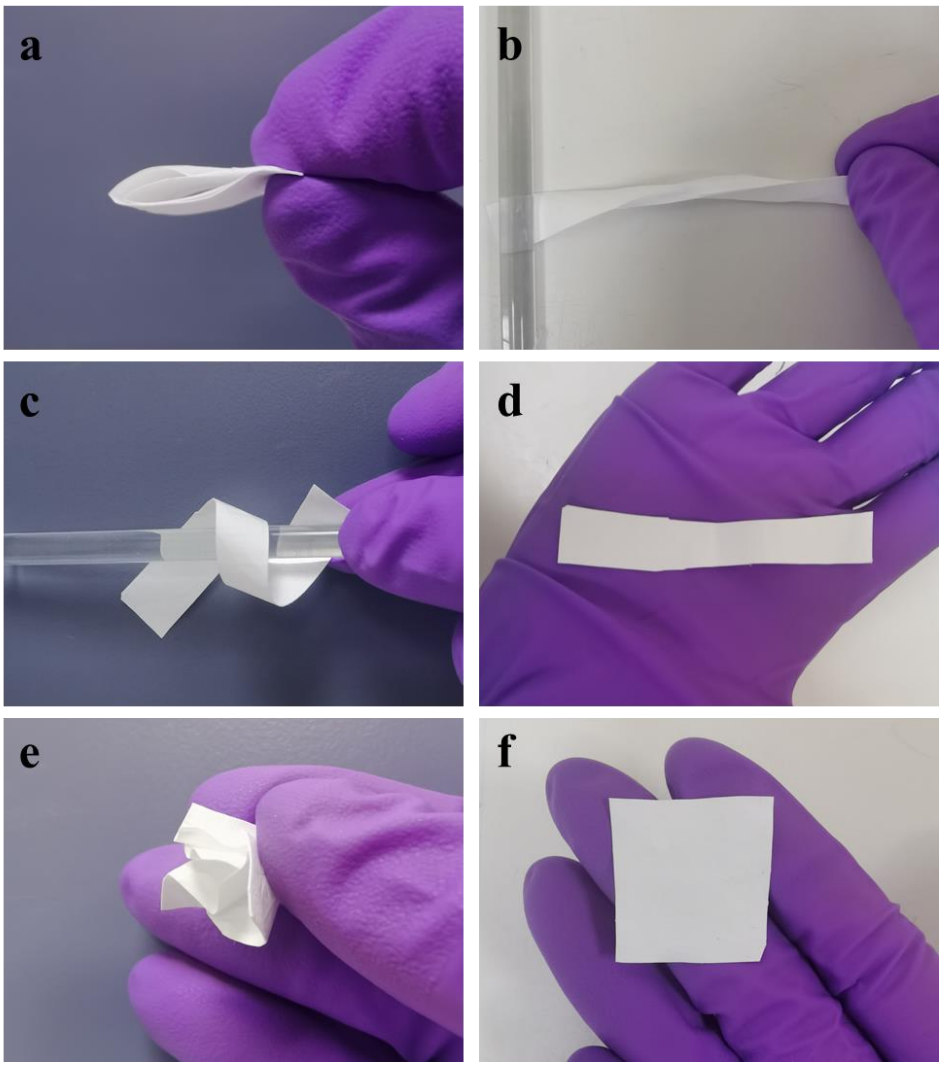

Figure S3. The flexibility performance of SiO_2 NFMs through various deformations: a-d) folding, twisting and bending and recovered NFMs, e-f) kneading and recovered NFMs.

Text S7. Surface optimization of SiO_2-PE NFMs

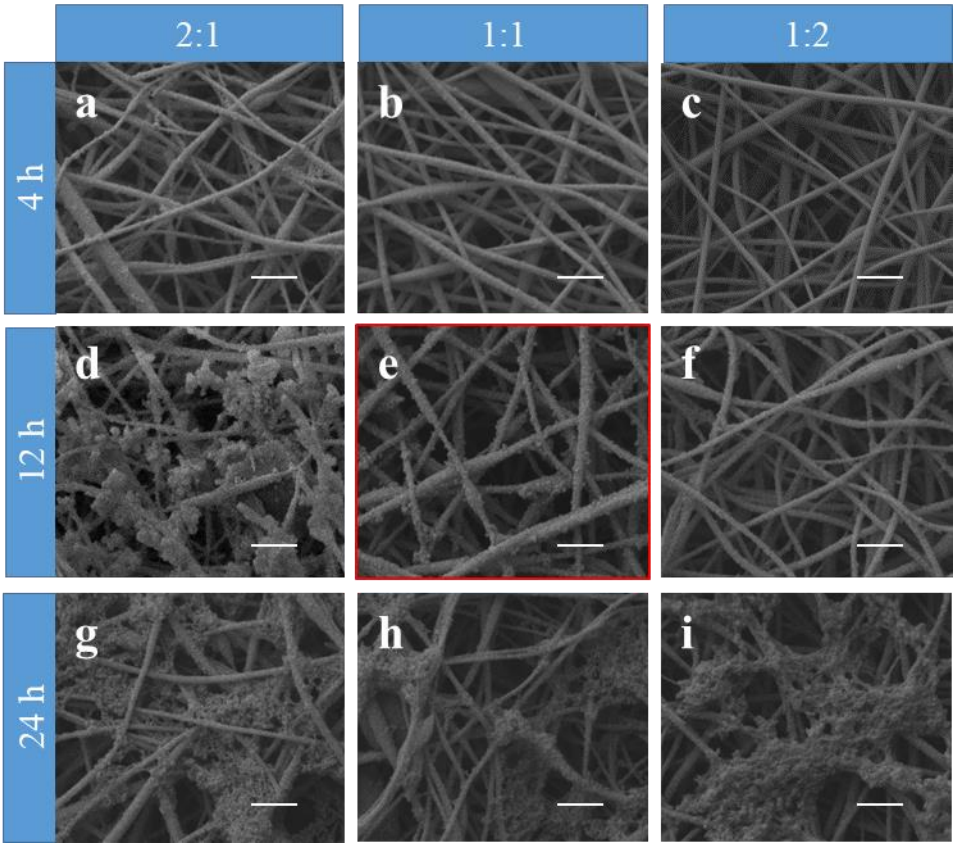

Figure S4. SEM images of SiO_2-PE nanofibers with different coating conditions. The mass ratio of DA: PEI is 2:1, 1:1, and 1:2 from left to right. The coating time of each condition is a-c) 4h, d-f) 12h, and g-i) 24h. The scale of the unlabeled bar is 1 μm. The optimized SiO_2-PE is highlighted in the red box.

Text S8. Transformation efficiency of free laccase

Figure S5 presented free laccase transformation rate on listed 20 EPs.

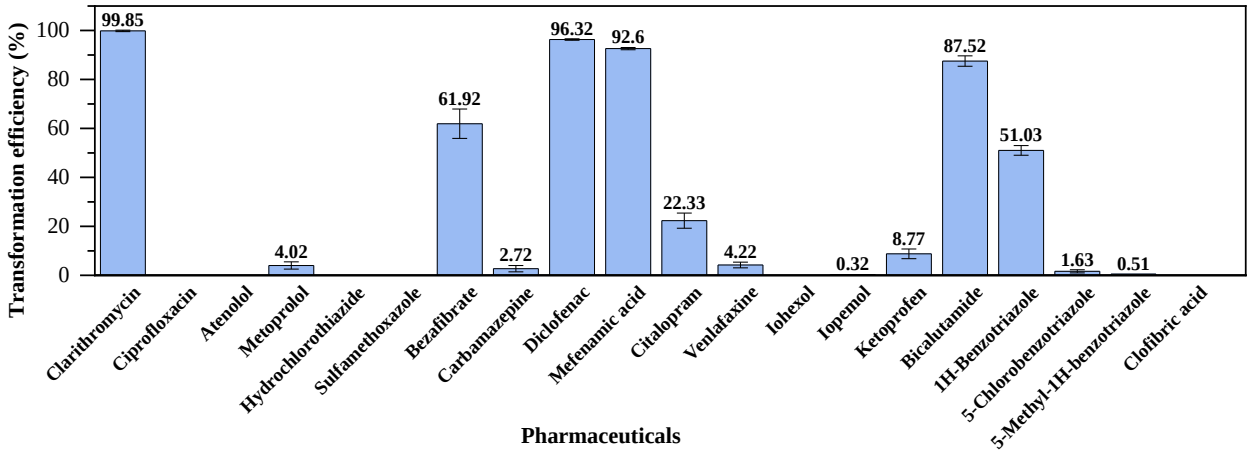

Figure S5. Eps transformation by free laccase

Text S9. Depletion efficiency of Control membrane

Figure S6 presented depletion efficiency of diclofenac achieved by control membranes on during the cycling experiment.

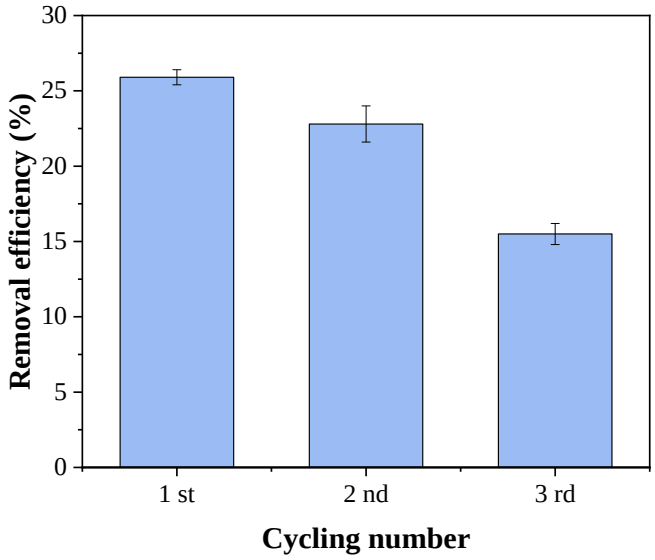

Figure S6. Diclofenac depletion efficiency during the cycling experiment.

Text S9. Morphology change on enzymatic NFMs after repeated used in filtration process.

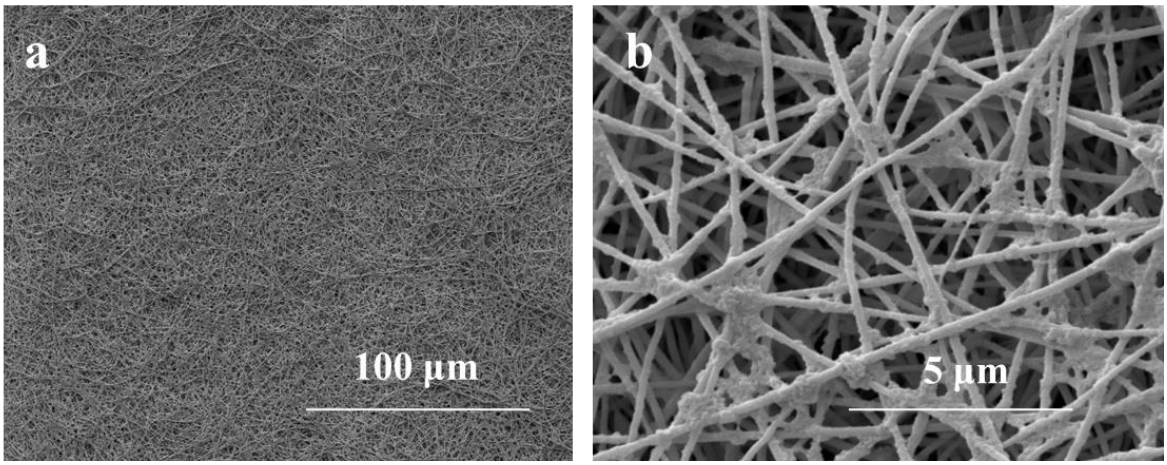

Figure S7. The SEM images of Lac-SiO_2-PE NFMs after 3 operational cycles use in dead-end filtration with different magnifications: a) 1000X, b) 20 000X